

The amazing diversity of Poaceae: trait variation across space, time, and lineage

by

Ryan Christopher Donnelly

B.S., Kansas State University, 2021

A THESIS

submitted in partial fulfillment of the requirements for the degree

MASTER OF SCIENCE

Division of Biology  
College of Arts and Sciences

KANSAS STATE UNIVERSITY  
Manhattan, Kansas

2022

Approved by:

Major Professor  
Jesse Nippert

# Copyright

© Ryan Donnelly 2022.

## Abstract

The grass family Poaceae is one of the most successful plant families on Earth. Poaceae is comprised of over 11,500 species, making it the fifth-largest plant family in current existence. It is also one of the most dominant – grasslands and savannas are found on every continent except Antarctica and cover over a quarter of the planet's terrestrial surface, impacting biogeochemical cycles on a global scale. Finally, grasses play fundamental roles in the development of human civilizations (forage, fiber, and fuels), ecosystem regulation of the water cycle, and regulation of biodiversity within plant and animal communities.

Given the global significance of grass species, it is important to understand the mechanisms of success within this plant family. Plant traits are typically used as ecological tools for assessing species adaptations to varying environments. Species that have a range of traits (morphological and physiological) are more likely to persist in environments that have complex spatial and temporal variability. Trait diversity has facilitated the great success of grasses. How can the traits of this vastly diverse group of plants be used to make predictions of grassland change in the future? In Chapter 2, I explored three methods of organizing grass species to better understand how trait diversity varies among photosynthetic pathway ( $C_3$  or  $C_4$ ), life history (annual or perennial), or evolutionary history. I accomplished this task by measuring 11 structural and physiological traits of 75 naturally-occurring species of grass on the Konza Prairie Biological Station (northeastern Kansas, USA). My results show that the traits of grasses are best represented by their evolutionary history. Photosynthetic pathway only revealed significant differences among physiological traits while structural traits varied by life history. Evolutionary history, on the other hand, was found to significantly explain differences found in both structural

and physiological traits when species were grouped by either Tribe or C<sub>4</sub> lineage. These findings indicate that models utilizing photosynthetic pathway to group grasses, a commonly used practice, likely minimize the existing variability and oversimplify landscape predictions of grassland change.

In Chapter 3, I examined how grass traits may vary temporally and spatially using two Panicoid species, *Dichanthelium oligosanthos* subsp. *scribnerianum* (C<sub>3</sub>) and *Panicum virgatum* (C<sub>4</sub>). To assess temporal variability, I measured leaf stomatal and isotopic/elemental composition traits from specimens dating back to 1887 at the Kansas State University Herbarium (KSC) and the McGregor Herbarium at the University of Kansas (KANU). To assess spatial variability, I measured a suite of traits from eight different grasslands across the Great Plains of North America representing six unique ecoregions. While differences in traits were found across space and time for both species, my results show that  $\Delta^{13}\text{C}$  has been increasing in *Dichanthelium oligosanthos* and decreasing in *Panicum virgatum* over time, illustrating differential responses to water stress for these species. Results from both chapters demonstrate that there is substantial inter- and intraspecific trait variation in Poaceae. My research suggests that incorporating aspects of evolutionary history, as well as spatial and temporal trait variability, better characterizes the natural variability in grass traits in the Great Plains and allows greater mechanistic insight into how these species respond to climate variability.

# Table of Contents

List of Figures .....	vii
List of Tables .....	ix
Acknowledgements .....	xi
Chapter 1 - Introduction.....	1
References.....	6
Chapter 2 - Evolutionary lineage, not plant functional type, explains the most trait variation among 75 coexisting grass species .....	10
Introduction.....	10
Materials and Methods.....	13
Site Description.....	13
Data Collection .....	14
Statistical Analysis.....	17
Results.....	18
Principal Component Analysis .....	18
Plant Structural Traits .....	18
Leaf Structural Traits .....	18
Leaf Physiological Traits .....	20
Discussion.....	21
Evolutionary lineage captures the most differences in trait variation.....	21
Trait variation within the C <sub>4</sub> photosynthetic pathway .....	23
PFTs, lineages, and grassland ecosystem modelling .....	24
Conclusions.....	25
References.....	26
Tables and Figures .....	33
Chapter 3 - Temporal and spatial trait variation of two Panicoid grasses: <i>Dichanthelium</i> <i>oligosanthes</i> subsp. <i>scribnerianum</i> and <i>Panicum virgatum</i> .....	45
Introduction.....	45
Materials and Methods.....	50
Study Sites and Collection of Herbarium Material.....	50

Trait Measurements .....	51
Statistical Analysis.....	54
Results.....	54
Temporal Trends .....	54
Spatial Trends .....	55
Discussion.....	57
Responses in traits to increasing CO <sub>2</sub> since 1887 .....	58
Trait variation across ecoregions .....	61
Conclusion .....	63
References.....	64
Tables and Figures .....	74
Chapter 4 - Conclusion .....	96
References.....	98

## List of Figures

Figure 2.1: A cladogram of all the genera of Poaceae species sampled in our study. We drew the tree following Soreng *et al.*, (2017) for relationships among subtribes, Skendzic *et al.*, (2007) for the relationships among the Andropogoninae, Catalán *et al.*, (2007) for the relationships among the Loliinae, and Peterson *et al.*, (2015) for relationships among the Eleusininae. C<sub>4</sub> markings indicate independent evolution of the C<sub>4</sub> pathway in that lineage. The cladogram was created using the ‘ape’ package in R (Paradis & Schliep, 2019)..... 41

Figure 2.2: PCA of 63 grass species and 9 functional traits sampled at KPBS. Points are classified by annual (open) and perennial (closed) and C<sub>3</sub> (circle) and C<sub>4</sub> (triangle). Colors represent grass tribes..... 42

Figure 2.3: Mean values of each trait that significantly differed by tribe. Error bars represent  $\pm 1$  SE. .... 43

Figure 2.4: Mean values for each trait that significantly differed by C<sub>4</sub> lineage. Error bars represent  $\pm 1$  SE. Each of these lineages represents an independent origin of C<sub>4</sub> photosynthesis (Fig. 2.1)..... 44

Figure 3.1: A map of the grassland sites and their ecoregions (US Environmental Protection Agency, 2013)..... 81

Figure 3.2: The change in stomatal densities of the abaxial ( $R^2 = 0.06492$ ;  $P = 0.1907$ ) and adaxial ( $R^2 = 0.001344$ ;  $P = 0.8531$ ) surfaces of *P. virgatum* leaves from the years 1887 – 2021..... 82

Figure 3.3: The change in total stomatal densities of *D. oligosanthos* ( $R^2 = 0.04249$ ;  $P = 0.2498$ ) and *P. virgatum* ( $R^2 = 0.02825$ ;  $P = 0.3926$ ) leaves from the years 1887 – 2021. .... 83

Figure 3.4: The change in stomatal densities of the abaxial ( $R^2 = 0.05433$ ;  $P = 0.1918$ ) and adaxial ( $R^2 = 0.01172$ ;  $P = 0.5487$ ) surfaces of *D. oligosanthos* leaves from the years 1887 – 2021..... 84

Figure 3.5: The change in stomatal lengths of the abaxial ( $R^2 = 0.1748$ ;  $P = 0.02685$ ) and adaxial ( $R^2 = 0.01798$ ;  $P = 0.4964$ ) surfaces of *P. virgatum* leaves from the years 1887 – 2021. ... 85

Figure 3.6: The change in stomatal lengths of the abaxial ( $R^2 = 0.01594$ ;  $P = 0.4838$ ) and adaxial ( $R^2 = 0.02762$ ;  $P = 0.3553$ ) surfaces of *D. oligosanthos* leaves from the years 1887 – 2021. .... 86

Figure 3.7: The change in stomatal ratios (adaxial:abaxial) of <i>D. oligosanthos</i> ( $R^2 = 0.0008576$ ; $P = 0.8715$ ) and <i>P. virgatum</i> ( $R^2 = 0.1052$ ; $P = 0.09219$ ) leaves from the years 1887 – 2021. .....	87
Figure 3.8: The change in $\Delta^{13}\text{C}$ of <i>D. oligosanthos</i> leaves from the years 1887 – 2020 ( $R^2 = 0.17$ ; $P = 0.007394$ ).....	88
Figure 3.9: The change in $\Delta^{13}\text{C}$ of <i>P. virgatum</i> leaves from the years 1887 – 2020 ( $R^2 = 0.3276$ ; $P = 0.0002649$ ).....	89
Figure 3.10: The change in C:N of <i>D. oligosanthos</i> leaves from the years 1887 – 2020 ( $R^2 =$ $0.08207$ ; $P = 0.06939$ ). .....	90
Figure 3.11: The change in C:N of <i>P. virgatum</i> leaves from the years 1887 – 2020 ( $R^2 = 0.07127$ ; $P = 0.1155$ ).....	91
Figure 3.12: The change in $\delta^{15}\text{N}$ of <i>D. oligosanthos</i> leaves from the years 1887 – 2020 ( $R^2 =$ $0.4493$ ; $P = 1.636e^{-06}$ ). .....	92
Figure 3.13: The change in $\delta^{15}\text{N}$ of <i>P. virgatum</i> leaves from the years 1887 – 2020 ( $R^2 = 0.3282$ ; $P = 0.0002608$ ).....	93
Figure 3.14: The change in %N of <i>D. oligosanthos</i> leaves from the years 1887 – 2020 ( $R^2 =$ $0.06826$ ; $P = 0.09895$ ). .....	94
Figure 3.15: The change in %N of <i>P. virgatum</i> leaves from the years 1887 – 2020 ( $R^2 =$ $0.0002608$ ; $P = 0.1997$ ). .....	95

## List of Tables

Table 2.1: A list of the 75 species sampled in the study.....	33
Table 2.2: A list of all traits measured in the study. ....	35
Table 2.3: $\chi^2$ , df, and $P$ , of all trait comparisons between tribe, photosynthetic pathway, life history, and $C_4$ lineage. ....	36
Table 2.4: Mean values for each trait comparing annuals to perennials and $C_3$ species to $C_4$ species. Error represents $\pm 1SE$ . Bolding denotes $P < 0.05$ , * denotes $0.01 < P < 0.05$ , ** denotes $0.001 < P < 0.01$ , *** denotes $P < 0.001$ .....	37
Table 2.5: $\chi^2$ , df, and $P$ of the interaction between life history and tribe using type III ANOVA. Only tribes that had both annual and perennial species measured for each trait are included in these analyses. Bolding indicates $P < 0.05$ . ....	38
Table 2.6: $\chi^2$ , df, and $P$ , of $\delta^{13}C$ comparisons between tribes with $C_3$ members and $C_4$ members, separately. We analyzed $\delta^{13}C$ separately for $C_3$ and $C_4$ species due to known differences in $\delta^{13}C$ between both photosynthetic pathways. Bolding indicates $P < 0.05$ . ....	39
Table 2.7: $\chi^2$ , df, and $P$ of $\delta^{13}C$ comparisons between $C_4$ subtypes. Under the “All Species” comparison, this places the three <i>Sporobolus</i> species (whose $C_4$ subtype is currently unknown) and <i>Bouteloua curtipendula</i> , a mixed NAD-ME/PCK species, each in their own group. The second comparison only compares species definitively known to be in the PCK, NAD-ME, and NADP-ME groups. Bolding indicates $P < 0.05$ . ....	40
Table 3.1: A list of traits measured in this study. ....	74
Table 3.2: A list of grasslands where sampling of traits of <i>D. oligosanthos</i> and <i>P. virgatum</i> occurred. Ecoregions were determined from US Environmental Protection Agency (2013). ....	75
Table 3.3: Mean values of stomatal traits of <i>D. oligosanthos</i> separated by ecoregion. Means within columns with different letters are statistically significant ( $P < 0.05$ ). ....	77
Table 3.4: Mean values of stomatal traits of <i>P. virgatum</i> separated by ecoregion. Means within columns with different letters are statistically significant ( $P < 0.05$ ). ....	78
Table 3.5: Mean values of leaf traits of <i>D. oligosanthos</i> separated by ecoregion. Means within columns with different letters are statistically significant ( $P < 0.05$ ). ....	79

Table 3.6: Mean values of leaf traits of *P. virgatum* separated by ecoregion. Means within columns with different letters are statistically significant ( $P < 0.05$ ). ..... 80

## Acknowledgements

There are many people to whom I owe gratitude for the completion of this degree. First and foremost, I thank my advisor, Dr. Jesse Nippert, for his mentorship to me as both an undergraduate and graduate student. Jesse encouraged me to pursue a master's degree at Kansas State University and inspired my love for grasses. He has been instrumental in reshaping the way I think about my life and the directions I want to take in the future. I also thank the other members of my committee, Dr. Carolyn Ferguson and Dr. John Blair, for their advice and feedback while I performed my research and wrote my thesis.

I also thank my lab mates, Dr. Seton Bachle, Rachel Keen, Emily Wedel, Greg Tooley, and Shahla Mohammadi, for the encouragement they have given me over the years. I am especially grateful to Rachel and Emily who have been invaluable in helping me learn to code in R and giving me feedback on my projects. I am also grateful to the undergraduates in our lab, Lauren, Meghan, and Sarah, who have spent many hours grinding leaf tissue and weighing biomass samples for me.

Additionally, I thank all my co-authors for their feedback and assistance in developing my first manuscript. They have all helped me become a better writer, thinker, and researcher. I extend an extra thanks to Dr. Daniel Griffith for setting so much time aside to discuss the manuscript with me and for his extremely thoughtful and meticulous feedback. I also thank Jeffrey Taylor for teaching me how to identify the grasses of Konza Prairie – a skill I cherish.

Thank you to my parents and sister for encouraging me to move from Los Angeles, California to Manhattan, Kansas for college. It remains one of the best decisions I have ever made in my life. Thank you to my partner, Paige, for being extremely supportive of my research and love for grasses. It can't be easy having to hear about every grass I see on walks or driving

14 hours round-trip with me to sample grasses in remote Nebraska, but she perseveres, nonetheless.

Lastly, I would like to thank all the organizations that made this research possible. Thank you to the National Science Foundation for funding this research. Thank you to Konza Prairie Biological Station for allowing me to sample grasses for my many projects, especially during the summer of 2020. Thank you to the Kansas State University Herbarium and the R. L. McGregor Herbarium at the University of Kansas and their curators for allowing me to sample traits of herbarium specimens. Finally, thank you to each of the grassland sites and those who helped me obtain permission to sample at those sites for my second research chapter: Joseph H. Williams Tallgrass Prairie Preserve, Kisk-Ke-Kosh Prairie, T. L. Davis Preserve, Cedar Creek Ecosystem Science Preserve, Wah'Kon-Tah Prairie, Woodworth Station Waterfowl Production Area, and Valentine National Wildlife Refuge.

## Chapter 1 - Introduction

Over the past 55-60 million years, the grass family Poaceae became one of the world's most diverse and dominant plant families (Strömberg, 2011). Currently, there are over 11,500 described species spread across 768 genera and 52 tribes (Soreng *et al.*, 2017). Grasses cover over one-quarter of the earth's terrestrial surface (Asner *et al.*, 2004) and sequester around 0.5 Pg C per year (Scurlock & Hall, 1998). Grasslands have been of great importance to humanity ever since savannas provided the landscape template upon which humans evolved (Bobe & Behrensmeyer, 2004). Furthermore, grasses have helped form the foundation of human civilization; humans depend on grasses for food both through direct consumption and indirectly via grazing livestock. Throughout history, humans have domesticated several wild grass species for use as crops, such as wheat, maize, rice, and sugarcane (Glémin & Bataillon, 2009). In the modern age, over two billion megatonnes of cereal are produced annually, providing a staple food source for most of the human population (Tilman *et al.*, 2002). Despite the critical contributions of grasslands towards the benefit of humans, they are currently one of the world's most endangered ecosystems (Henwood, 2010).

Grasslands are characterized and maintained through disturbances; they are a product of interactions among fire, herbivory, and climate (Blair *et al.*, 2014). However, throughout the Anthropocene, humans have greatly modified each of these drivers such that the future of grassland ecosystems is uncertain. These human activities include fire suppression, extirpation of native megafauna herbivores, and increased greenhouse gas emissions into the atmosphere, causing climate change. While fire suppression and the removal of megafauna can be combatted at the local level, the effects of climate change cannot. Symptoms of climate change, such as increased drought, more frequent extreme precipitation events, and generally warmer

temperatures will affect grassy ecosystems globally (Gibson & Newman, 2019). Therefore, it is necessary to understand how grasslands will respond to various climate scenarios. This requires a knowledge of how grasses and grasslands have changed under past conditions as well as creating models to predict how grasslands may change in the future.

In this thesis, I describe how traits of grass species vary across space, time, and lineage in an effort to better understand the trait diversity of our grasslands. In Chapter 2, I explore three methods of organizing grass species to better understand how trait diversity varies among photosynthetic pathway ( $C_3$  or  $C_4$ ), life history (annual or perennial), or evolutionary history. In Chapter 3, I examine how traits of two Panicoid species, *Dichanthelium oligosanthes* subsp. *scribnerianum* ( $C_3$ ) and *Panicum virgatum* ( $C_4$ ) vary across spatial and temporal scales.

Plant traits are commonly used as predictors of plant performance in certain environmental conditions (Violle *et al.*, 2007). Over the past couple decades, the use of plant traits to make predictions about species or groups of species has risen to prominence in the field of ecology (Laughlin, 2014). What started out as using simple leaf traits to uncover patterns in plant life histories and species distributions, such as in Wright *et al.*, (2004), is now a large part of the field where entire databases are dedicated to hosting massive amounts of information on plant traits, such as the TRY database (Kattge *et al.*, 2011). For any given species, the values of its traits are subject to change, as plants can perform differently under varying environmental conditions or as time passes (Violle *et al.*, 2007). Traits may vary intraspecifically across spatial scales due to differences in environmental conditions across a species' range or across temporal scales due to environmental change (Violle *et al.*, 2007); this intraspecific variation may be due to phenotypic plasticity (Sultan, 2000; Violle *et al.*, 2012). The traits of each species of plant are products of its evolutionary history, in part due to the traits its ancestors evolved to combat

certain stressors in the environment (Valladares *et al.*, 2007). Thus, entire lineages of plants may have species with very similar traits because these traits originated from a common ancestor adapted to a specific biome (Crisp *et al.*, 2009).

While plant traits may be useful as proxies of plant performance, they are also highly valuable measurements that can be used to predict how a species will fare in new or altered environments and are especially important in assessing how species will respond to climate change. Many ecosystem models incorporate plant traits into their analyses to determine how not just one species will perform under novel climactic scenarios, but whole ecosystems. To make these models feasible, the species in an ecosystem are grouped into several categories based upon some common factor, commonly a species' function in an environment (Verheijen *et al.*, 2013). These functional types are incredibly useful because it becomes impossible to account for species-specific differences in structure and function when creating large-scale models of ecosystem function (Woodward & Cramer, 1996).

A variety of plant functional groups can be created for ecosystem models depending on the system. In grasslands, it is common to have separate functional groups for woody species, grasses and grass-like species (such as sedges), and forbs. However, because grasses are extremely biodiverse and do not all share the same traits, grasses have been further organized into their own functional groups to better represent their functional diversity. One of the most common methods of placing grasses into functional groups is grouping species into plant functional types (PFTs) based on whether they perform either C<sub>3</sub> or C<sub>4</sub> photosynthesis (Griffith *et al.*, 2020). However, PFTs based on photosynthetic pathways overlook large amounts of trait variation within Poaceae, especially within the C<sub>4</sub> PFT, as C<sub>4</sub> photosynthesis has evolved independently many times (Grass Phylogeny Working Group II, 2012). Instead, organizing

grasses by their evolutionary lineage may better represent grass trait diversity by capturing more ecologically meaningful differences than PFTs (Griffith *et al.*, 2020; Anderegg *et al.*, 2022).

In North America, there are three lineages of grasses that dominate the landscape: the tribe Andropogoneae (C<sub>4</sub>) and the subfamilies Chloridoideae (C<sub>4</sub>) and Pooideae (C<sub>3</sub>). These three lineages have evolved to occupy different climate spaces. The Pooideae are cold-climate specialists, having evolved traits to deal with freezing and other side effects of cold temperatures (Edwards & Smith, 2010; Schubert *et al.*, 2019). Both the Pooideae and Chloridoideae live in dry climates, though droughts are not as pronounced in Pooideae-dominated areas (Edwards & Smith, 2010; Lehmann *et al.*, 2019). The Andropogoneae and Chloridoideae are warm-climate specialists, with the Chloridoideae living in hotter, drier environments and the Andropogoneae inhabiting more mesic sites (Lehmann *et al.*, 2019). Geographically, the Pooideae dominate the northwest Midwest, the Andropogoneae dominate the eastern Midwest, and the Chloridoideae dominate the south and southwestern Midwest.

In some regions, these three lineages of grasses can co-dominate the landscape due to temporal differences in environmental conditions, such as mean annual temperature (Still *et al.*, 2003). Kansas is one of these places, occurring at the crossover point where neither C<sub>3</sub> nor C<sub>4</sub> species have the physiological advantage (Ehleringer & Björkman, 1977), creating a range of overlap among the dominant grass lineages (Lehmann *et al.*, 2019). Here, cool-season grasses, such as members of the Pooideae lineage, take advantage of cooler temperatures by growing in the spring to early summer. As summer progresses, the warm-season grasses (a mix of Andropogoneae and Chloridoideae) become the dominant grasses on the landscape.

The research in this thesis was conducted at the Konza Prairie Biological Station near Manhattan, Kansas, a place where all three dominant lineages of grasses co-occur and are found abundantly (Taylor *et al.*, unpublished). The second chapter of this thesis highlights the amazing diversity of grasses occurring in this region. In this chapter, I measure structural and physiological traits of 75 species of naturally-occurring grasses to determine the best method of capturing the large amount of functional diversity of grasses in grassland ecosystem models. I accomplish this by testing whether traits significantly differed among species grouped by photosynthetic pathway (C<sub>3</sub> or C<sub>4</sub>), life history (annual or perennial), or evolutionary lineage (tribe or C<sub>4</sub> lineage). The second chapter aims to improve how grassland ecosystem modeling is conducted and improve our understanding of how grasslands will respond to future environmental conditions. In the third chapter of this thesis, I utilize the impressive collections of the herbaria at both Kansas State University (KSC) and the University of Kansas (KANU) to investigate temporal changes in grass traits. This chapter describes how the traits of two species of grasses, *Dichanthelium oligosanthos* and *Panicum virgatum* have been changing over the past 140 years in response to anthropogenic CO<sub>2</sub> emissions. Coupled with this analysis of temporal trends in traits, I also investigate how traits of these species vary spatially by collecting traits of *Dichanthelium oligosanthos* and *Panicum virgatum* at 8 grassland ecosystems across the Great Plains of the United States. Combined, these chapters provide an increased understanding of the incredible diversity of traits found in Poaceae and how these traits can be used to predict what will happen to our grasslands in the future.

## References

- Anderegg LDL, Griffith DM, Cavender-Bares J, Riley WJ, Berry JA, Dawson TE, Still CJ. 2022.** Representing plant diversity in land models: an evolutionary approach to make “Functional Types” more functional. *Global Change Biology* **28**: 2541–2554.
- Asner GP, Elmore AJ, Olander LP, Martin RE, Harris AT. 2004.** Grazing systems, ecosystem responses, and global change. *Annual Review of Environment and Resources* **29**: 261–299.
- Blair J, Nippert J, Briggs J. 2014.** Grassland ecology. In: Monson RK, ed. *Ecology and the environment*. New York, NY, USA: Springer, 389–423.
- Bobe R. 2004.** The expansion of grassland ecosystems in Africa in relation to mammalian evolution and the origin of the genus *Homo*. *Palaeogeography, Palaeoclimatology, Palaeoecology* **207**: 399–420.
- Crisp MD, Arroyo MTK, Cook LG, Gandolfo MA, Jordan GJ, McGlone MS, Weston PH, Westoby M, Wilf P, Linder HP. 2009.** Phylogenetic biome conservatism on a global scale. *Nature* **458**: 754–756.
- Edwards EJ, Smith SA. 2010.** Phylogenetic analyses reveal the shady history of C<sub>4</sub> grasses. *Proceedings of the National Academy of Sciences* **107**: 2532–2537.
- Ehleringer J, Björkman O. 1977.** Quantum Yields for CO<sub>2</sub> Uptake in C<sub>3</sub> and C<sub>4</sub> Plants: Dependence on Temperature, CO<sub>2</sub>, and O<sub>2</sub> Concentration. *Plant Physiology* **59**: 86–90.
- Gibson DJ, Newman JA (Eds.). 2019.** *Grasslands and Climate Change*. Cambridge University Press.
- Glémin S, Bataillon T. 2009.** A comparative view of the evolution of grasses under domestication. *New Phytologist* **183**: 273–290.

**Grass Phylogeny Working Group II. 2012.** New grass phylogeny resolves deep evolutionary relationships and discovers C<sub>4</sub> origins. *New Phytologist* **193**: 304–312.

**Griffith DM, Osborne CP, Edwards EJ, Bachle S, Beerling DJ, Bond WJ, Gallaher TJ, Helliker BR, Lehmann CER, Leatherman L, et al. 2020.** Lineage-based functional types: characterising functional diversity to enhance the representation of ecological behaviour in Land Surface Models. *New Phytologist* **228**: 15–23.

**Henwood WD. 2020.** Toward a strategy for the conservation and protection of the world's temperate grasslands. *Great Plains Research* **20**: 121–134.

**Kattge J, Díaz S, Lavorel S, Prentice IC, Leadley P, Bönlisch G, Garnier E, Westoby M, Reich PB, Wright IJ, et al. 2011.** TRY - a global database of plant traits. *Global Change Biology* **17**: 2905–2935.

**Laughlin DC. 2014.** The intrinsic dimensionality of plant traits and its relevance to community assembly (S Wilson, Ed.). *Journal of Ecology* **102**: 186–193.

**Lehmann CE, Griffith DM, Simpson KJ, Anderson TM, Archibald S, Beerling DJ, Bond WJ, Denton E, Edwards EJ, Forrestel EJ et al. 2019.** Functional diversification enabled grassy biomes to fill global climate space. *BioRxiv*: 583625.

**Schubert M, Grønvold L, Sandve SR, Hvidsten TR, Fjellheim S. 2019.** Evolution of cold acclimation and its role in niche transition in the temperate grass subfamily Pooideae. *Plant Physiology* **180**: 404–419.

**Scurlock JMO, Hall DO. 1998.** The global carbon sink: a grassland perspective. *Global Change Biology* **4**: 229–233.

**Soreng RJ, Peterson PM, Romaschenko K, Davidse G, Teisher JK, Clark LG, Barberá P, Gillespie LJ, Zuloaga FO. 2017.** A worldwide phylogenetic classification of the Poaceae

(Gramineae) II: an update and a comparison of two 2015 classifications. *Journal of Systematics and Evolution* **55**: 259–290.

**Still CJ, Berry JA, Collatz GJ, DeFries RS. 2003.** Global distribution of C<sub>3</sub> and C<sub>4</sub> vegetation: carbon cycle implications. *Global Biogeochemical Cycles* **17**: 6-1-6–14.

**Strömberg CAE. 2011.** Evolution of grasses and grassland ecosystems. *Annual Review of Earth and Planetary Sciences* **39**: 517–544.

**Sultan SE. 2000.** Phenotypic plasticity for plant development, function and life history. *Trends in Plant Science* **5**: 537–542.

**Taylor JH, Breckon GJ, Mayfield MH. 2021.** An annotated checklist of the vascular flora of Konza Prairie Biological Station. Unpublished manuscript.

**Tilman D, Cassman KG, Matson PA, Naylor R, Polasky S. 2002.** Agricultural sustainability and intensive production practices. *Nature* **418**: 671–677.

**Valladares F, Gianoli E, Gómez JM. 2007.** Ecological limits to plant phenotypic plasticity. *New Phytologist* **176**: 749–763.

**Verheijen LM, Brovkin V, Aerts R, Bönisch G, Cornelissen JHC, Kattge J, Reich PB, Wright IJ, van Bodegom PM. 2013.** Impacts of trait variation through observed trait–climate relationships on performance of an Earth system model: a conceptual analysis. *Biogeosciences* **10**: 5497–5515.

**Violle C, Navas M-L, Vile D, Kazakou E, Fortunel C, Hummel I, Garnier E. 2007.** Let the concept of trait be functional! *Oikos* **116**: 882–892.

**Violle C, Enquist BJ, McGill BJ, Jiang L, Albert CH, Hulshof C, Jung V, Messier J. 2012.** The return of the variance: intraspecific variability in community ecology. *Trends in Ecology & Evolution* **27**: 244–252.

**Woodward FI, Cramer W. 1996.** Plant functional types and climatic change: introduction.  
*Journal of Vegetation Science* **7**: 306–308.

**Wright IJ, Reich PB, Westoby M, Ackerly DD, Baruch Z, Bongers F, Cavender-Bares J,  
Chapin T, Cornelissen JHC, Diemer M, *et al.* 2004.** The worldwide leaf economics spectrum.  
*Nature* **428**: 821–827.

## **Chapter 2 - Evolutionary lineage, not plant functional type, explains the most trait variation among 75 coexisting grass species**

### **Introduction**

Over the past 55-60 million years, the grass family Poaceae has become one of the world's most diverse and dominant plant families. Currently, there are over 11,500 described species spread across 768 genera and 52 tribes (Soreng *et al.*, 2017), with grasslands and savannas covering over one-quarter of the earth's terrestrial surface (Asner *et al.*, 2004) and sequestering around 0.5 Pg C per year (Scurlock & Hall, 1998). The global-scale emergence of grass-inhabited biomes and the more local-scale grass lineages that came to populate these early biomes led to lineage-specific environmental selection, and clear examples of both divergent and convergent evolution within the Poaceae. For example, the Pooideae lineage evolved to be cold-climate specialists (Edwards & Smith, 2010), and the warm-climate Chloridoideae species are divergent from the warm-climate Andropogoneae species; Chloridoideae species are arid-land specialists and Andropogoneae species tend to inhabit more mesic sites (Lehmann *et al.*, 2019). One of the clearest examples of convergent evolution in the grasses— and one of the most critical aspects of Poaceae success globally— has been the evolution of the C<sub>4</sub> pathway. Despite accounting for only ~1% of all species of plants and less than half of all grass species (Osborne *et al.*, 2014; Christenhusz & Byng, 2016), C<sub>4</sub> grasses cover around 19 million km<sup>2</sup>, accounting for nearly a quarter of total terrestrial gross productivity (Still *et al.*, 2003).

In Poaceae, the C<sub>4</sub> pathway has evolved independently more than 20 times over a ~30 million year period (Grass Phylogeny Working Group II, 2012). C<sub>4</sub> evolution is thought to always be selected for by high temperature, but the primacy of additional selective agents changed through time: water limitation in the mid-Oligocene, lower CO<sub>2</sub> concentrations and

increased aridity in the mid-to-late Miocene (Ehleringer *et al.*, 1997; Sage *et al.*, 2018; Zhou *et al.*, 2018). So even within this oft-cited example of convergent evolution, C<sub>4</sub> physiology within the grasses should not be viewed as a single functional type because of the previous divergences and changing selective agents through time. Such a consideration extends even more broadly to the whole of the Poaceae, where millions of years of physiological and structural diversity has been selected for, and preserved, within separate taxonomic lineages.

Due to the inherent physiological differences between the C<sub>3</sub> and C<sub>4</sub> photosynthetic pathways, C<sub>4</sub> grasses are normally lumped into one plant functional type (PFT) in macroecological analyses (Griffith *et al.*, 2020). These highly abstracted PFTs are also typically used to represent grass functional biodiversity in most Land Surface Models (LSMs), which include a comprehensive array of physical, biological, and chemical processes that simulate biosphere processes and are crucial for climate-related decision making and policy. PFTs are popular for capturing first-order ecosystem properties because it becomes nearly impossible to account for species-specific structure and function when creating large-scale models of ecosystem function (Woodward & Cramer, 1996). While PFTs may simplify the modeling process, important aspects of C<sub>4</sub> diversity may be overlooked, such as potential functional differences within PFTs due to the independent origins of C<sub>4</sub> grass species (Edwards *et al.*, 2007; Edwards *et al.*, 2010; Liu *et al.*, 2012). This is problematic, as differences in traits and growth responses of C<sub>4</sub> grasses have been linked to their lineages rather than photosynthetic pathway (Kellogg *et al.*, 1999; Taylor *et al.*, 2010).

One prominent idea to improve PFTs is to categorize grasses into lineage-based functional types (LFTs), where grasses are grouped based on their phylogenetic relatedness to one another (Griffith *et al.*, 2020). Grouping grass species by evolutionary lineage, as in LFTs,

rather than by PFTs, presents a key method of capturing the broad diversity of species' traits. This may help prevent oversimplifications of C<sub>3</sub> or C<sub>4</sub> PFTs, where a single PFT may include species in distantly related lineages, each potentially having evolved traits unrelated to C<sub>3</sub> or C<sub>4</sub> pathways (Edwards *et al.*, 2007; Edwards *et al.*, 2010). Grouping traits by lineage can also explain trait variation, as seen in Edwards *et al.*, (2007), where traits of *Echinochloa* appeared to be outliers in its C<sub>4</sub> PFT group suggesting that the genus may have traits unique to its independent C<sub>4</sub> lineage. Furthermore, LFT approaches have the potential to be broadly applicable in other ecosystem types and for remote sensing (Anderegg *et al.*, 2022). Thus, using the LFT approach, functional trait variation within PFTs can be captured (Griffith *et al.*, 2020) since many important plant traits are known to be phylogenetically conserved (Edwards *et al.*, 2007; Liu *et al.*, 2012; Coelho de Souza *et al.*, 2016). However, not all traits are phylogenetically conserved (Cadotte *et al.*, 2017), and factors such as photosynthetic type and life history (i.e., whether a species is annual or perennial) can also explain a large proportion of trait variation. For example, Liu *et al.*, (2019) showed that life history explained more of the variation in structural traits than photosynthetic pathway in grasses, while the C<sub>3</sub>-C<sub>4</sub> contrast in species explained most of the variation in physiological traits. Thus, trait variation within LFTs is not well characterized, and recent work has called for increased collection of grass traits across lineages (Griffith *et al.*, 2020).

To that end, we measured 75 species of Poaceae (Table 2.1) and analyzed physiological and structural traits (Table 2.2) from *in situ* tallgrass prairie populations located at the Konza Prairie Biological Station (KPBS; Manhattan, KS USA). Our objective was to understand how evolutionary lineage influences traits in species that are growing within similar environments. For each trait across all species, we assessed the ability of life history, lineage, and

photosynthetic pathway to explain variability. Of the 12 subfamilies and 52 tribes that are currently recognized in Poaceae (Soreng *et al.*, 2017), our study measured species representing 5 subfamilies (Aristidoideae, Chloridoideae, Oryzoideae, Panicoideae, and Pooideae) and 14 tribes (Table 2.1; Andropogoneae, Aristideae, Bromeae, Cynodonteae, Diarrheneae, Eragrostideae, Meliceae, Oryzae, Paniceae, Paspaleae, Poeae, Stipeae, Triticeae, and Zoysieae). Importantly, this represented species from 7 of the independent C<sub>4</sub> origins in grasses (Fig. 2.1; Andropogoneae, *Aristida*, Chloridoideae, *Digitaria*, *Echinochloa*, *Paspalum*, and the MPC Clade – the clade which constitutes the subtribes Cenchrinae, Melinidinae, and Panicinae), including the two most dominant lineages globally (Lehmann *et al.*, 2019). Measuring a suite of traits from a large diversity of species growing at the same site allowed us to determine which factor best explains trait variation. We hypothesized that lineage would be the best predictor of traits, more so than either photosynthetic pathway or life history. We further predicted that there would be substantial variation of traits in C<sub>4</sub> species among the seven C<sub>4</sub> lineages represented in our research. One reason we expected this variation is because the evolution of C<sub>4</sub> lineages varies biogeographically and it is expected that these lineages will conserve traits from the climate of the biomes in which they evolved (Edwards *et al.*, 2007; Crisp *et al.*, 2009).

## Materials and Methods

### Site Description

Field work and data collection were conducted at the Konza Prairie Biological Station (KPBS), a historically unplowed 3,487 ha tallgrass prairie located in the Flint Hills region of northeastern Kansas, USA (39°05', 96°35'W). KPBS is divided into 52 different watersheds, each experimentally manipulated in terms of fire frequency (burned once every 1, 2, 4, or 20 years) and grazing (cattle, bison, or ungrazed). This landscape of grazing by burning creates a

mosaic of microsite conditions that contribute to the high plant species diversity and is representative of the broader tallgrass prairie ecosystem. Mean annual precipitation is 812 mm (1983-2020), the majority (~70%) of which is received during the growing season (April-September). Mean growing season temperature is 21°C (1983-2020).

## **Data Collection**

The flora of KPBS includes 98 grass species comprising annuals, perennials, native, and non-native species (Taylor *et al.*, unpublished). In 2020, we sampled 75 grass species that exist within the boundaries of KPBS (Table 2.1). Sampling occurred throughout the entirety of the site – there was no specific location for measuring all the species given that we measured naturally-established individuals growing within their own viable habitat. We collected samples from plants in representative habitats for each species to facilitate species comparisons. Five replicate populations were marked for each species. The replicates varied at distances ranging from a few meters to a few kilometers depending on the abundance of the species to ensure independence. For rare species, it was often difficult to find more than a few individuals across all of KPBS, so replicates of rare species tended to be in closer proximity than the replicates of dominant species. For the dominant species (e.g., *Andropogon gerardii*) that number in the hundreds of millions of individuals on-site, capturing the breadth of the population differences was beyond the scope of this project.

A suite of plant traits was collected for each individual in coordination with the initiation of flowering for each species (Table 2.2). We used flowering as a key phenological event to synchronize trait measurements. Traits measured include photosynthetic A- $c_i$  response curves (to derive  $V_{p_{max}}$ ,  $V_{c_{max}}$ , and  $J_{max}$ ), leaf osmotic potential at full turgor (MPa), specific leaf area (SLA;  $\text{cm}^2 \text{g}^{-1}$ ), leaf dry matter content (LDMC), leaf thickness (mm), maximum plant flowering

and vegetative heights (cm), leaf C:N, and  $\delta^{13}\text{C}$  compositions (Table 2.2).  $V_{c_{\max}}$  is the maximum rate of carboxylation of Rubisco ( $\mu\text{mol m}^{-2} \text{s}^{-1}$ ),  $J_{\max}$  is the maximum rate of electron transport ( $\mu\text{mol electrons m}^{-2} \text{s}^{-1}$ ), and  $V_{p_{\max}}$  is the maximum rate of carboxylation of PEPc ( $\mu\text{mol m}^{-2} \text{s}^{-1}$ ).

Leaf gas exchange was measured with a LI-6400XT Portable Photosynthesis System (Li-COR, Inc., Lincoln, Nebraska, USA) on leaves for two to three replicates of each species. Measurements were taken from 9:00 to 15:00 on healthy, fully expanded leaves. Gas exchange measurements for A-C<sub>i</sub> response curves were collected by taking measurements at eight concentrations of CO<sub>2</sub> in the following order: 400, 300, 200, 100, 50, 500, 800, and 1000  $\mu\text{mol CO}_2 \text{ mol}^{-1}$ . The PAR intensity was 2000  $\mu\text{mol m}^{-2} \text{s}^{-1}$ , relative humidity was maintained between 40%-60%, and the leaf was allowed a minimum of 90 seconds to a maximum of 450 seconds to equilibrate between changes in CO<sub>2</sub>. Measurements were taken in optimal ambient light conditions with little to no cloud cover. Electron transport rate ( $J_{\max}$ ), and maximum carboxylation ( $V_{c_{\max}}$ ) for C<sub>3</sub> species were determined using the curve-fitting procedures described in the 'plantecophys' R package (Duursma, 2015). For C<sub>4</sub> species, we used the Excel curve fitting procedure described by Zhou *et al.*, (2019).

Osmotic potential, a trait linked to drought tolerances of species and related to the turgor loss point (Bartlett *et al.*, 2012a; Bartlett *et al.*, 2012b), was measured using a VAPRO® Vapor Pressure Osmometer (Model 5600; Logan, Utah, USA) for three leaf replicates of each species. For each replicate, one individual grass tiller was removed from the field and subsequently clipped with the stem underwater. The stems remained underwater overnight before osmotic potential measurements were taken the next day. Our measurement protocol followed Griffin-Nolan *et al.*, (2019). In brief, a single, fully hydrated leaf was removed from the grass tiller,

punched with a 5 mm leaf tissue punch, and quickly wrapped in aluminum foil before being submerged in liquid nitrogen for one minute. Once taken out, the frozen tissue was immediately pierced to lyse cell contents. This tissue was then equilibrated in the osmometer's tissue chamber for ten minutes before measurement.

For leaf measurements, one leaf was taken from each replicate. Leaf area was measured in the field using Leafscan, a mobile app for measuring the surface area of individual leaves (Anderson & Rosas-Anderson, 2017). Leaf wet mass was measured after leaf rehydration and leaf dry mass was measured after the leaf had been dried for at least 48 hours at 60 °C. Rehydration was performed by submerging the leaf in water for 24-72 hours. Leaf thickness was derived from  $(SLA * LDMC)^{-1}$  (Vile *et al.*, 2005) and multiplied by 10 to convert to mm. Maximum flowering height and maximum vegetative height were measured from the ground to the highest point of the inflorescence or the uppermost leaf, respectively. At each replicate, five randomly selected individuals were measured; the tallest inflorescence and tallest leaf were used for maximum heights.

Leaf C and N content and stable C isotopic composition were measured at the Stable Isotope Mass Spectrometry Laboratory at Kansas State University. For each replicate, five leaves were dried at 60 °C for a minimum of 48 hours and then homogenized using an amalgamator. Total C and N of homogenized leaf samples were measured following combustion using an Elementar vario Pyro cube coupled to an Elementar Vision mass spectrometer for isotope analysis. Isotopic abundance ratios were converted to  $\delta$  notation using:

$$\delta = \left[ \frac{R_{sample}}{R_{standard}} - 1 \right] * 1000$$

where R is the ratio of heavy (<sup>13</sup>C) to light (<sup>12</sup>C) isotopes for the sample and standard, respectively. Working laboratory standards were annually calibrated against the internationally

accepted standard, Vienna Pee-Dee Belemnite for  $\delta^{13}\text{C}$ . Within-run and across-run variability of the laboratory working standard was  $< 0.05\text{‰}$ .

## **Statistical Analysis**

All statistical analyses were performed in R V4.1.2 (R Core Team, 2021). For each trait, we used separate linear mixed effects models with either with species as a random effect for each of the following factors: photosynthetic pathway, life history, tribe, or  $\text{C}_4$  lineage as a predictor and species as a random effect using the ‘lme4’ package (Bates *et al.*, 2015). In this way, we assessed what the strongest predictors were for how traits are related within each factor.

We tested whether interactions were present between tribe and life history for tribes that included both annual and perennial species in our data. We did not test whether interactions were present between tribe and photosynthetic pathway in this study due to the factors being confounded with one another. Photosynthetic pathway among species within a tribe is non-independent. For instance, only one out of the fourteen tribes sampled in this study included both  $\text{C}_3$  and  $\text{C}_4$  species (Paniceae).

We used PCA to visualize if certain traits were associated with grass life history, photosynthetic pathway, and tribe. Trait values were averaged across the five replicates for each species. We removed eight species with poor A- $\text{C}_i$  curves and four species that were the only species within the tribe. We did not include traits that were highly correlated with one another ( $R^2 > 0.80$ ) in the PCA analysis. Data were log transformed and standardized to linearize relationships among traits and ensure each variable held equal weight in the analysis. We used a permutational multivariate ANOVA to assess the amount of trait variation explained by life history, photosynthetic pathway, and tribe using the adonis function in the ‘vegan’ package (Oksanen *et al.*, 2020) within R.

## Results

### Principal Component Analysis

PC1 and PC2 explained 33.54% and 18.13% of the variation in PFTs, respectively (Fig. 2.2). Life history tended to divide along PC1 and species tended to cluster by tribe. Similar to the results above, leaf structural traits tended to correlate with life history. For example, leaf structural traits such as LDMC and C:N were highly correlated and associated with perennial C<sub>4</sub> grasses, while high SLA was associated with annual species, which tend to grow fast and have high leaf N content. Tribe explained the most variation among traits ( $R^2 = 0.288$ ) followed by life history and photosynthetic type ( $R^2 = 0.081$  and  $0.075$ , respectively).

### Plant Structural Traits

Significant differences in maximum flowering and vegetative heights were found among tribe, life history, and C<sub>4</sub> lineage ( $P < 0.003$ ), but not photosynthetic pathway (Table 2.3). Perennials were taller than annuals (Table 2.4). For both maximum flowering and vegetative heights, Andropogoneae was the tallest tribe ( $117.6 \pm 6.8$  cm and  $92.6 \pm 6.3$  cm, respectively) and Eragrostideae was the shortest ( $28.1 \pm 3.1$  cm and  $21.0 \pm 1.8$  cm, respectively; Fig. 2.3a,b). Within the C<sub>4</sub> lineages, for both maximum flowering and vegetative heights, Andropogoneae was the tallest ( $117.6 \pm 6.8$  cm and  $92.6 \pm 6.3$  cm, respectively) and *Aristida* was the shortest ( $40.9 \pm 2.9$  cm and  $24.2 \pm 0.7$  cm, respectively; Fig. 2.4a,b).

### Leaf Structural Traits

All differences in leaf structural traits (SLA, LDMC, C:N, and leaf thickness) measured in this study showed significant differences between tribes and life histories, and some differences were found within C<sub>4</sub> lineages. Only one leaf structural trait (leaf C:N) differed by photosynthetic pathway.

SLA significantly differed among tribes and life histories ( $P < 0.001$ ; Table 2.3). On average, annuals had significantly higher SLA than perennials (Table 2.4). Among the tribes, there was large variation in SLA; Stipeae had the lowest SLA ( $87.6 \pm 5.6 \text{ cm}^2 \text{ g}^{-1}$ ) and Oryzeae had the highest SLA ( $451.9 \pm 49.7 \text{ cm}^2 \text{ g}^{-1}$ ; Fig. 2.3c).

Significant differences in leaf dry matter content (LDMC) were found among tribes, life histories, and  $C_4$  lineages ( $P < 0.001$ ; Table 2.3). On average, perennials had higher LDMC than annuals (Table 2.4). Values differed greatly among tribes; Paspaleae had the lowest LDMC ( $0.230 \pm 0.014$ ) and Zoysieae had the highest LDMC ( $0.424 \pm 0.011$ ; Fig. 2.3d). There was also large variation among  $C_4$  lineages; *Aristida* had the highest LDMC ( $0.397 \pm 0.009$ ) and *Echinochloa* had the lowest LDMC ( $0.227 \pm 0.012$ ; Fig. 2.4c). We found that weak interactions were present for LDMC ( $P = 0.03$ ; Table 2.5).

Significant differences in leaf carbon to nitrogen ratios (C:N) existed among tribes, photosynthetic pathways ( $P < 0.001$ ), and life histories ( $P = 0.015$ ), but not  $C_4$  lineages (Table 2.3). On average,  $C_4$  grasses had higher C:N than  $C_3$  grasses and perennials had higher C:N than annuals (Table 2.4). Among the tribes there was large variation of C:N; Zoysieae had the highest C:N ( $40.47 \pm 1.94$ ) and Diarrheneae had the lowest ( $15.47 \pm 0.86$ ; Fig. 2.3e).

Significant variation in leaf thickness was found among tribes ( $P = 0.008$ ) and life histories ( $P = 0.017$ ), but not photosynthetic pathways or  $C_4$  lineages. On average, leaves from perennial species were thicker than leaves from annual species. Among the tribes, Stipeae had the thickest leaves ( $0.357 \pm 0.027 \text{ mm}$ ) and Oryzeae had the thinnest leaves ( $0.071 \pm 0.007 \text{ mm}$ ; Fig. 2.3f).

## Leaf Physiological Traits

Multiple physiological traits (osmotic potential,  $V_{c_{max}}$ , and  $\delta^{13}C$ ), showed significant differences between tribe and photosynthetic pathway. Two physiological traits (osmotic potential and  $\delta^{13}C$ ) significantly differed according to their  $C_4$  lineage, while only one physiological trait (osmotic potential) differed by life history.

Osmotic potential significantly differed by tribe, life history,  $C_4$  lineage ( $P < 0.001$ ), and photosynthetic pathway ( $P = 0.034$ ; Table 2.3). Osmotic potential varied greatly among tribes, where Diarrheneae had the lowest osmotic potential (mean  $\pm$  SE,  $-2.09 \pm 0.09$  MPa), and Paniceae had the highest osmotic potential ( $-1.09 \pm 0.04$  MPa; Fig. 2.3g). On average,  $C_3$  grasses had significantly lower osmotic potentials than  $C_4$  grasses and perennials had significantly lower osmotic potentials than annuals (Table 2.4). Among the  $C_4$  lineages, *Aristida* had the lowest osmotic potential ( $-1.68 \pm 0.12$  MPa) and *Digitaria* had the highest osmotic potential ( $-0.95 \pm 0.02$  MPa; Fig. 2.4e).

$V_{c_{max}}$  was significantly different among tribes ( $P = 0.001$ ) and photosynthetic pathways ( $P < 0.001$ ), but not life history or  $C_4$  lineage (Table 2.3).  $C_3$  grasses had significantly higher  $V_{c_{max}}$  than  $C_4$  grasses (Table 2.4), where Poeae ( $C_3$ ) had the highest  $V_{c_{max}}$  ( $78.15 \pm 7.12$   $\mu\text{mol m}^{-2} \text{s}^{-1}$ ) and Andropogoneae ( $C_4$ ) had the lowest  $V_{c_{max}}$  ( $24.78 \pm 4.37$   $\mu\text{mol m}^{-2} \text{s}^{-1}$ ; Fig. 2.3h). We found that weak interactions were present for  $V_{c_{max}}$  ( $P = 0.02$ ; Table 2.5). No factor significantly affected  $J_{max}$  and  $V_{p_{max}}$ .

We analyzed  $\delta^{13}C$  separately for  $C_3$  and  $C_4$  species due to known differences in  $\delta^{13}C$  between both photosynthetic pathways (Table 2.4).  $\delta^{13}C$  showed significant differences by tribe for  $C_3$  ( $P = 0.018$ ) and  $C_4$  ( $P < 0.001$ ) grasses (Table 2.6). Among  $C_3$  grasses, Diarrheneae had the lowest  $\delta^{13}C$  ( $-31.27 \pm 0.28\text{‰}$ ) and Paniceae had the highest  $\delta^{13}C$  ( $-28.23 \pm 0.14\text{‰}$ ; Fig. 2.3i).

Among C<sub>4</sub> grasses, Cynodonteae had the lowest  $\delta^{13}\text{C}$  ( $-14.21 \pm 0.10\text{‰}$ ) and Paniceae had the highest  $\delta^{13}\text{C}$  ( $-12.65 \pm 0.08\text{‰}$ ; Fig. 2.3j).  $\delta^{13}\text{C}$  also significantly differed by C<sub>4</sub> lineages ( $P < 0.001$ ; Fig. 2.4d); Chloridoideae had the lowest  $\delta^{13}\text{C}$  ( $-14.01 \pm 0.08\text{‰}$ ) and *Digitaria* had the highest  $\delta^{13}\text{C}$  values ( $-12.34 \pm 0.10\text{‰}$ ).

In addition to C<sub>4</sub> lineage, we found significant differences in  $\delta^{13}\text{C}$  by C<sub>4</sub> subtype (PCK, NAD-ME, and NADP-ME;  $P < 0.001$ ; Table 2.7). PCK species had the lowest  $\delta^{13}\text{C}$  ( $-13.99 \pm 0.17\text{‰}$ ), a similar value to that of NAD-ME species ( $-13.84 \pm 0.09\text{‰}$ ). NADP-ME species had the highest  $\delta^{13}\text{C}$  ( $-12.70 \pm 0.06\text{‰}$ ). *Bouteloua curtipendula*, a mixed NAD-ME/PCK species (Gutierrez *et al.*, 1974), had a  $\delta^{13}\text{C}$  value of  $-13.96 \pm 0.11\text{‰}$ . Lastly, the three *Sporobolus* species (*Sporobolus compositus*, *Sporobolus heterolepis*, and *Sporobolus vaginiflorus*) had an average  $\delta^{13}\text{C}$  of  $-13.59 \pm 0.11\text{‰}$ . It is not currently known whether these three species utilize NAD-ME or PCK pathways.

## Discussion

### Evolutionary lineage captures the most differences in trait variation

In this study, we measured a suite of traits from 75 species of grasses and assessed if traits differed among lineages, life histories, and photosynthetic pathways to determine which factor captures the most differences in trait variation. Our results show that a naturally-occurring suite of grass species within a single grassland has a comparable degree of variability in trait responses as has been typically reported at regional scales (Yang *et al.*, 2019; Dong *et al.*, 2020). This variability was better explained by evolutionary lineage (grasses grouped by taxonomy) than either life history (annual/perennial) or photosynthetic type (C<sub>3</sub>/C<sub>4</sub>) and grouping species by photosynthetic type oversimplifies this community and misses important variation required for more precise predictions from grassland ecosystem models (Griffith *et al.*, 2020).

Most of the traits explained by photosynthetic type were physiological traits. Photosynthetic type did not explain any differences found in structural traits except for C:N. Structural traits are commonly measured in plant surveys to draw inference on plant growth strategies and physiology at large scales (Wright *et al.*, 2004; Reich, 2014). Our results show these structural traits do not significantly vary by photosynthetic type in this grassland despite known growth advantages of the C<sub>4</sub> photosynthetic pathway in hot environments (Atkinson *et al.*, 2016; Simpson *et al.*, 2020). Therefore, grouping grasses by lineage or life history performed better than grouping by photosynthetic type to capture differences in structural traits.

However, grouping grasses by life history presents similar issues as photosynthetic type because life history tends to explain much more variation in structural traits than physiological traits, similar to how grouping by PFT explains a large amount of variation in strictly physiological traits (Liu *et al.*, 2019). This phenomenon is expected, because whether a plant is annual or perennial dictates the economics of resource usage and investment strategies into plant tissue growth (Adler *et al.*, 2014). For instance, the species we measured in Andropogoneae, a globally dominant tribe in high precipitation, fire-prone grassy ecosystems, were all C<sub>4</sub> perennial species with lower SLA and higher LDMC and C:N than other tribes. Slower growing, perennial species tend to allocate greater resources towards non-photosynthesizing tissues, trading off maximizing photosynthesis for expensive, more durable leaves and stems, along with a high investment in the root system for acquiring water, nutrients, and prolonging life span (Grime, 1977; Monaco *et al.*, 2003; Reich, 2014). In contrast, we found that less dominant tribes with mostly annual species, such as Paniceae, are shorter, with higher SLA, thinner leaves, lower LDMC, and lower leaf C:N. These fast-growing annual species allocate most resources towards producing thin, broad leaves to quickly maximize photosynthesis, investing energy into

reproductive tissue prior to senescence (Grime, 1977; Garnier & Laurent, 1994; Garnier *et al.*, 1997; Reich, 2014). While life history was a good predictor of structural traits, these grasslands are dominated by perennial species, which make up 68% of Poaceae species on KPBS (Taylor *et al.*, unpublished). Grouping grasses solely by life history undoubtedly overlooks important physiological traits within a life history type.

However, these general trends related to life history and photosynthetic type are not always present. One tribe that directly contrasts common trends for perennial grasses is Oryzae, which in our study included two perennial, C<sub>3</sub> species. These two grasses (*Leersia virginica* and *Leersia oryzoides*) exhibited characteristics typical of annual species. In fact, out of all 14 tribes, Oryzae had the highest average SLA and the thinnest leaves, with relatively average LDMC and leaf C:N. This outlier may seem strange until lineage is considered. Both species share the same genus and occupy similar niches in the tallgrass ecosystem: they are rhizomatous species that grow near streams and within wet areas (Darris & Bartow, 2004; Ritz, 2012) and bloom later in the season than almost any other C<sub>3</sub> grass species at KPBS (Taylor *et al.*, unpublished). It may not be as important for these species to invest heavily into expensive stem or leaf tissues since they occupy entirely different habitats than dominant species on KPBS. The unusual nature of Oryzae demonstrates the problems associated with PFT groupings of grasses; the tribe's trait variation is much better represented when grouped by lineage.

### **Trait variation within the C<sub>4</sub> photosynthetic pathway**

Beyond analyzing trait variation solely from different tribes, we also analyzed how traits differed in unique lineages of the C<sub>4</sub> photosynthetic pathway. We found that C<sub>4</sub> lineages explained variation for nearly half the traits we measured. When all C<sub>4</sub> species are grouped into a singular PFT, this variation is inherently overlooked, adding further evidence to the benefits of

grouping species by evolutionary lineage. Focusing on the two dominant lineages of C<sub>4</sub> grasses in North America (Andropogoneae and Chloridoideae) highlights this point, as the Andropogoneae lineage evolved to occupy wetter environments than the arid-specializing Chloridoideae (Lehmann *et al.*, 2019). Andropogoneae were taller and had higher average  $\delta^{13}\text{C}$  and osmotic potential, which may reflect differences in water use strategies among C<sub>4</sub> plants. Systematic differences in  $\delta^{13}\text{C}$  within C<sub>4</sub> plants (a novel finding not previously reported) seem to be associated with water use differences among photosynthetic subtypes and are of sufficient magnitude to be considered when choosing endmembers in isotope studies. These trait differences suggest grouping grasses by photosynthetic type likely overlooks large differences in ecosystem water and carbon cycling among C<sub>4</sub> plants (Liu & Osborne, 2015). These differences may reflect differences in photosynthetic subtype between Chloridoideae (primarily NAD-ME) and Andropogoneae (NADP-ME) that is better captured when grouping grasses by lineage (Liu & Osborne, 2015; Griffith *et al.*, 2020).

### **PFTs, lineages, and grassland ecosystem modelling**

Our results are consistent with other studies (Taylor *et al.*, 2010; Liu *et al.*, 2012; Griffith *et al.*, 2020) which demonstrate the importance of incorporating phylogenetic history into trait comparison analyses. Grouping grasses by lineage will allow LSMs to account for the evolutionary histories of species, where important functional traits may be conserved (Edwards *et al.*, 2007; Liu *et al.*, 2012; Coelho de Souza *et al.*, 2016). LFTs are a valid approach because lineage explains variation in both physiological and structural traits. This eliminates problems with grouping species into PFTs or based on life histories; each approach only explains variation in physiological or structural traits, respectively. However, we do acknowledge that accounting for a vast number of tribes in modelling analyses may be impractical, especially when some

tribes only consist of one or two species that may not be ecologically important at the ecosystem level. Rather, it might be better to account for lineage-based trait variation at a higher taxonomic level, such as subfamily, or to only include lineages for dominant species. For instance, LFTs in Griffith *et al.*, (2020) are structured based on the globally dominant lineages of C<sub>3</sub> and C<sub>4</sub> grasses. The large variation of traits observed among different lineages in this study further validates the call to move away from PFTs and incorporate lineage-based functional types (LFTs) into ecosystem models.

Additionally, it is important to note that we were able to see these differences in trait variation among tribes from species growing in the same local environment within a relatively small site. Despite all these species possessing traits to survive in the tallgrass prairie, evolutionary history still played a significant role as the main predictor of trait variation. If species were sampled across different regions or environments, we might expect to see even more distinct trait variation among lineages. Regarding their impacts on ecosystem models, the differences in traits among lineages shown in this study are likely conservative because differences in traits were found among lineages occurring in the same environment. Further work comparing the traits of grass species globally is warranted to more accurately determine how traits vary among lineages.

## **Conclusions**

We found that evolutionary lineage best represented trait variation among the 75 species of grasses we measured. While life history and photosynthetic pathway also explained variation among traits, they explained less variation and mostly explained only structural traits or physiological traits, respectively. We conclude that grouping grasses by lineage represents a better method of organizing species in vegetative models to account for trait diversity. This

strategy will hopefully improve how grass diversity is represented in LSMs and increase accuracy in making predictions of how grassland ecosystems will change in the future.

## References

**Adler PB, Salguero-Gómez R, Compagnoni A, Hsu JS, Ray-Mukherjee J, Mbeau-Ache C, Franco M. 2014.** Functional traits explain variation in plant life history strategies. *Proceedings of the National Academy of Sciences* **111**: 740–745.

**Anderegg LDL, Griffith DM, Cavender-Bares J, Riley WJ, Berry JA, Dawson TE, Still CJ. 2022.** Representing plant diversity in land models: an evolutionary approach to make “Functional Types” more functional. *Global Change Biology* **28**: 2541–2554.

**Anderson CJR, Rosas-Anderson PJ. 2017.** Leafscan (Version 1.3.21). [Mobile application software]. Retrieved from leafscanapp.com.

**Asner GP, Elmore AJ, Olander LP, Martin RE, Harris AT. 2004.** Grazing systems, ecosystem responses, and global change. *Annual Review of Environment and Resources* **29**: 261–299.

**Atkinson RRL, Mockford EJ, Bennett C, Christin P-A, Spriggs EL, Freckleton RP, Thompson K, Rees M, Osborne CP. 2016.** C<sub>4</sub> photosynthesis boosts growth by altering physiology, allocation and size. *Nature Plants* **2**: 16038.

**Bartlett MK, Scoffoni C, Ardy R, Zhang Y, Sun S, Cao K, Sack L. 2012a.** Rapid determination of comparative drought tolerance traits: using an osmometer to predict turgor loss point. *Methods in Ecology and Evolution* **3**: 880–888.

**Bartlett MK, Scoffoni C, Sack L. 2012b.** The determinants of leaf turgor loss point and prediction of drought tolerance of species and biomes: a global meta-analysis. *Ecology Letters* **15**: 393–405.

- Bates D, Mächler M, Bolker B, Walker S. 2015.** Fitting linear mixed-effects models using **lme4**. *Journal of Statistical Software* **67**.
- Cadotte MW, Davies TJ, Peres-Neto PR. 2017.** Why phylogenies do not always predict ecological differences. *Ecological Monographs* **87**: 535–551.
- Catalán P, Torrecilla P, López-Rodríguez J, Müller J, Stace C. 2007.** A systematic approach to subtribe Loliinae (Poaceae: Pooideae) based on phylogenetic evidence. *Aliso* **23**: 380–405.
- Christenhusz MJM, Byng JW. 2016.** The number of known plants species in the world and its annual increase. *Phytotaxa* **261**: 201.
- Coelho de Souza F, Dexter KG, Phillips OL, Brienen RJW, Chave J, Galbraith DR, Lopez Gonzalez G, Monteagudo Mendoza A, Pennington RT, Poorter L, et al. 2016.** Evolutionary heritage influences Amazon tree ecology. *Proceedings of the Royal Society B: Biological Sciences* **283**: 20161587.
- Crisp MD, Arroyo MTK, Cook LG, Gandolfo MA, Jordan GJ, McGlone MS, Weston PH, Westoby M, Wilf P, Linder HP. 2009.** Phylogenetic biome conservatism on a global scale. *Nature* **458**: 754–756.
- Darris D, Bartow A. 2004.** Plant Fact Sheet for rice cutgrass (*Leersia oryzoides*). USDA Natural Resources Conservation Service, Plant Materials Center, Corvallis, OR.
- Dong N, Prentice IC, Wright IJ, Evans BJ, Togashi HF, Caddy-Retalic S, McInerney FA, Sparrow B, Leitch E, Lowe AJ. 2020.** Components of leaf-trait variation along environmental gradients. *New Phytologist* **228**: 82–94.
- Duursma RA. 2015.** Plantecophys - an R package for analysing and modelling leaf gas exchange data. *PLoS ONE* **10**: e0143346.

- Edwards EJ, Still CJ, Donoghue MJ. 2007.** The relevance of phylogeny to studies of global change. *Trends in Ecology & Evolution* **22**: 243–249.
- Edwards EJ, Smith SA. 2010.** Phylogenetic analyses reveal the shady history of C<sub>4</sub> grasses. *Proceedings of the National Academy of Sciences* **107**: 2532–2537.
- Edwards EJ, Osborne CP, Strömberg CAE, Smith SA, C Grasses Consortium, Bond WJ, Christin P-A, Cousins AB, Duvall MR, Fox DL, et al. 2010.** The origins of C<sub>4</sub> grasslands: integrating evolutionary and ecosystem science. *Science* **328**: 587–591.
- Ehleringer JR, Cerling TE, Helliker BR. 1997.** C<sub>4</sub> photosynthesis, atmospheric CO<sub>2</sub>, and climate. *Oecologia* **112**: 285–299.
- Garnier E, Laurent G. 1994.** Leaf anatomy, specific mass and water content in congeneric annual and perennial grass species. *New Phytologist* **128**: 725–736.
- Garnier E, Cordonnier P, Guillerm J-L, Sonié L. 1997.** Specific leaf area and leaf nitrogen concentration in annual and perennial grass species growing in Mediterranean old-fields. *Oecologia* **111**: 490–498.
- Grass Phylogeny Working Group II. 2012.** New grass phylogeny resolves deep evolutionary relationships and discovers C<sub>4</sub> origins. *New Phytologist* **193**: 304–312.
- Griffin-Nolan RJ, Ocheltree TW, Mueller KE, Blumenthal DM, Kray JA, Knapp AK. 2019.** Extending the osmometer method for assessing drought tolerance in herbaceous species. *Oecologia* **189**: 353–363.
- Griffith DM, Osborne CP, Edwards EJ, Bachle S, Beerling DJ, Bond WJ, Gallaher TJ, Helliker BR, Lehmann CER, Leatherman L, et al. 2020.** Lineage-based functional types: characterising functional diversity to enhance the representation of ecological behaviour in Land Surface Models. *New Phytologist* **228**: 15–23.

**Grime JP. 1977.** Evidence for the existence of three primary strategies in plants and its relevance to ecological and evolutionary theory. *The American Naturalist* **111**: 1169–1194.

**Gutierrez M, Gracen VE, Edwards GE. 1974.** Biochemical and cytological relationships in C<sub>4</sub> plants. *Planta* **119**: 279–300.

**Kellogg E. 1999.** Growth responses of C<sub>4</sub> grasses of contrasting origin to elevated CO<sub>2</sub>. *Annals of Botany* **84**: 279–288.

**Lehmann CE, Griffith DM, Simpson KJ, Anderson TM, Archibald S, Beerling DJ, Bond WJ, Denton E, Edwards EJ, Forrestel EJ et al. 2019.** Functional diversification enabled grassy biomes to fill global climate space. *BioRxiv*: 583625.

**Liu H, Edwards EJ, Freckleton RP, Osborne CP. 2012.** Phylogenetic niche conservatism in C<sub>4</sub> grasses. *Oecologia* **170**: 835–845.

**Liu H, Osborne CP. 2015.** Water relations traits of C<sub>4</sub> grasses depend on phylogenetic lineage, photosynthetic pathway, and habitat water availability. *Journal of Experimental Botany* **66**: 761–773.

**Liu H, Taylor SH, Xu Q, Lin Y, Hou H, Wu G, Ye Q. 2019.** Life history is a key factor explaining functional trait diversity among subtropical grasses, and its influence differs between C<sub>3</sub> and C<sub>4</sub> species. *Journal of Experimental Botany* **70**: 1567–1580.

**Monaco TA, Johnson DA, Norton JM, Jones TA, Connors KJ, Norton JB, Redinbaugh MB. 2003.** Contrasting responses of intermountain west grasses to soil nitrogen. *Journal of Range Management* **56**: 282.

**Oksanen JF, Blanchet G, Friendly M, Kindt R, Legendre P, McGlinn D, Minchin PR, O'Hara RB, Simpson GL, Solymos P, et al. 2020.** vegan: community ecology package. R package version 2.5-7.

**Osborne CP, Salomaa A, Kluyver TA, Visser V, Kellogg EA, Morrone O, Vorontsova MS, Clayton WD, Simpson DA. 2014.** A global database of C<sub>4</sub> photosynthesis in grasses. *New Phytologist* **204**: 441–446.

**Paradis E, Schliep K. 2019.** ape 5.0: an environment for modern phylogenetics and evolutionary analyses in R. *Bioinformatics* **35**: 526–528.

**Peterson PM, Romaschenko K, Arrieta YH. 2015.** A molecular phylogeny and classification of the Eleusininae with a new genus, *Micrachne* (Poaceae: Chloridoideae: Cynodonteae). *Taxon* **64**: 445–467.

**R Core Team. 2021.** R: A language and environment for statistical computing. R Foundation for Statistical Computing, Vienna, Austria.

**Reich PB. 2014.** The world-wide ‘fast-slow’ plant economics spectrum: a traits manifesto. *Journal of Ecology* **102**: 275–301.

**Ritz SE. 2012.** Plant guide for whitegrass (*Leersia virginica*). USDA Natural Resources Conservation Service, Appalachian Plant Materials Center, Alderson, WV.

**Sage RF, Monson RK, Ehleringer JR, Adachi S, Percy RW. 2018.** Some like it hot: the physiological ecology of C<sub>4</sub> plant evolution. *Oecologia* **187**: 941–966.

**Scurlock JMO, Hall DO. 1998.** The global carbon sink: a grassland perspective. *Global Change Biology* **4**: 229–233.

**Simpson KJ, Bennett C, Atkinson RRL, Mockford EJ, McKenzie S, Freckleton RP, Thompson K, Rees M, Osborne CP. 2020.** C<sub>4</sub> photosynthesis and the economic spectra of leaf and root traits independently influence growth rates in grasses. *Journal of Ecology* **108**: 1899–1909.

- Skendzic E, Columbus T, Cerros-Tlatilpa R. 2007.** Phylogenetics of Andropogoneae (Poaceae: Panicoideae) based on nuclear ribosomal internal transcribed spacer and chloroplast trnL–F sequences. *Aliso* **23**: 530–544.
- Soreng RJ, Peterson PM, Romaschenko K, Davidse G, Teisher JK, Clark LG, Barberá P, Gillespie LJ, Zuloaga FO. 2017.** A worldwide phylogenetic classification of the Poaceae (Gramineae) II: an update and a comparison of two 2015 classifications. *Journal of Systematics and Evolution* **55**: 259–290.
- Still CJ, Berry JA, Collatz GJ, DeFries RS. 2003.** Global distribution of C<sub>3</sub> and C<sub>4</sub> vegetation: carbon cycle implications. *Global Biogeochemical Cycles* **17**: 6-1-6–14.
- Taylor SH, Hulme SP, Rees M, Ripley BS, Ian Woodward F, Osborne CP. 2010.** Ecophysiological traits in C<sub>3</sub> and C<sub>4</sub> grasses: a phylogenetically controlled screening experiment. *New Phytologist* **185**: 780–791.
- Taylor JH, Breckon GJ, Mayfield MH. 2021.** An annotated checklist of the vascular flora of Konza Prairie Biological Station. Unpublished manuscript.
- Vile D, Garnier É, Shipley B, Laurent G, Navas M-L, Roumet C, Lavorel S, Díaz S, Hodgson JG, Lloret F, et al. 2005.** Specific leaf area and dry matter content estimate thickness in laminar leaves. *Annals of Botany* **96**: 1129–1136.
- Woodward FI, Cramer W. 1996.** Plant functional types and climatic change: introduction. *Journal of Vegetation Science* **7**: 306–308.
- Wright IJ, Reich PB, Westoby M, Ackerly DD, Baruch Z, Bongers F, Cavender-Bares J, Chapin T, Cornelissen JHC, Diemer M, et al. 2004.** The worldwide leaf economics spectrum. *Nature* **428**: 821–827.

**Yang Y, Wang H, Harrison SP, Prentice IC, Wright IJ, Peng C, Lin G. 2019.** Quantifying leaf-trait covariation and its controls across climates and biomes. *New Phytologist* **221**: 155–168.

**Zhou H, Helliker BR, Huber M, Dicks A, Akçay E. 2018.** C<sub>4</sub> photosynthesis and climate through the lens of optimality. *Proceedings of the National Academy of Sciences* **115**: 12057–12062.

**Zhou H, Akçay E, Helliker BR. 2019.** Estimating C<sub>4</sub> photosynthesis parameters by fitting intensive A/C<sub>i</sub> curves. *Photosynthesis Research* **141**: 181–194.

## Tables and Figures

**Table 2.1: A list of the 75 species sampled in the study.**

Tribe	Photosynthetic Type	Life History	Species
Andropogoneae	C <sub>4</sub>	Perennial	<i>Andropogon gerardii</i> <i>Andropogon virginicus</i> <i>Bothriocloa bladhii</i> <i>Bothriochloa ischaemum</i> <i>Bothriochloa laguroides</i> <i>Schizachyrium scoparium</i> <i>Sorghastrum nutans</i> <i>Sorghum halepense</i> <i>Tripsacum dactyloides</i>
Aristidae	C <sub>4</sub>	Annual	<i>Aristida oligantha</i>
Bromeae	C <sub>3</sub>	Annual	<i>Bromus japonicus</i> <i>Bromus tectorum</i>
		Perennial	<i>Bromus inermis</i> <i>Bromus pubescens</i>
Cynodonteae	C <sub>4</sub>	Annual	<i>Eleusine indica</i> <i>Leptochloa fusca</i>
		Perennial	<i>Bouteloua curtipendula</i> <i>Bouteloua dactyloides</i> <i>Bouteloua gracilis</i> <i>Bouteloua hirsuta</i> <i>Chloris verticillata</i> <i>Muhlenbergia bushii</i> <i>Muhlenbergia cuspidata</i> <i>Muhlenbergia frondosa</i> <i>Muhlenbergia schreberi</i> <i>Schedonnardus paniculatus</i> <i>Tridens flavus</i>
Diarrheneae	C <sub>3</sub>	Perennial	<i>Diarrhena obovata</i>
Eragrostideae	C <sub>4</sub>	Annual	<i>Eragrostis cilianensis</i> <i>Eragrostis pectinacea</i>
		Perennial	<i>Eragrostis spectabilis</i>
Meliceae	C <sub>3</sub>	Perennial	<i>Glyceria striata</i>
Oryzeae	C <sub>3</sub>	Perennial	<i>Leersia oryzoides</i> <i>Leersia virginica</i>

Paniceae	C <sub>3</sub>	Perennial	<i>Dichantherium linearifolium</i> <i>Dichantherium oligosanthes</i> <i>Dichantherium praecocius</i>
	C <sub>4</sub>	Annual	<i>Cenchrus longispinus</i> <i>Digitaria ciliaris</i> <i>Digitaria ischaemum</i> <i>Echinochloa crus-galli</i> <i>Echinochloa muricata</i> <i>Eriochloa contracta</i> <i>Panicum capillare</i> <i>Panicum dichotomiflorum</i> <i>Setaria pumila</i> <i>Setaria viridis</i>
		Perennial	<i>Digitaria cognata</i> <i>Panicum virgatum</i>
Paspaleae	C <sub>4</sub>	Perennial	<i>Hopia obtusa</i> <i>Paspalum pubiflorum</i> <i>Paspalum setaceum</i>
Poeae	C <sub>3</sub>	Annual	<i>Alopecurus carolinianus</i> <i>Vulpia octoflora</i>
		Perennial	<i>Agrostis gigantea</i> <i>Agrostis hyemalis</i> <i>Dactylis glomerata</i> <i>Koeleria macrantha</i> <i>Lolium perenne</i> <i>Phalaris arundinacea</i> <i>Poa compressa</i> <i>Poa pratensis</i> <i>Schedonorus arundinaceus</i> <i>Sphenopholis obtusata</i>
Stipeae	C <sub>3</sub>	Perennial	<i>Hesperostipa spartea</i>
Triticeae	C <sub>3</sub>	Annual	<i>Aegilops cylindrica</i> <i>Hordeum pusillum</i>
		Perennial	<i>Elymus canadensis</i> <i>Elymus villosus</i> <i>Elymus virginicus</i> <i>Pascopyrum smithii</i>
Zoysieae	C <sub>4</sub>	Annual	<i>Sporobolus vaginiflorus</i>
		Perennial	<i>Spartina pectinata</i> <i>Sporobolus compositus</i> <i>Sporobolus heterolepis</i>

**Table 2.2: A list of all traits measured in the study.**

Trait	Type
Maximum Flowering Height (cm)	Structural
Maximum Vegetative Height (cm)	
Specific Leaf Area (SLA; cm <sup>2</sup> g <sup>-1</sup> )	
Leaf Dry Matter Content (LDMC)	
Leaf Thickness (mm)	
C:N	
Osmotic Potential (MPa)	Physiological
δ <sup>13</sup> C (‰)	
V <sub>cmax</sub> (μmol m <sup>-2</sup> s <sup>-1</sup> )	
J <sub>max</sub> (μmol m <sup>-2</sup> s <sup>-1</sup> )	
V <sub>pmax</sub> (μmol m <sup>-2</sup> s <sup>-1</sup> )	

**Table 2.3:  $\chi^2$ , df, and  $P$ , of all trait comparisons between tribe, photosynthetic pathway, life history, and C<sub>4</sub> lineage.**

Trait	Tribe			Photosynthetic Pathway			Life History			C <sub>4</sub> Lineage		
	$\chi^2$	df	$P$	$\chi^2$	df	$P$	$\chi^2$	df	$P$	$\chi^2$	df	$P$
Maximum Flowering Height (cm)	35.40	13	<b>&lt;0.001</b>	0.004	1	0.948	10.03	1	<b>0.002</b>	21.38	6	<b>0.002</b>
Maximum Vegetative Height (cm)	31.93	13	<b>0.002</b>	0.06	1	0.801	10.26	1	<b>0.001</b>	19.81	6	<b>0.003</b>
Specific Leaf Area (SLA; cm <sup>2</sup> g <sup>-1</sup> )	34.75	13	<b>&lt;0.001</b>	0.009	1	0.924	16.46	1	<b>&lt;0.001</b>	11.57	6	0.072
Leaf Dry Matter Content (LDMC)	81.04	13	<b>&lt;0.001</b>	3.03	1	0.081	12.10	1	<b>&lt;0.001</b>	41.06	6	<b>&lt;0.001</b>
Leaf Thickness (mm)	28.46	13	<b>0.008</b>	0.52	1	0.473	5.68	1	<b>0.017</b>	3.19	6	0.785
C:N	40.30	13	<b>&lt;0.001</b>	14.51	1	<b>&lt;0.001</b>	5.91	1	<b>0.015</b>	9.29	6	0.158
Osmotic Potential (Mpa)	58.47	13	<b>&lt;0.001</b>	4.48	1	<b>0.034</b>	12.73	1	<b>&lt;0.001</b>	39.58	6	<b>&lt;0.001</b>
$\delta^{13}\text{C}$ (‰)	Data in Table 2.6			6706.7	1	<b>&lt;0.001</b>	2.57	1	0.109	83.37	6	<b>&lt;0.001</b>
V <sub>c</sub> <sub>max</sub> (μmol m <sup>-2</sup> s <sup>-1</sup> )	33.37	13	<b>0.001</b>	36.60	1	<b>&lt;0.001</b>	0.07	1	0.797	11.62	6	0.071
J <sub>max</sub> (μmol m <sup>-2</sup> s <sup>-1</sup> )	12.45	13	0.491	0.47	1	0.492	0.16	1	0.687	8.41	6	0.209
*V <sub>p</sub> <sub>max</sub> (μmol m <sup>-2</sup> s <sup>-1</sup> )	2.40	6	0.880	-	-	-	1.74	1	0.187	3.02	6	0.807

\*V<sub>p</sub><sub>max</sub>, the maximum rate of carboxylation of PEPC, is a C<sub>4</sub>-specific trait, so all analyses done with V<sub>p</sub><sub>max</sub> only include C<sub>4</sub> species. Bolding indicates  $P < 0.05$ .

**Table 2.4: Mean values for each trait comparing annuals to perennials and C<sub>3</sub> species to C<sub>4</sub> species. Error represents  $\pm 1$ SE. Bolding denotes  $P < 0.05$ , \* denotes  $0.01 < P < 0.05$ , \*\* denotes  $0.001 < P < 0.01$ , \*\*\* denotes  $P < 0.001$ .**

Trait	Annual	Perennial	C <sub>3</sub>	C <sub>4</sub>
Maximum Flowering Height	<b>42.0 <math>\pm</math> 2.2**</b>	<b>71.6 <math>\pm</math> 2.7**</b>	62.4 $\pm$ 2.7	63.2 $\pm$ 3.1
Maximum Vegetative Height	<b>32.5 <math>\pm</math> 1.7**</b>	<b>59.7 <math>\pm</math> 2.5**</b>	50.5 $\pm$ 2.3	52.7 $\pm$ 2.8
Specific Leaf Area (SLA)	<b>275.2 <math>\pm</math> 9.0***</b>	<b>198.0 <math>\pm</math> 6.4***</b>	218.4 $\pm$ 8.6	221.3 $\pm$ 7.2
Leaf Dry Matter Content (LDMC)	<b>0.279 <math>\pm</math> 0.007 ***</b>	<b>0.335 <math>\pm</math> 0.005***</b>	0.298 $\pm$ 0.005	0.332 $\pm$ 0.006
Leaf Thickness	<b>0.149 <math>\pm</math> .004*</b>	<b>0.189 <math>\pm</math> .005*</b>	0.189 $\pm$ 0.007	0.171 $\pm$ 0.004
C:N	<b>21.69 <math>\pm</math> 0.85*</b>	<b>26.63 <math>\pm</math> 0.60*</b>	<b>20.56 <math>\pm</math> 0.47***</b>	<b>28.21 <math>\pm</math> 0.71***</b>
Osmotic Potential	<b>-1.18 <math>\pm</math> 0.04***</b>	<b>-1.53 <math>\pm</math> 0.03***</b>	<b>-1.54 <math>\pm</math> 0.05*</b>	<b>-1.36 <math>\pm</math> 0.03*</b>
$\delta^{13}\text{C}$	-17.44 $\pm$ 0.72	-20.70 $\pm$ 0.49	<b>-29.68 <math>\pm</math> 0.10***</b>	<b>-13.32 <math>\pm</math> 0.06***</b>
V <sub>c</sub> <sub>max</sub>	51.72 $\pm$ 5.61	51.86 $\pm$ 3.41	<b>73.50 <math>\pm</math> 4.49***</b>	<b>37.27 <math>\pm</math> 2.72***</b>
J <sub>max</sub>	172.0 $\pm$ 10.7	165.9 $\pm$ 6.7	162.3 $\pm$ 9.4	171.4 $\pm$ 7.1
V <sub>p</sub> <sub>max</sub>	49.60 $\pm$ 4.95	41.12 $\pm$ 2.78	n/a	n/a

**Table 2.5:  $\chi^2$ , df, and P of the interaction between life history and tribe using type III ANOVA. Only tribes that had both annual and perennial species measured for each trait are included in these analyses. Bolding indicates  $P < 0.05$ .**

Trait	$\chi^2$	df	$P$
Maximum Flowering Height (cm)	8.56	6	0.200
Maximum Vegetative Height (cm)	8.94	6	0.177
Specific Leaf Area (SLA; cm <sup>2</sup> g <sup>-1</sup> )	6.03	6	0.420
Leaf Dry Matter Content (LDMC)	13.67	6	<b>0.034</b>
Leaf Thickness (mm)	3.48	6	0.747
C:N	11.23	6	0.081
Osmotic Potential (Mpa)	11.99	6	0.062
$\delta^{13}\text{C}$ (‰)	Data in Table 2.6		
$V_{c_{\max}}$ ( $\mu\text{mol m}^{-2} \text{s}^{-1}$ )	13.50	5	<b>0.020</b>
$J_{\max}$ ( $\mu\text{mol m}^{-2} \text{s}^{-1}$ )	10.35	5	0.066
* $V_{p_{\max}}$ ( $\mu\text{mol m}^{-2} \text{s}^{-1}$ )	0.46	2	0.795

\* $V_{p_{\max}}$ , the maximum rate of carboxylation of PEPc, is a C<sub>4</sub>-specific trait, so all analyses done with  $V_{p_{\max}}$  only include C<sub>4</sub> species.

**Table 2.6:  $\chi^2$ , df, and  $P$ , of  $\delta^{13}\text{C}$  comparisons between tribes with  $\text{C}_3$  members and  $\text{C}_4$  members, separately. We analyzed  $\delta^{13}\text{C}$  separately for  $\text{C}_3$  and  $\text{C}_4$  species due to known differences in  $\delta^{13}\text{C}$  between both photosynthetic pathways. Bolding indicates  $P < 0.05$ .**

	Tribe, $\text{C}_3$ Species Only			Tribe, $\text{C}_4$ Species Only		
	$\chi^2$	df	$P$	$\chi^2$	df	$P$
$\delta^{13}\text{C}$	16.88	7	<b>0.018</b>	77.27	6	<b>&lt;0.001</b>
Life History*Tribe	1.36	2	0.506	0.17	3	0.982

**Table 2.7:  $\chi^2$ , df, and  $P$  of  $\delta^{13}\text{C}$  comparisons between  $\text{C}_4$  subtypes. Under the “All Species” comparison, this places the three *Sporobolus* species (whose  $\text{C}_4$  subtype is currently unknown) and *Bouteloua curtipendula*, a mixed NAD-ME/PCK species, each in their own group. The second comparison only compares species definitively known to be in the PCK, NAD-ME, and NADP-ME groups. Bolding indicates  $P < 0.05$ .**

	All Species			Not Including <i>Sporobolus</i> or <i>Bouteloua curtipendula</i>		
	$\chi^2$	df	$P$	$\chi^2$	df	$P$
$\delta^{13}\text{C}$	40.52	4	<b>&lt;0.001</b>	37.09	2	<b>&lt;0.001</b>

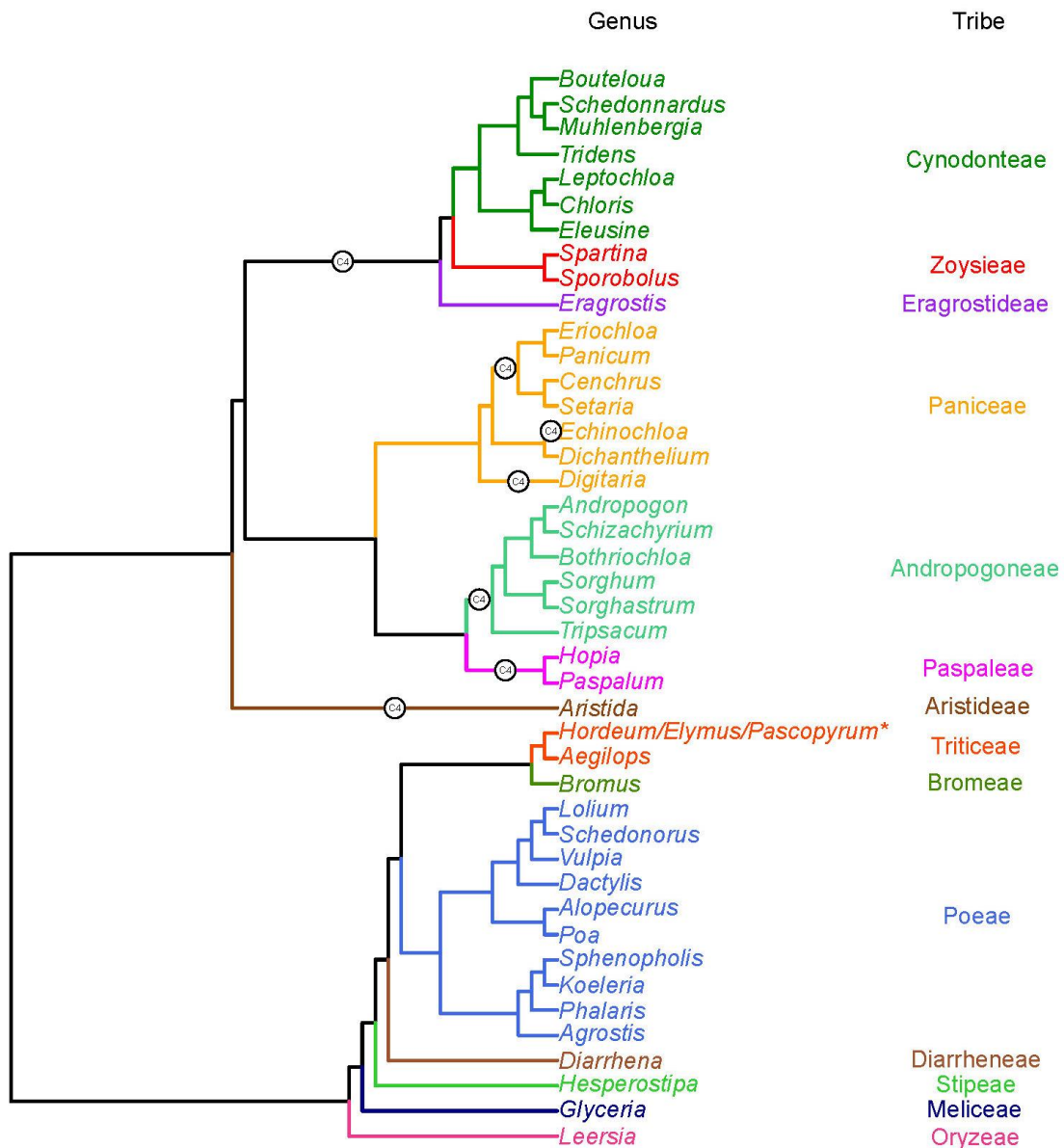


**Figure 2.1:** A cladogram of all the genera of Poaceae species sampled in our study. We drew the tree following Soreng *et al.*, (2017) for relationships among subtribes, Skendzic *et al.*, (2007) for the relationships among the Andropogoninae, Catalán *et al.*, (2007) for the relationships among the Loliinae, and Peterson *et al.*, (2015) for relationships among the Eleusininae. C<sub>4</sub> markings indicate independent evolution of the C<sub>4</sub> pathway in that lineage. The cladogram was created using the ‘ape’ package in R (Paradis & Schliep, 2019).

\*Due to the complicated phylogenetic history among the Triticeae, which involves multiple hybrid origins (R. J. Mason-Gamer, pers. comm), we have chosen to depict these three genera together on the same node.

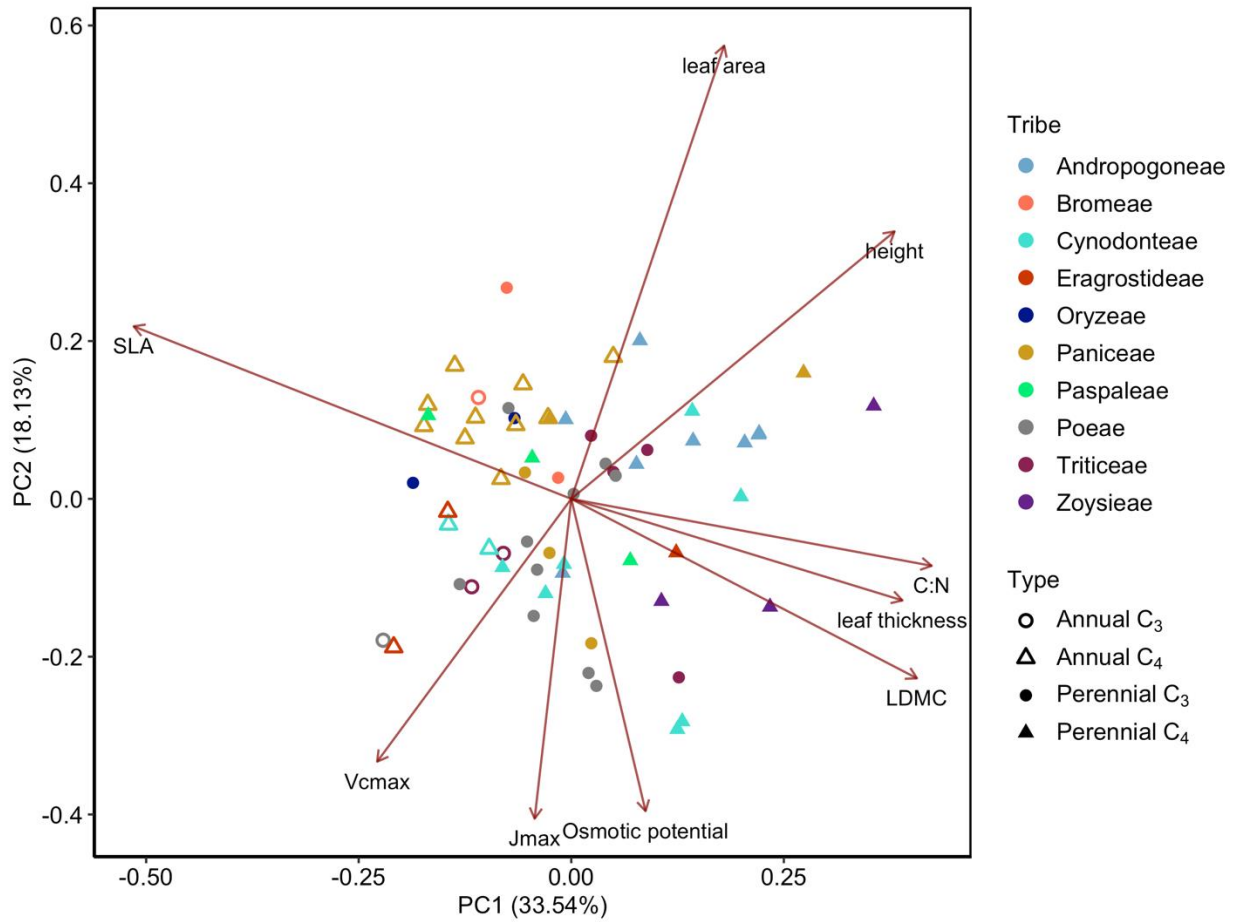


**Figure 2.2: PCA of 63 grass species and 9 functional traits sampled at KPBS. Points are classified by annual (open) and perennial (closed) and C<sub>3</sub> (circle) and C<sub>4</sub> (triangle). Colors represent grass tribes.**

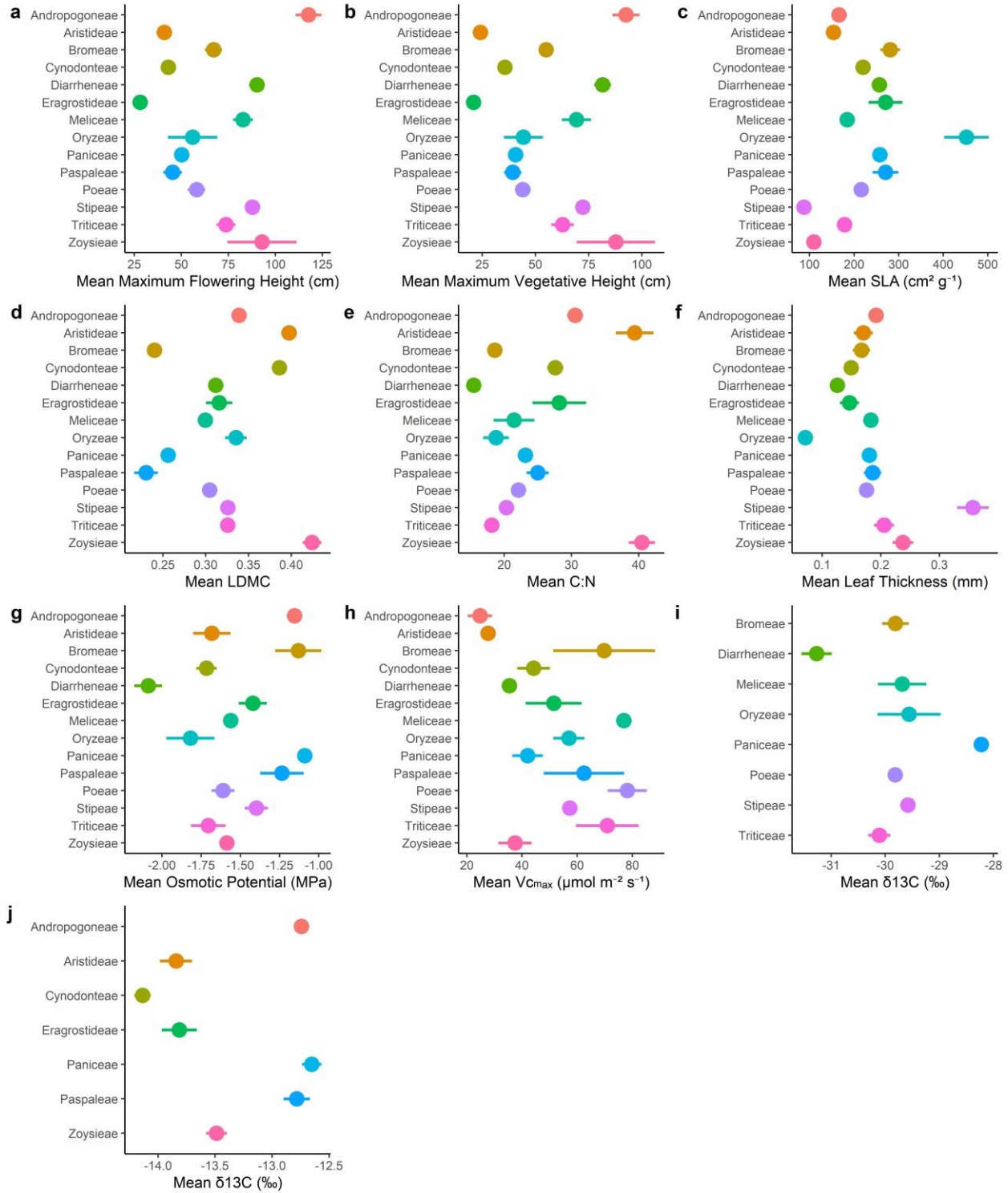


**Figure 2.3: Mean values of each trait that significantly differed by tribe. Error bars represent  $\pm 1$  SE.**

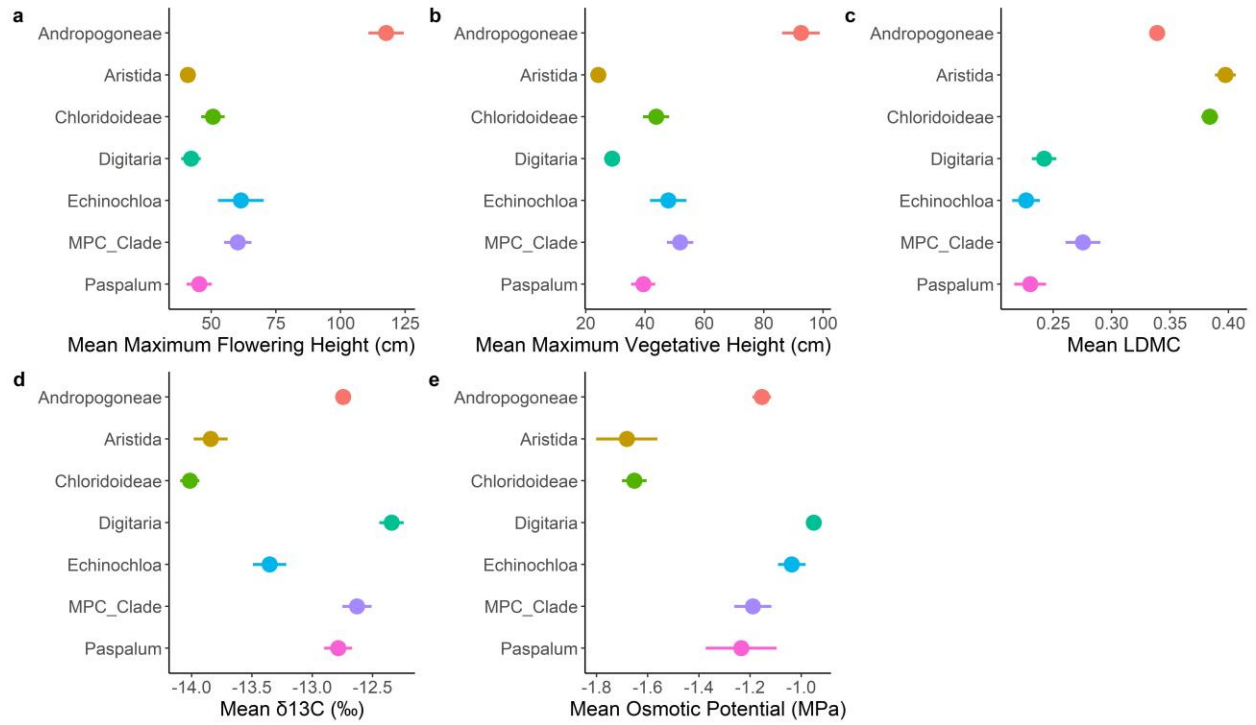


**Figure 2.4: Mean values for each trait that significantly differed by C<sub>4</sub> lineage. Error bars represent  $\pm 1SE$ . Each of these lineages represents an independent origin of C<sub>4</sub> photosynthesis (Fig. 2.1).**

# **Chapter 3 - Temporal and spatial trait variation of two Panicoid grasses: *Dichanthelium oligosanthos* subsp. *scribnerianum* and *Panicum virgatum***

## **Introduction**

Plant traits are commonly used to predict how species will respond under certain environmental conditions (Violle *et al.*, 2007). This is especially useful in the modern era, as humans have rapidly influenced a myriad of environmental conditions that plants must respond to, including human-induced climate change (Parmesan & Hanley, 2015), shifts in nutrient cycling (Bouwman *et al.*, 2009), and habitat loss (Helm *et al.*, 2006). Because traits of any given plant species may vary intraspecifically, it is important to estimate the full range of a species' traits to make accurate predictions of how the species will respond to future environmental conditions (Violle *et al.*, 2012). This includes both an assessment of variation in traits across the species' range, as well as a look at how the trajectory of its traits have changed in recent history.

Herbaria worldwide house nearly 400 million specimens of plants, providing incredibly valuable material to measure spatial and temporal changes in plant traits (Heberling, 2022). In addition to documenting species occurrence over time, herbarium specimens can also be used to investigate changes in leaf physiology and morphology through time (Heberling, 2022). For example, herbarium specimens have been used to assess how plants have responded to increased atmospheric CO<sub>2</sub> concentrations over the past several hundred years. Since the Industrial Revolution, atmospheric CO<sub>2</sub> concentrations have increased from anthropogenic emissions via burning fossil fuels. Atmospheric CO<sub>2</sub> levels have increased from around 285 parts per million (ppm) since year 1850 (McCarroll & Loader, 2004) to over 420 ppm as of May 2022 (Keeling *et*

*al.*, 2005). One major response has been the increased ratio of carbon (C) to nitrogen (N) in plant tissues (Peñuelas & Matamala, 1990, McLauchlan *et al.*, 2010; McLauchlan *et al.*, 2017; Peñuelas *et al.*, 2020). All else equal, as atmospheric CO<sub>2</sub> has become more readily available for plants to take up, plants proportionally acquire more molecules of C than other elements, such as N. This proportional decrease of nutrients in plant biomass has broad implications for global C and N cycling (Reich *et al.*, 2006). As low-quality (high C:N) plant litter becomes available for decomposition by microorganisms, decomposition may slow and lead to increased immobilization or decreased rates of N mineralization, which ultimately can feedback to decrease future available N for plants (Reich *et al.*, 2006).

One key indicator of changes due to increased anthropogenic CO<sub>2</sub> is directional changes in  $\delta^{13}\text{C}$  values, the ratio of  $^{13}\text{C}:^{12}\text{C}$  relative to the ratio of the standard, in plant tissue. Burning fossil fuels, which are primarily composed of ancient terrestrial photosynthetic organisms with  $\delta^{13}\text{C}$  values of about -25‰ (Friedli *et al.*, 1986), has decreased atmospheric  $\delta^{13}\text{C}$  from -6.44‰ prior to 1800 to about -8.5‰ in 2022 (Friedli *et al.*, 1986; Keeling *et al.*, 2005). This change in isotopic signature is reflected in plant tissues. During the photosynthetic reactions, plants discriminate against  $^{13}\text{CO}_2$  in favor of the lighter  $^{12}\text{CO}_2$  molecule (Farquhar *et al.*, 1989). In C<sub>3</sub> plants, the bulk of carbon fractionation occurs during the carboxylation by RuBisCO and fractionation in C<sub>4</sub> plants occurs during the carboxylation of PEP carboxylase, causing differences in  $\delta^{13}\text{C}$  between C<sub>3</sub> and C<sub>4</sub> species (Farquhar *et al.*, 1989). Carbon isotopic discrimination,  $\Delta^{13}\text{C}$ , is commonly used instead of  $\delta^{13}\text{C}$  when analyzing changes in carbon isotopes over time, since  $\Delta^{13}\text{C}$  accounts for temporal differences in atmospheric  $\delta^{13}\text{C}$  due to burning of fossil fuels.  $\delta^{13}\text{C}$  in C<sub>3</sub> plants is known to decrease over time (Peñuelas & Azcón-Bieto, 1992; Beerling *et al.*, 1993; Zhao *et al.*, 2001; Pedicino *et al.*, 2002), but null results have

also been observed (Pedicino *et al.*, 2002). Temporal studies of  $\Delta^{13}\text{C}$  in  $\text{C}_3$  plants reveal decreasing (Peñuelas & Azcón-Bieto, 1992; Araus & Buxó, 1993; Pedicino *et al.*, 2002), increasing (Zhao *et al.*, 2001; Pedicino *et al.*, 2002), and unchanging (Pedicino *et al.*, 2002) trends.  $\Delta^{13}\text{C}$  may be linked to phylogeny or be species-specific in  $\text{C}_3$  plants (Stein *et al.*, 2021). In contrast,  $\delta^{13}\text{C}$  has often been found to remain unchanged in  $\text{C}_4$  species over time, and consequently used as a proxy for historic atmospheric concentrations (Marino & McElroy, 1991; Toolin & Eastoe, 1993), though decreases in  $\delta^{13}\text{C}$  have been found as well (Eastoe & Toolin, 2018).  $\Delta^{13}\text{C}$  in  $\text{C}_4$  plants has been found to both increase (Pedicino *et al.*, 2002; Eastoe & Toolin, 2018) and remain unchanged (Marino & McElroy, 1991; Pedicino *et al.*, 2002) over time.

Leaf  $\Delta^{13}\text{C}$  can also be used as a proxy of integrated water use efficiency (WUE; Farquhar & Richards, 1984; Farquhar *et al.*, 1989). WUE is defined as the ratio of water lost to the atmosphere to the amount of carbon fixed and utilized by the plant (Farquhar *et al.*, 1989). When plants open their stomata for  $\text{CO}_2$  assimilation, water escapes into the atmosphere. Thus, the regulation of stomatal conductance of a plant over time, coupled with the concentration gradients of  $\text{CO}_2$  inside and outside the leaf, influences how much  $\text{CO}_2$  the plant assimilates and consequently its WUE. When plants are immersed in relatively rich  $\text{CO}_2$  environments (specifically,  $\text{C}_3$  plants), the carbon-fixing enzyme RuBisCO will increase carbon discrimination against  $^{13}\text{C}$ , causing a negative relationship between  $\Delta^{13}\text{C}$  and WUE (Farquhar *et al.*, 1989). While some species have been found to have increased WUE when exposed to higher levels of  $\text{CO}_2$  (Jackson *et al.*, 1994; Haworth *et al.*, 2011), this is not the case for every species (Miller-Rushing *et al.*, 2009). Furthermore,  $\Delta^{13}\text{C}$  may be linked more tightly to phylogenetic relationships and species identity rather than  $\text{CO}_2$  levels (Stein *et al.*, 2021).

Plants may also change stomatal densities and sizes in efforts to reduce water loss. Data from herbarium specimens and greenhouse studies have revealed that some plant species reduce the number of stomata on their leaves in response to increased CO<sub>2</sub> (Peñuelas & Matamala, 1990; Beerling & Chaloner, 1993a; Beerling & Chaloner, 1993b; Woodward & Kelly, 1995; Bettarini *et al.*, 1998; Doheny-Adams *et al.*, 2012; Large *et al.*, 2017). Guard cell length (stomatal size) may also decrease (Miglietta & Raschi, 1993). With higher CO<sub>2</sub> concentrations, plants can reduce their stomatal densities to reduce water loss while maintaining similar photosynthetic production. However, this response is not uniform across all species; some species have shown increases or no changes in stomatal density over time (Beerling *et al.*, 1992; Bettarini *et al.*, 1998, Ydenberg *et al.*, 2021).

To date, most studies investigating temporal changes in traits such as stomatal densities, leaf C:N, and leaf  $\Delta^{13}\text{C}$  have measured non-grasses, leaving grasses (Poaceae) underrepresented. It is important to understand how grassy ecosystems, which cover at least 25% of the earth's terrestrial surface (Asner *et al.*, 2004), have been affected by this surplus of CO<sub>2</sub> in the atmosphere. Grasses are major players in the C cycle and are responsible for trapping nearly 0.5 Pg C per year (Scurlock & Hall, 1998). The differences between how C<sub>3</sub> and C<sub>4</sub> grass species respond to increased CO<sub>2</sub> are especially important, as grasslands across the world vary in composition of C<sub>3</sub> and C<sub>4</sub> species (Osborne *et al.*, 2014). Because C<sub>4</sub> photosynthesis evolved in response to decreases in atmospheric CO<sub>2</sub> and increases in aridity and water limitations (Ehleringer *et al.*, 1997; Sage *et al.*, 2018; Zhou *et al.*, 2018), there are large implications for future performance and competition among grass species.

In addition to temporal trait variation, species exhibit varying degrees of intraspecific trait variation across their ranges (Li *et al.*, 2016; Moran *et al.*, 2016), including dominant grass

species in the Great Plains of North America (Bachle *et al.*, 2018). On a broad scale, this may be due to plastic responses to differing environmental factors, such as precipitation, temperature, and soil characteristics (Bernard-Verdier *et al.*, 2012; Westerband *et al.*, 2021). Across the Great Plains, climate varies substantially. For instance, a strong east-west precipitation gradient exists across the Great Plains, with the driest western sites receiving 25-40 cm of annual rainfall and the wettest eastern sites receiving about 150 cm (Nielsen, 2018). There is also a north-south temperature gradient in effect, where mean annual temperatures in the north are much colder than regions in the southern Great Plains (Kunkel *et al.*, 2013). Ultimately, these patterns and differences in environmental factors create distinct ecoregions (Bailey, 2004), of which there are many in the Great Plains (US Environmental Protection Agency, 2013). Ecoregions are thus useful for assessing differences among traits while considering multiple environmental differences.

To assess spatial and temporal differences among traits of a C<sub>3</sub> and a C<sub>4</sub> grass species, we measured a suite of traits (Table 3.1) on two species of grass, *Dichanthelium oligosanthos* subsp. *scribnerianum* (C<sub>3</sub>) and *Panicum virgatum* (C<sub>4</sub>). These two species are common throughout their large ranges in the Great Plains (Great Plains Flora Association, 1986) and abundant in local herbarium collections. *D. oligosanthos* subsp. *scribnerianum* (hereafter referred to as simply *D. oligosanthos*) and *P. virgatum* both have perennial life histories and are closely related species; despite having different photosynthetic pathways, they are both in the tribe Paniceae. In this study, we evaluate how leaf traits of these two grass species vary over time as atmospheric CO<sub>2</sub> has increased by measuring traits from herbarium specimens collected in Kansas. We also assess the intraspecific variability of these species' traits by measuring traits at eight grasslands in six unique ecoregions (Table 3.2; Fig. 1). For temporal trends, we predicted  $\Delta^{13}\text{C}$  to decrease in *D.*

*oligosanthes* and exhibit no change in *P. virgatum*. *D. oligosanthes* is a C<sub>3</sub> species, which we predict will respond to increased CO<sub>2</sub> concentrations by increasing its WUE to conserve water while maintaining the same rates of photosynthesis, thus decreasing  $\Delta^{13}\text{C}$ . We did not expect  $\Delta^{13}\text{C}$  of *P. virgatum* to respond over time because discrimination in C<sub>4</sub> species is minimally affected by CO<sub>2</sub> concentrations (O'Leary, 1988). We also predicted both species of plants will increase tissue C:N ratios and decrease stomatal density and stomatal lengths on both sides of the leaves in response to increased CO<sub>2</sub> over time. For spatial trends, we expected to see intraspecific differences across ecoregions in all traits we measured for both species due to the large differences in environmental factors across ecoregions; both species are widely distributed within North America and individuals are known to have various leaf morphologies (Barkworth *et al.*, 2003). At the very least, we expected at least two ecoregions to exhibit significant differences for each trait.

## **Materials and Methods**

### **Study Sites and Collection of Herbarium Material**

To compare how *D. oligosanthes* and *P. virgatum* vary in traits throughout their range, we sampled individuals at a variety of grasslands across the Great Plains of the United States over the course of the summers of 2021 and 2022 (Table 3.2; Fig. 1). These grasslands included Konza Prairie Biological Station (Manhattan, Kansas), Wah'Kon-Tah Prairie (El Dorado Springs, Missouri), Kisk-Ke-Kosh Prairie (Reasnor, Iowa), Joseph H. Williams Tallgrass Prairie Preserve (Pawhuska, Oklahoma), Valentine National Wildlife Refuge (Valentine, Nebraska), T. L. Davis Preserve (Elkhorn, Nebraska), Cedar Creek Ecosystem Science Reserve (East Bethel, Minnesota), and the Woodworth Station Waterfowl Production Area (Woodworth, North Dakota). We sampled plants growing from remnant portions of all grasslands except the

Woodworth Station Waterfowl Production Area, Wah’Kon-Tah Prairie, and Cedar Creek Ecosystem Science Reserve. At the Woodworth Station Waterfowl Production Area, all *P. virgatum* represented restored populations. At Wah’Kon-Tah Prairie, two replicates of *P. virgatum* came from restored populations. Both restored populations were seeded with locally sourced seeds. The restored populations at the Cedar Creek Ecosystem Science Reserve were recovered from the seed bank.

To measure temporal trends in traits, we sampled 14 specimens each of *D. oligosanthes* and *P. virgatum* at the Kansas State University Herbarium (KSC) and 17 specimens each at the McGregor Herbarium at Kansas University (KANU). KSC boasts a large (ca. 200,000) collection of plant specimens, many of which are historical specimens dating prior to 1900. KANU hosts approximately double (~400,000) the number of plant specimens as KSC, most of which were collected post-1950. Together these herbaria complement each other, allowing us to sample across a wider range of dates than would have been possible at just one herbarium.

When selecting specimens to sample, we used specific criteria to standardize our sampling efforts. First, specimens needed to have ample leafy material, a prerequisite for approval for destructive sampling. Second, specimens sampled were collected in the eastern third of the state of Kansas to minimize environmental variation by location. Third, all specimens sampled were collected during the species’ respective growing season to avoid senesced specimens. Specimens of *D. oligosanthes* were collected during the months May-July and specimens of *P. virgatum* were collected from June-August.

### **Trait Measurements**

At each sampling site, five replicates of each species (when possible) were measured for their specific leaf area (SLA), leaf dry matter content (LDMC), fresh leaf thickness, C:N, and

$\delta^{13}\text{C}$ . SLA ( $\text{cm}^2 \text{g}^{-1}$ ) is the ratio of leaf area to dry mass, LDMC is the ratio of leaf dry mass to wet mass, fresh leaf thickness (mm) is the thickness of the leaf in the field, C:N is the ratio of carbon to nitrogen, and  $\delta^{13}\text{C}$  is the ratio of the isotope  $^{13}\text{C}$  to  $^{12}\text{C}$  compared to the standard. Two of the five replicates were measured for their stomatal densities and stomatal lengths. For leaf measurements (SLA, LDMC, and leaf thickness), one leaf was sampled from each replicate. Leaf area and fresh leaf thickness were measured in the field. Leaf area was measured using Leafscan, a mobile app for measuring the surface area of leaves (Anderson & Rosas-Anderson, 2017), and fresh leaf thickness using calipers. Leaves were rehydrated by being submerged in water for 24-72 hours for wet mass measurements, and dried in a drying oven at  $60^\circ\text{C}$  for at least 48 hours for dry mass.

Stable isotope measurements for leaf  $\delta^{13}\text{C}$ , total C, and total N were done at the Stable Isotope Mass Spectrometry Laboratory at Kansas State University. Multiple leaves from each replicate were dried for at least 48 hours at  $60^\circ\text{C}$  and homogenized with an amalgamator. Total C and N of homogenized leaf samples was measured following combustion using an Elementar vario Pyro cube coupled to an Elementar Vision mass spectrometer for isotope analysis. Isotopic abundance ratios were converted to  $\delta$  notation using:

$$\delta = \left[ \frac{R_{\text{sample}}}{R_{\text{standard}}} - 1 \right] * 1000$$

where R is the ratio of heavy ( $^{13}\text{C}$ ) to light ( $^{12}\text{C}$ ) isotopes for the sample and standard, respectively. Working laboratory standards were annually calibrated against the internationally accepted standard, Vienna Pee-Dee Belemnite for  $\delta^{13}\text{C}$ . Within-run and across-run variability of the laboratory working standard was  $< 0.05\%$ . For temporal trends, all  $\delta^{13}\text{C}$  values were

corrected for changes in atmospheric  $\delta^{13}\text{C}$  by converting to carbon isotope discrimination values  $\Delta^{13}\text{C}$  according to Farquhar et al. 1982:

$$\Delta^{13}\text{C} = \frac{\delta^{13}\text{C}_{\text{air}} - \delta^{13}\text{C}_{\text{plant}}}{1 + \delta^{13}\text{C}_{\text{plant}}/1000}$$

$\delta^{13}\text{C}_{\text{air}}$  was estimated using measurements from McCarroll & Loader (2004) for the years preceding 2004 and measurements from the Moana Observatory Data were used for years 2004-2022 (Keeling *et al.*, 2005).

Stomatal peels were measured on samples from both herbaria and pressed and dried collections from each study site. Stomatal peels were made by applying clear nail varnish to leaves on the herbarium specimens and peeling the varnish once dry with clear tape. Both *D. oligosanthos* and *P. virgatum* are amphistomatous, so peels were made on both the abaxial and adaxial surfaces of the leaves. Due to the nature of herbarium specimens, where stems and leaves are affixed to herbarium paper, we were unable to sample exact opposite sides of each leaf. However, the leaves of *P. virgatum* were long and folded to fit on the herbarium sheet, exposing both sides of the same leaf. Thus, abaxial and adaxial peels were taken from the same leaf where the leaf was folded. For *D. oligosanthos*, the leaves were short and not folded to fit on the herbarium sheets, so only one side of each leaf was available to perform peels. To circumvent this issue, peels of the abaxial and adaxial surfaces were made on different (but similarly-developed) leaves of the same individual.

Two counts of stomatal density were taken for each peel, and five replicates of stomatal lengths were measured for each count of stomatal density (10 total per specimen). Stomata were counted under 20x magnification on the objective lens and 10x magnification on the ocular lens using an Olympus BH-2 Microscope (Shinjuku City, Tokyo, Japan). An image was taken of each

leaf section using a Lumenera Infinity 2 microscopy camera (Ottawa, Canada). The area of the image field of view was determined by using a stage micrometer and was 0.120 mm<sup>2</sup> for each image. Stomatal densities were then converted to per 1 mm<sup>2</sup>. Total stomatal density was measured as the sum of the abaxial and adaxial stomatal densities. Stomatal length (horizontal length of the guard cell from end to end) was measured using ImageJ; pixel length was converted to mm using a reference length determined from the stage micrometer. Five specimens of *P. virgatum* that were measured for stable isotopes were unable to be sampled for stomatal densities or lengths, as either the specimens had leaves that were too folded or wrinkled to obtain peels, or stomata were too sunken and not visible on the peels.

### **Statistical Analysis**

All statistical analyses were performed in R V4.2.1 (R Core Team, 2022). For temporal trait responses, we used linear regression models to determine if traits significantly differed over time. We performed separate linear regression for each trait (Table 3.1) with year as the predictor variable. For spatial trait responses, we used one-way ANOVA for each trait with ecoregion as the predictor variable. For significant predictor values, a Tukey's HSD test was used to make pairwise comparisons using the package 'emmeans' (Lenth 2022). All models were performed separately for each species.

## **Results**

### **Temporal Trends**

We measured stomatal traits (total stomatal density, abaxial stomatal density, adaxial stomatal density, stomatal ratio, abaxial stomatal length, and adaxial stomatal length) and isotopic/elemental composition traits ( $\Delta^{13}\text{C}$  and C:N) on leaves of *D. oligosanthos* and *P. virgatum* from the years 1887 – 2021 collected from eastern Kansas (Table 3.1). For stomatal

traits, we found that only the abaxial stomatal density of *P. virgatum* significantly changed over time, exhibiting a weakly positive correlation ( $R^2 = 0.1748$ ,  $P = 0.027$ ; Fig. 3.2). All other stomatal traits for both species did not significantly change across time (Figs. 3.3-3.7,  $P > 0.05$ ).

Of the two leaf isotopic and elemental composition traits measured, only  $\Delta^{13}\text{C}$  significantly increased or decreased over time. We found that the  $\Delta^{13}\text{C}$  of *D. oligosanthes* exhibited a significant, weakly positive correlation across time ( $R^2 = 0.17$ ,  $P = 0.007$ ; Fig. 3.8), and that the  $\Delta^{13}\text{C}$  of *P. virgatum* responded in the opposite manner, with a significant, weakly negative correlation across time ( $R^2 = 0.3276$ ,  $P < 0.001$ ; Fig. 3.9). C:N did not change significantly over time for either species (Figs. 3.10-3.11).

We also report temporal trends of two additional traits, leaf  $\delta^{15}\text{N}$  and %N. While these traits were not the focus of this study, they are of interest in the field and we find it valuable to report the results. We found that  $\delta^{15}\text{N}$  showed significant, moderately negative correlations with time for both *D. oligosanthes* ( $R^2 = 0.4493$ ,  $P < 0.001$ ; Fig. 3.12) and *P. virgatum* ( $R^2 = 0.3282$ ,  $P < 0.001$ ; Fig. 3.13). %N, however, did not change significantly over time (Figs. 3.14-3.15). These results are consistent with other studies (McLauchlan *et al.*, 2010; Tang *et al.*, 2022).

## **Spatial Trends**

We collected measurements on traits of *D. oligosanthes* and *P. virgatum* from eight different grasslands found in six ecoregions of the Great Plains of the United States (Table 3.2; Fig. 3.1). We measured the same stomatal traits (total stomatal density, abaxial stomatal density, adaxial stomatal density, stomatal ratio, abaxial stomatal length, and adaxial stomatal length) as we did for our temporal trend analysis (Table 3.1). However, an additional suite of leaf traits were measured and analyzed, including leaf SLA, LDMC, fresh thickness,  $\delta^{13}\text{C}$ , and C:N (Table

3.1). We compared how each of these traits varied for *D. oligosanthos* and *P. virgatum* across the ecoregions where each of our sites were located (Table 3.2; Fig. 1).

Only one stomatal trait significantly differed among ecoregions for *D. oligosanthos*: stomatal ratio. Stomatal ratios from plants growing in the Flint Hills ( $1.47 \pm 0.14$ ; Table 3.3) and the Western Corn Belt Plains ( $1.47 \pm 0.24$ ; Table 3.3) were significantly smaller than stomatal ratios from plants growing in the North Central Hardwood Forests ecoregion ( $3.35 \pm 0.65$ ; Table 3.3). No other stomatal traits showed any significant differences among ecoregions (Table 3.3). Significant differences among stomatal traits across ecoregions for *P. virgatum* existed for adaxial stomatal density and adaxial stomatal length (Table 3.4). Adaxial stomatal densities were significantly higher in the Central Irregular Plains ( $358.3 \pm 41.7$  stomata/mm<sup>2</sup>; Table 3.4) than they were in the Flint Hills ( $190.6 \pm 23.8$  stomata/mm<sup>2</sup>; Table 3.4) and the Western Corn Belt Plains ( $154.2 \pm 25.0$  stomata/mm<sup>2</sup>; Table 3.4). Adaxial stomatal lengths were significantly larger in the Flint Hills ( $0.0286 \pm 0.0016$  mm; Table 3.4) and the Northwest Glaciated Plains ( $0.0294 \pm 0.0010$  mm; Table 3.4) than in the Central Irregular Plains ( $0.0214 \pm 0.0011$  mm; Table 3.4).

Significant differences among leaf traits across ecoregions for *D. oligosanthos* existed for LDMC, fresh leaf thickness, C:N, and  $\delta^{13}\text{C}$  (Table 3.5). LDMC was found to be significantly higher among individuals growing in the Central Irregular Plains ( $0.344 \pm 0.006$ ; Table 3.5) than the Flint Hills ( $0.295 \pm 0.010$ ; Table 3.5), North Central Hardwood Forests ( $0.281 \pm 0.014$ ; Table 3.5), and Western Corn Belt Plains ( $0.286 \pm 0.009$ ; Table 3.5). Fresh leaf thickness was significantly greater in the Nebraska Sandhills ( $0.212 \pm 0.010$  mm; Table 3.5) than in the North Central Hardwood Forests ( $0.167 \pm 0.011$  mm; Table 3.5). C:N was significantly higher in the Central Irregular Plains ( $31.81 \pm 2.42$ ; Table 3.5) than the Nebraska Sandhills ( $22.88 \pm 1.37$ ; Table 3.5), North Central Hardwood Forests ( $24.09 \pm 1.12$ ; Table 3.5), and the Western Corn

Belt Plains ( $20.92 \pm 1.54$ ; Table 3.5). The Flint Hills had higher C:N ( $29.33 \pm 1.37$ ; Table 3.5) than the North Central Hardwood Forests and the Western Corn Belt Plains. Finally,  $\delta^{13}\text{C}$  was significantly higher in the Nebraska Sandhills ( $-26.54 \pm 0.11$ ; Table 3.5) than in the Flint Hills ( $-28.09 \pm 0.20$ ; Table 3.5) and the Western Corn Belt Plains ( $-27.87 \pm 0.32$ ; Table 3.5).  $\delta^{13}\text{C}$  was also significantly higher in the North Central Hardwood Forests ( $-26.86 \pm 0.22$ ; Table 3.5) compared to the Flint Hills. Significant differences in SLA was not found in *D. oligosanthos* (Table 3.5).

For the leaf traits of *P. virgatum*, significant differences across ecoregions were found in SLA and LDMC (Table 3.6). *P. virgatum* growing in the Central Irregular Plains ( $164.1 \pm 13.4$ ; Table 3.6) and Northwest Glaciated Plains ( $190.3 \pm 7.9$ ; Table 3.6) had significantly higher SLA on average than individuals of the Flint Hills ( $131.4 \pm 4.4$ ; Table 3.6). LDMC was significantly higher in the Flint Hills ( $0.393 \pm 0.009$ ; Table 3.6) than the Northwest Glaciated Plains ( $0.308 \pm 0.017$ ; Table 3.6). Significant differences were not found for fresh leaf thickness, C:N, or  $\delta^{13}\text{C}$  in *P. virgatum* across ecoregions.

## Discussion

In this study, we measured a suite of leaf traits on two widespread Panicoid species of grass (*D. oligosanthos* and *P. virgatum*) representative of either  $\text{C}_3$  or  $\text{C}_4$  photosynthetic pathways in the Great Plains of North America. The goal was to assess temporal (within eastern Kansas) and spatial (across the broader Great Plains) intraspecific variation in common leaf-level plant traits. Our results highlight trait plasticity and local adaptation across species, location, and time of measurement. The nature of this variability among two species from the same tribe of grasses (but differing photosynthetic pathway) illustrates the importance of measuring traits on

members of underrepresented groups of plants, such as grasses, as trait responses may be species-specific.

### **Responses in traits to increasing CO<sub>2</sub> since 1887**

We measured six stomatal traits on both *D. oligosanthos* and *P. virgatum* (Table 3.1). We hypothesized both species would exhibit a decrease in stomatal density and stomatal length over time due to increasing atmospheric CO<sub>2</sub> (Peñuelas & Matamala, 1990; Miglietta & Raschi, 1993). However, this hypothesis was not supported by the data; the general lack of change in stomatal density and length was contrary to previous studies that have found decreasing stomatal densities in response to elevated CO<sub>2</sub> (Peñuelas & Matamala, 1990; Beerling & Chaloner, 1993a; Beerling & Chaloner, 1993b; Woodward & Kelly, 1995; Bettarini *et al.*, 1998; Doheny-Adams *et al.*, 2012; Large *et al.*, 2017). While not statistically significant, there was an increasing trend in total stomatal density for both species over time (Fig. 3.3). Studies reporting decreasing stomatal densities have focused primarily on non-grass species. Woodward & Kelly (1995) assessed changes in stomatal density of 100 species in response to increasing CO<sub>2</sub>, including seven grass species. Of these seven grass species, four exhibited decreases in stomatal densities (one C<sub>3</sub>, three C<sub>4</sub>) and three species exhibited increases (two C<sub>3</sub>, one C<sub>4</sub>). Interestingly, the proportion of grasses showing a decreasing response towards increased CO<sub>2</sub> is 57%, which is less than the proportion of all species included in the analysis (74%). Coupled with the responses of stomatal densities of *D. oligosanthos* and *P. virgatum* found in this study, the percentage of grass species showing decreasing stomatal density falls to 44%. While still a small sample size, this suggests that the stomatal densities of grass species may respond more variably to increases in CO<sub>2</sub> (or other changing environmental factors, such as water availability) than in other plant lineages.

Although the trends were not significant, *D. oligosanthos* and *P. virgatum* both had increasing C:N and decreasing %N through time. Increasing atmospheric CO<sub>2</sub> is expected to increase foliar C:N ratios as plants have access to more carbon, but changes in %N through time seem to be less consistent (Peñuelas & Matamala, 1990, McLauchlan *et al.*, 2010; McLauchlan *et al.*, 2017; Brookshire *et al.*, 2020; Peñuelas *et al.*, 2020). While the majority of species measured in these studies were non-grasses, Brookshire *et al.*, (2020) found increasing C:N and decreasing %N in both species of C<sub>3</sub> grasses sampled. McLauchlan *et al.*, (2010) found decreasing %N in only four of the eight grass species sampled, and these were a mix of C<sub>3</sub> and C<sub>4</sub> species. The other four grass species sampled exhibited no change in %N through time. This suggests that effect of increased atmospheric CO<sub>2</sub> on %N may be species-specific, as grasses belonging to the same genus in McLauchlan *et al.*, (2010) exhibited both no change and decreasing %N. Additionally, the effects of increased anthropogenic N deposition over time (Matson *et al.*, 2002) may also play a role in suppressing increased C:N ratios. These null results may also be a result of small sampling sizes in the study.

Based on their differing photosynthetic pathways, we hypothesized that  $\Delta^{13}\text{C}$  of *D. oligosanthos* would decrease in response to increased atmospheric CO<sub>2</sub> and the  $\Delta^{13}\text{C}$  of *P. virgatum* would be unaffected. However, neither prediction was supported by our data.  $\Delta^{13}\text{C}$  of *D. oligosanthos* significantly increased over time, indicating that integrated water use efficiency (WUE) has actually decreased through time in this species.  $\Delta^{13}\text{C}$  of C<sub>3</sub> species are typically expected to decrease over time in response to elevated CO<sub>2</sub> due to increased stomatal closure to limit water loss, thus increasing WUE (Francey & Farquhar, 1982). This trend has been observed in several studies (Peñuelas & Azcón-Bieto, 1992; Pedicino *et al.*, 2002), including in C<sub>3</sub> grasses (Araus & Buxó, 1993). However,  $\Delta^{13}\text{C}$  in C<sub>3</sub> plants has also been found to increase (Zhao *et al.*,

2001; Pedicino *et al.*, 2002) or remain unchanged (Pedicino *et al.*, 2002) over time as atmospheric CO<sub>2</sub> has increased. There are many reasons why a species may exhibit changes in  $\Delta^{13}\text{C}$ . Environmental factors such as mean annual precipitation, nutrient availability, and irradiance all may influence  $\Delta^{13}\text{C}$  of C<sub>3</sub> species (Cernusak *et al.*, 2013). Furthermore,  $\Delta^{13}\text{C}$  may also depend on a species' genotype or phylogeny (Cernusak *et al.*, 2013; Stein *et al.*, 2021).

The decrease in  $\Delta^{13}\text{C}$  of *P. virgatum* was surprising. While few studies have measured temporal changes in  $\Delta^{13}\text{C}$  on C<sub>4</sub> species, only increasing (Pedicino *et al.*, 2002; Eastoe & Toolin, 2018) and unchanging (Marino & McElroy, 1991; Pedicino *et al.*, 2002) trends have previously been reported. To our knowledge, this is the first time a decreasing response of  $\Delta^{13}\text{C}$  over time has been reported for a C<sub>4</sub> species. There may be several reasons why this change in  $\Delta^{13}\text{C}$  was observed. In C<sub>4</sub> species,  $\Delta^{13}\text{C}$  may increase when plants are subjected to dry conditions, usually only by 0.5‰-1‰ (Buchmann *et al.*, 1996, Fravolini *et al.*, 2002; Ghannoum *et al.*, 2002).  $\Delta^{13}\text{C}$  of C<sub>4</sub> plants is also influenced by light availability. When shaded, the  $\Delta^{13}\text{C}$  of C<sub>4</sub> species increases (Buchmann *et al.*, 1996), and changes in  $\Delta^{13}\text{C}$  in response to light are greater than that of responses to water (Cernusak *et al.*, 2013). Additionally, the responses of  $\Delta^{13}\text{C}$  of C<sub>4</sub> grasses to changes in environmental factors vary by C<sub>4</sub> subtype – the  $\Delta^{13}\text{C}$  of the NADP-ME subtype responds the least, followed by PCK then NAD-ME (Buchmann *et al.*, 1996). As *P. virgatum* has the NAD-ME subtype, the ~1‰ decrease observed since 1887 is reasonable. A decrease in  $\Delta^{13}\text{C}$  as a response to increased light availability seems unlikely, as *P. virgatum* normally grows in full sunlight. Thus, it appears plausible that increased water availability may be responsible for the  $\Delta^{13}\text{C}$  decrease seen in *P. virgatum* over time. The results of  $\Delta^{13}\text{C}$  measured over time for both *D. oligosanthos* and *P. virgatum* may both be responses to increased water availability in the region; precipitation data from Manhattan, Kansas, USA (located within the region of specimens

sampled) shows increasing mean annual precipitation throughout the last century (Nippert, 2019).

### **Trait variation across ecoregions**

A suite of traits was measured on individuals of *D. oligosanthos* and *P. virgatum* across eight grassland locations found in six ecoregions of the Great Plains of North America. We predicted that we would find differences between at least two ecoregions for every trait because these species persist across a wide range of environments with complex spatial and temporal variability. However, across the suite of stomatal traits we measured, there were few differences between ecoregions for either species. Only one stomatal trait of *D. oligosanthos* (stomatal ratio) and two stomatal traits of *P. virgatum* (adaxial stomatal density and adaxial stomatal length) showed differences among ecoregions. We attribute this substantial lack of differences to our sample sizes. Only two replicates were taken at each site for each trait, limiting significant statistical differences between sites. We believe that more significant differences may have been found if additional replicates were included in the analyses, as differences in stomatal traits have been reported to vary across temperature and precipitation gradients (Pyakurel & Wang, 2014; Carlson *et al.*, 2016; Du *et al.*, 2021).

In contrast to stomatal traits, we found more differences among non-stomatal leaf traits (SLA, LDMC, fresh leaf thickness, C:N, and  $\delta^{13}\text{C}$ ) among ecoregions for both *D. oligosanthos* and *P. virgatum*. Due to the larger number of replicates for these traits, we expect the results to better reflect ecological differences rather than sample size. Of these four traits, only differences in LDMC were found between both species, though not among the same ecoregions. The LDMC of *D. oligosanthos* was higher in the Central Irregular Plains than all other ecoregions except the Nebraska Sandhills, which showed no difference. The Central Irregular Plains is the most

southwestern ecoregion in our study and has greater precipitation and warmer temperatures throughout the year compared to the other ecoregions. LDMC is known to increase with increasing precipitation across rainfall gradients in both forests and grasslands (Wang *et al.*, 2016; Zuo *et al.*, 2021), which explains the differences found in our study. However, LDMC in *P. virgatum* was not found to be higher in the drier western ecoregions compared to the wetter eastern ecoregions.

In contrast to LDMC, SLA has been found to decrease with increasing precipitation (Wang *et al.*, 2016, Brody & Low, 2019; Zuo *et al.*, 2021). While no changes in SLA were observed among ecoregions for *D. oligoanthes*, SLA differed in *P. virgatum* among many ecoregions, but with no clear divide along precipitation gradients. Like SLA, leaf thickness decreases with increasing precipitation in grasslands (Zuo *et al.*, 2021), though no similar trends were found in forests (Wang *et al.*, 2016). Fresh leaf thickness was only different among ecoregions in *D. oligoanthes*, where individuals growing in the driest ecoregion (Nebraska Sandhills) had the greatest leaf thickness. One reason precipitation gradients may not explain all of the variability among these leaf traits is that the precipitation gradients across our ecoregions did not extend throughout the entire precipitation gradient of the Great Plains. While our eastern ecoregions tended to be close to the wettest regions of the Great Plains, our western ecoregions only extended to the middle of the Great Plains that receive moderate precipitation. Without including extreme western sites in our analysis, the picture remains incomplete.

$\delta^{13}\text{C}$  only differed among ecoregions in *D. oligoanthes*. In  $\text{C}_3$  plants, differences in  $\delta^{13}\text{C}$  are strongly driven by instantaneous  $c_i/c_a$ , the ratio of intracellular  $\text{CO}_2$  to the ratio of atmospheric  $\text{CO}_2$  (Cernusak *et al.*, 2013). Instantaneous  $c_i/c_a$  has a negative relationship with leaf  $\delta^{13}\text{C}$  (Cernusak *et al.*, 2013) and is influenced by many environmental factors including water

availability, nutrient availability, irradiance, and reduced CO<sub>2</sub> partial pressures due to elevation (Tieszen, 1991). Tieszen (1991) predicts irradiance affects  $c_i/c_a$  the most and water availability second, but *D. oligoanthes* was collected in open grasslands at all sites in this study, so differences in irradiance are likely unimportant as drivers of  $\delta^{13}\text{C}$ . Water stress decreases  $c_i/c_a$  (Tieszen, 1991) by increasing stomatal regulation and decreasing discrimination against  $^{13}\text{C}$ , resulting in higher foliar  $\delta^{13}\text{C}$  values (Cernusak *et al.*, 2013). This trend has been observed in C<sub>3</sub> grasses across a precipitation gradient (Weiguo *et al.*, 2005). In our study, the highest  $\delta^{13}\text{C}$  values measured in *D. oligoanthes* came from the driest ecoregion (Nebraska Sandhills) and the lowest  $\delta^{13}\text{C}$  came from one of the wettest ecoregions sampled in this study (Flint Hills).

## Conclusion

We found that traits of two species of Panicoid grasses, *D. oligoanthes* (C<sub>3</sub>) and *P. virgatum* (C<sub>4</sub>), varied in response to changes in environmental conditions across spatial and temporal scales. Observed trait variation across spatial scales in traits such as SLA, LDMC, leaf thickness, and  $\delta^{13}\text{C}$  has likely influenced the ability of these species to persist across the Great Plains of North America, where environmental conditions vary substantially among its ecoregions (similar to Bachle *et al.*, 2021). Temporally, we found contrasting responses of  $\Delta^{13}\text{C}$  between the species, indicating that these species have been responding differently to environmental change over time, which may be linked to the difference in photosynthetic pathways. The decreasing response of  $\Delta^{13}\text{C}$  of *P. virgatum* over time is the first time this type of trend has been reported for a C<sub>4</sub> species. In addition, we found that many traits, such as stomatal density and C:N, did not respond across time, which contrasts with results from other studies. This is likely due to the underrepresentation of Poaceae in the literature; predictions in the field of trait ecology are founded primarily on non-grass species. However, we acknowledge that the

limited number of older samples (pre-1900) may have also played a role in these trends. We argue that the evolutionary history of species is important when assessing trait variability across temporal and spatial scales. If we are to make predictions about global ecosystem change, we need to include all relevant phylogenies in trait analyses, especially C<sub>3</sub> and C<sub>4</sub> species of the highly diverse and dominant Poaceae.

## References

- Anderson CJR, Rosas-Anderson PJ. 2017.** Leafscan (Version 1.3.21). [Mobile application software]. Retrieved from leafscanapp.com.
- Araus J, Buxo R. 1993.** Changes in carbon isotope discrimination in grain cereals from the north-western Mediterranean Basin during the past seven millenia. *Functional Plant Biology* **20**: 117.
- Asner GP, Elmore AJ, Olander LP, Martin RE, Harris AT. 2004.** Grazing systems, ecosystem responses, and global change. *Annual Review of Environment and Resources* **29**: 261–299.
- Bachle S, Griffith DM, Nippert JB. 2018.** Intraspecific trait variability in *Andropogon gerardii*, a dominant grass species in the US Great Plains. *Frontiers in Ecology and Evolution* **6**: 217.
- Bachle S, Nippert JB. 2021.** Microanatomical traits track climate gradients for a dominant C<sub>4</sub> grass species across the Great Plains, USA. *Annals of Botany* **127**: 451–459.
- Bailey RG. 2004.** Identifying ecoregion boundaries. *Environmental Management* **34**: S14–S26.
- Barkworth ME, Capels KM, Long S, Piep MB. 2003.** Flora of North America. 25: Magnoliophyta: Commelinidae: Poaceae, part 2. New York: Oxford Univ. Press.
- Beerling DJ, Chaloner WG, Huntley B, Pearson JA, Tooley MJ, Woodward FI. 1992.** Variations in the stomatal density of *Salix herbacea* L. under the changing atmospheric CO<sub>2</sub>

concentrations of late- and post-glacial time. *Philosophical Transactions of the Royal Society of London. Series B: Biological Sciences* **336**: 215–224.

**Beerling DJ, Chaloner WG. 1993a.** Stomatal density responses of Egyptian *Olea europaea* L. leaves to CO<sub>2</sub> change since 1327 BC. *Annals of Botany* **71**: 431–435.

**Beerling DJ, Chaloner WG. 1993b.** The impact of atmospheric CO<sub>2</sub> and temperature changes on stomatal density: observation from *Quercus robur* lammas leaves. *Annals of Botany* **71**: 231–235.

**Beerling, DJ, Matthey DP, Chaloner WG. 1993.** Shifts in the  $\delta^{13}\text{C}$  composition of *Salix herbacea* L. leaves in response to spatial and temporal gradients of atmospheric CO<sub>2</sub> concentration. *Proceedings of the Royal Society of London. Series B: Biological Sciences* **253**: 53–60.

**Bernard-Verdier M, Navas M-L, Vellend M, Violle C, Fayolle A, Garnier E. 2012.** Community assembly along a soil depth gradient: contrasting patterns of plant trait convergence and divergence in a Mediterranean rangeland. *Journal of Ecology* **100**: 1422–1433.

**Bettarini I, Vaccari FP, Miglietta F. 1998.** Elevated CO<sub>2</sub> concentrations and stomatal density: observations from 17 plant species growing in a CO<sub>2</sub> spring in central Italy. *Global Change Biology* **4**: 17–22.

**Bouwman AF, Beusen AHW, Billen G. 2009.** Human alteration of the global nitrogen and phosphorus soil balances for the period 1970–2050: Nitrogen and phosphorous soil balances. *Global Biogeochemical Cycles* **23**.

**Brookshire ENJ, Stoy PC, Currey B, Finney B. 2020.** The greening of the Northern Great Plains and its biogeochemical precursors. *Global Change Biology* **26**: 5404–5413.

- Buchmann N, Brooks JR, Rapp KD, Ehleringer JR. 1996.** Carbon isotope composition of C<sub>4</sub> grasses is influenced by light and water supply. *Plant, Cell and Environment* **19**: 392–402.
- Carlson JE, Adams CA, Holsinger KE. 2016.** Intraspecific variation in stomatal traits, leaf traits and physiology reflects adaptation along aridity gradients in a South African shrub. *Annals of Botany* **117**: 195–207.
- Cernusak LA, Ubierna N, Winter K, Holtum JAM, Marshall JD, Farquhar GD. 2013.** Environmental and physiological determinants of carbon isotope discrimination in terrestrial plants. *New Phytologist* **200**: 950–965.
- Doheny-Adams T, Hunt L, Franks PJ, Beerling DJ, Gray JE. 2012.** Genetic manipulation of stomatal density influences stomatal size, plant growth and tolerance to restricted water supply across a growth carbon dioxide gradient. *Philosophical Transactions of the Royal Society B: Biological Sciences* **367**: 547–555.
- Du B, Zhu Y, Kang H, Liu C. 2021.** Spatial variations in stomatal traits and their coordination with leaf traits in *Quercus variabilis* across Eastern Asia. *Science of The Total Environment* **789**: 147757.
- Eastoe C, Toolin L. 2018.** A multi-century  $\delta^{13}\text{C}$  record of the C<sub>4</sub> grass *Setaria macrostachya* in the US Southwest: identifying environmental causes of variability. *Palaeogeography, Palaeoclimatology, Palaeoecology* **489**: 129–136.
- Ehleringer JR, Cerling TE, Helliker BR. 1997.** C<sub>4</sub> photosynthesis, atmospheric CO<sub>2</sub>, and climate. *Oecologia* **112**: 285–299.
- Farquhar G, Richards R. 1984.** Isotopic composition of plant carbon correlates with water-use efficiency of wheat genotypes. *Functional Plant Biology* **11**: 539.

- Farquhar GD, Ehleringer JR, Hubick KT. 1989.** Carbon isotope discrimination and photosynthesis. *Annual Review of Plant Physiology and Plant Molecular Biology* **40**: 503– 537.
- Francey RJ, Farquhar GD. 1982.** An explanation of  $^{13}\text{C}/^{12}\text{C}$  variations in tree rings. *Nature* **297**: 28–31.
- Fravolini A, Williams DG, Thomspen TL. 2002.** Carbon isotope discrimination and bundle sheath leakiness in three  $\text{C}_4$  subtypes grown under variable nitrogen, water and atmospheric  $\text{CO}_2$  supply. *Journal of Experimental Botany* **53**: 2261–2269.
- Friedli H, Löttscher H, Oeschger H, Siegenthaler U, Stauffer B. 1986.** Ice core record of the  $^{13}\text{C}/^{12}\text{C}$  ratio of atmospheric  $\text{CO}_2$  in the past two centuries. *Nature* **324**: 237–238.
- Ghannoum O, Caemmerer S von, Conroy JP. 2002.** The effect of drought on plant water use efficiency of nine NAD – ME and nine NADP – ME Australian  $\text{C}_4$  grasses. *Functional Plant Biology* **29**: 1337.
- Great Plains Flora Association 1986.** *Flora of the Great Plains*. Lawrence, Kan: University Press of Kansas.
- Haworth M, Elliott-Kingston C, McElwain JC. 2011.** The stomatal  $\text{CO}_2$  proxy does not saturate at high atmospheric  $\text{CO}_2$  concentrations: evidence from stomatal index responses of Araucariaceae conifers. *Oecologia* **167**: 11–19.
- Heberling JM. 2022.** Herbaria as big data sources of plant traits. *International Journal of Plant Sciences* **183**: 87–118.
- Helm A, Hanski I, Partel M. 2005.** Slow response of plant species richness to habitat loss and fragmentation. *Ecology Letters* **9**: 72-77.
- Jackson RB, Sala OE, Field CB, Mooney HA. 1994.**  $\text{CO}_2$  alters water use, carbon gain, and yield for the dominant species in a natural grassland. *Oecologia* **98**: 257–262.

- Keeling CD, Piper SC, Bacastow RB, Wahlen M, Whorf TP, Heimann M, Meijer HA. 2005.** Atmospheric CO<sub>2</sub> and <sup>13</sup>CO<sub>2</sub> exchange with the terrestrial biosphere and oceans from 1978 to 2000: observations and carbon cycle implications. *In: Ehleringer JR, Cerling TE, Dearing MD, eds. A history of atmospheric CO<sub>2</sub> and its effects on plants, animals, and ecosystems. New York, NY, USA: Springer, 83–113.*
- Kunkel KE, Stevens LE, Stevens SE, Sun L, Janssen E, Wuebbles D, Kruk MC, Thomas DP, Shulski M, Umphlett N, et al. 2013.** Regional climate trends and scenarios for the U.S. National Climate Assessment. Part 4. Climate of the U.S. Great Plains. *NOAA.*
- Large MF, Nessia HR, Cameron EK, Blanchon DJ. 2017.** Changes in stomatal density over time (1769–2015) in the New Zealand endemic tree *Corynocarpus laevigatus* J. R. Forst. & G. Forst. (Corynocarpaceae). *Pacific Science* **71**: 319–328.
- Lenth R. 2019.** Emmeans: Estimated marginal means, aka least-squares means. *R package v.1.3.4. [WWW document] URL <https://CRAN.R-project.org/package=emmeans>.*
- Li H, Yu K, Ratajczak Z, Nippert JB, Tondrob D, Xu D, Li W, Du G. 2016.** When variability outperforms the mean: trait plasticity predicts plant cover and biomass in an alpine wetland. *Plant and Soil* **407**: 401–415.
- Marino BD, McElroy MB. 1991.** Isotopic composition of atmospheric CO<sub>2</sub> inferred from carbon in C<sub>4</sub> plant cellulose. *Nature* **349**: 127–131.
- Matson P, Lohse KA, Hall SJ. 2002.** The globalization of nitrogen deposition: consequences for terrestrial ecosystems. *AMBIO: A Journal of the Human Environment* **31**: 113–119.
- McCarroll D, Loader NJ. 2004.** Stable isotopes in tree rings. *Quaternary Science Reviews* **23**: 771–801.

- McLauchlan KK, Ferguson CJ, Wilson IE, Ocheltree TW, Craine JM. 2010.** Thirteen decades of foliar isotopes indicate declining nitrogen availability in central North American grasslands. *New Phytologist* **187**: 1135–1145.
- McLauchlan KK, Gerhart LM, Battles JJ, Craine JM, Elmore AJ, Higuera PE, Mack MC, McNeil BE, Nelson DM, Pederson N, et al. 2017.** Centennial-scale reductions in nitrogen availability in temperate forests of the United States. *Scientific Reports* **7**: 7856.
- Miglietta F, Raschi A. 1993.** Studying the effect of elevated CO<sub>2</sub> in the open in a naturally enriched environment in central Italy. *Vegetatio* **104–105**: 391–400.
- Miller-Rushing AJ, Primack RB, Templer PH, Rathbone S, Mukunda S. 2009.** Long-term relationships among atmospheric CO<sub>2</sub>, stomata, and intrinsic water use efficiency in individual trees. *American Journal of Botany* **96**: 1779–1786.
- Moran EV, Hartig F, Bell DM. 2016.** Intraspecific trait variation across scales: implications for understanding global change responses. *Global Change Biology* **22**: 137–150.
- Nielsen DC. 2018.** Influence of latitude on the US Great Plains east–west precipitation gradient. *Agricultural & Environmental Letters* **3**: 170040.
- Nippert J. 2019.** APT02 Monthly temperature and precipitation records from Manhattan, KS.
- O’Leary MH. 1988.** Carbon isotopes in photosynthesis. *BioScience* **38**: 328–336.
- Osborne CP, Salomaa A, Kluyver TA, Visser V, Kellogg EA, Morrone O, Vorontsova MS, Clayton WD, Simpson DA. 2014.** A global database of C<sub>4</sub> photosynthesis in grasses. *New Phytologist* **204**: 441–446.
- Parmesan C, Hanley ME. 2015.** Plants and climate change: complexities and surprises. *Annals of Botany* **116**: 849–864.

**Pedicino L, Leavitt S, Betancourt J, Van de Water P. 2002.** Historical variations in  $\delta^{13}\text{C}$  leaf of herbarium specimens in the southwestern U.S. *Western North American Naturalist* **62**: 348–359.

**Peñuelas J, Matamala R. 1990.** Changes in N and S leaf content, stomatal density and specific leaf area of 14 plant species during the last three centuries of  $\text{CO}_2$  increase. *Journal of Experimental Botany* **41**: 1119–1124.

**Peñuelas J, Azcon-Bieto J. 1992.** Changes in leaf  $\Delta^{13}\text{C}$  of herbarium plant species during the last 3 centuries of  $\text{CO}_2$  increase. *Plant, Cell and Environment* **15**: 485–489.

**Peñuelas J, Fernández-Martínez M, Vallicrosa H, Maspons J, Zuccarini P, Carnicer J, Sanders TGM, Krüger I, Obersteiner M, Janssens IA, et al. 2020.** Increasing atmospheric  $\text{CO}_2$  concentrations correlate with declining nutritional status of European forests. *Communications Biology* **3**: 125.

**Pyakurel A, Wang JR. 2014.** Leaf morphological and stomatal variations in paper birch populations along environmental gradients in Canada. *American Journal of Plant Sciences* **05**: 1508–1520.

**R Core Team. 2022.** R: A language and environment for statistical computing. R Foundation for Statistical Computing, Vienna, Austria.

**Reich PB, Hungate BA, Luo Y. 2006.** Carbon-nitrogen interactions in terrestrial ecosystems in response to rising atmospheric carbon dioxide. *Annual Review of Ecology, Evolution, and Systematics* **37**: 611–636.

**Sage RF, Monson RK, Ehleringer JR, Adachi S, Pearcy RW. 2018.** Some like it hot: the physiological ecology of  $\text{C}_4$  plant evolution. *Oecologia* **187**: 941–966.

- Sandel B, Low R. 2019.** Intraspecific trait variation, functional turnover and trait differences among native and exotic grasses along a precipitation gradient. *Journal of Vegetation Science* **30**: 633–643.
- Scurlock JMO, Hall DO. 1998.** The global carbon sink: a grassland perspective. *Global Change Biology* **4**: 229–233.
- Stein RA, Sheldon ND, Smith SY. 2021.** C<sub>3</sub> plant carbon isotope discrimination does not respond to CO<sub>2</sub> concentration on decadal to centennial timescales. *New Phytologist* **229**: 2576–2585.
- Tang S, Liu J, Gilliam FS, Hietz P, Wang Z, Lu X, Zeng F, Wen D, Hou E, Lai Y, et al. 2022.** Drivers of foliar <sup>15</sup>N trends in southern China over the last century. *Global Change Biology* **28**: 5441–5452.
- Tieszen LL. 1991.** Natural variations in the carbon isotope values of plants: implications for archaeology, ecology, and paleoecology. *Journal of Archaeological Science* **18**: 227–248.
- Toolin LJ, Eastoe CJ. 1993.** Late Pleistocene-recent atmospheric δ<sup>13</sup>C record in C<sub>4</sub> grasses. *Radiocarbon* **35**: 263–269.
- U.S. Environmental Protection Agency. 2013.** Level III ecoregions of the continental United States: Corvallis, Oregon, U.S. EPA, National Health and Environmental Effects Research Laboratory, map scale 1:7,500,000. <https://www.epa.gov/eco-research/level-iii-and-iv-ecoregions-continental-united-states>
- Violle C, Navas M-L, Vile D, Kazakou E, Fortunel C, Hummel I, Garnier E. 2007.** Let the concept of trait be functional! *Oikos* **116**: 882–892.

**Violle C, Enquist BJ, McGill BJ, Jiang L, Albert CH, Hulshof C, Jung V, Messier J. 2012.**

The return of the variance: intraspecific variability in community ecology. *Trends in Ecology & Evolution* **27**: 244–252.

**Wang R, Yu G, He N, Wang Q, Zhao N, Xu Z. 2016.** Latitudinal variation of leaf

morphological traits from species to communities along a forest transect in eastern China.

*Journal of Geographical Sciences* **26**: 15–26.

**Weiguo L, Xiahong F, Youfeng N, Qingle Z, Yunning C, Zhisheng AN. 2005.**  $\Delta^{13}\text{C}$  variation of  $\text{C}_3$  and  $\text{C}_4$  plants across an Asian monsoon rainfall gradient in arid northwestern China. *Global Change Biology* **11**: 1094–1100.

**Westerband AC, Funk JL, Barton KE. 2021.** Intraspecific trait variation in plants: a renewed focus on its role in ecological processes. *Annals of Botany* **127**: 397–410.

**Woodward FI, Kelly CK. 1995.** The influence of  $\text{CO}_2$  concentration on stomatal density. *New Phytologist* **131**: 311–327.

**Ydenberg R, Leyland B, Hipfner M, Prins HHT. 2021.** Century-long stomatal density record of the nitrophyte, *Rubus spectabilis* L., from the Pacific Northwest indicates no effect of changing atmospheric carbon dioxide but a strong response to nutrient subsidy. *Ecology and Evolution* **11**: 18081–18088.

**Zhao F-J, Spiro B, McGrath SP. 2001.** Trends in  $^{13}\text{C}/^{12}\text{C}$  ratios and C isotope discrimination of wheat since 1845. *Oecologia* **128**: 336–342.

**Zhou H, Helliker BR, Huber M, Dicks A, Akçay E. 2018.**  $\text{C}_4$  photosynthesis and climate through the lens of optimality. *Proceedings of the National Academy of Sciences* **115**: 12057–12062.

**Zuo X, Zhao S, Cheng H, Hu Y, Wang S, Yue P, Liu R, Knapp AK, Smith MD, Yu Q, et al.**

**2021.** Functional diversity response to geographic and experimental precipitation gradients

varies with plant community type. *Functional Ecology* **35**: 2119–2132.

## Tables and Figures

**Table 3.1: A list of traits measured in this study.**

Traits measured across time	Traits measured across space
Total Stomatal Density (stomata/mm <sup>2</sup> )	Total Stomatal Density (stomata/mm <sup>2</sup> )
Adaxial Stomatal Density (stomata/mm <sup>2</sup> )	Adaxial Stomatal Density (stomata/mm <sup>2</sup> )
Abaxial Stomatal Density (stomata/mm <sup>2</sup> )	Abaxial Stomatal Density (stomata/mm <sup>2</sup> )
Top Stomatal Length (mm)	Top Stomatal Length (mm)
Bottom Stomatal Length (mm)	Bottom Stomatal Length (mm)
Stomatal Ratio (Adaxial:Abaxial)	Stomatal Ratio (Adaxial:Abaxial)
$\Delta^{13}\text{C}$ (‰)	$\delta^{13}\text{C}$ (‰)
C:N	C:N
	SLA (cm <sup>2</sup> g <sup>-1</sup> )
	LDMC
	Fresh Leaf Thickness (mm)

**Table 3.2: A list of grasslands where sampling of traits of *D. oligosanthos* and *P. virgatum* occurred. Ecoregions were determined from US Environmental Protection Agency (2013).**

Site	Locality	Ecoregion	Species Sampled
Konza Prairie Biological Station	Manhattan, Kansas, USA	Flint Hills	<i>D. oligosanthos</i> and <i>P. virgatum</i>
Wah'Kon-Tah Prairie	El Dorado Springs, Missouri, USA	Central Irregular Plains	<i>D. oligosanthos</i> and <i>P. virgatum</i>
Kisk-Ke-Kosh Prairie	Reasnor, Iowa, USA	Western Corn Belt Plains	<i>D. oligosanthos</i>
Joseph H. Williams Tallgrass Prairie Preserve	Pawhuska, Oklahoma, USA	Flint Hills	<i>D. oligosanthos</i> and <i>P. virgatum</i>
Valentine National Wildlife Refuge	Valentine, Nebraska, USA	Nebraska Sandhills	<i>D. oligosanthos</i> and <i>P. virgatum</i>
T. L. Davis Preserve	Elkhorn, Nebraska, USA	Western Corn Belt Plains	<i>D. oligosanthos</i> and <i>P. virgatum</i>
Cedar Creek Ecosystem Science Reserve	East Bethel, Minnesota, USA	North Central Hardwood Forests	<i>D. oligosanthos</i> and <i>P. virgatum</i>

Woodworth Station	Woodworth, North	Northwestern	<i>P. virgatum</i>
Waterfowl Production Area	Dakota, USA	Glaciated Plains	

**Table 3.3: Mean values of stomatal traits of *D. oligosanthus* separated by ecoregion. Means within columns with different letters are statistically significant ( $P < 0.05$ ).**

Trait	Total Stomatal Density (per mm <sup>2</sup> )	Adaxial Stomatal Density (per mm <sup>2</sup> )	Abaxial Stomatal Density (per mm <sup>2</sup> )	Adaxial Stomatal Length (mm)	Abaxial Stomatal Length (mm)	Stomatal Ratio (Adaxial:Abaxial)
Central Irregular Plains	343.8 ± 52.1 <i>a</i>	225.0 ± 62.5 <i>a</i>	118.7 ± 10.4 <i>a</i>	0.0303 ± 0.0018 <i>a</i>	0.0339 ± 0.0020 <i>a</i>	1.96 ± 0.70 <i>ab</i>
Flint Hills	277.1 ± 8.1 <i>a</i>	163.5 ± 5.7 <i>a</i>	113.5 ± 7.5 <i>a</i>	0.0329 ± 0.0013 <i>a</i>	0.0381 ± 0.0019 <i>a</i>	1.47 ± 0.14 <i>a</i>
Nebraska Sandhills	391.7 ± 87.5 <i>a</i>	279.2 ± 79.2 <i>a</i>	112.5 ± 8.3 <i>a</i>	0.0295 ± 0.0009 <i>a</i>	0.0344 ± 0.0041 <i>a</i>	2.44 ± 0.52 <i>ab</i>
North Central Hardwood Forests	366.7 ± 33.3 <i>a</i>	279.2 ± 12.5 <i>a</i>	87.5 ± 20.8 <i>a</i>	0.0305 ± 0.0022 <i>a</i>	0.0369 ± 0.0040 <i>a</i>	3.35 ± 0.65 <i>b</i>
Western Corn Belt Plains	314.6 ± 21.3 <i>a</i>	184.4 ± 20.0 <i>a</i>	130.2 ± 12.8 <i>a</i>	0.0303 ± 0.0015 <i>a</i>	0.0328 ± 0.0010 <i>a</i>	1.47 ± 0.24 <i>a</i>

**Table 3.4: Mean values of stomatal traits of *P. virgatum* separated by ecoregion. Means within columns with different letters are statistically significant ( $P < 0.05$ ).**

Trait	Total Stomatal Density (per mm <sup>2</sup> )	Adaxial Stomatal Density (per mm <sup>2</sup> )	Abaxial Stomatal Density (per mm <sup>2</sup> )	Adaxial Stomatal Length (mm)	Abaxial Stomatal Length (mm)	Stomatal Ratio (Adaxial:Abaxial)
Central Irregular Plains	620.8 ± 100.0 <i>a</i>	358.3 ± 41.7 <i>a</i>	262.5 ± 58.3 <i>a</i>	0.0214 ± 0.0011 <i>a</i>	0.0301 ± 0.0040 <i>a</i>	1.40 ± 0.15 <i>a</i>
Flint Hills	349.0 ± 39.0 <i>a</i>	190.6 ± 23.8 <i>b</i>	158.3 ± 16.2 <i>a</i>	0.0286 ± 0.0016 <i>b</i>	0.0356 ± 0.0013 <i>a</i>	1.20 ± 0.07 <i>a</i>
Nebraska Sandhills	375.0 ± 16.7 <i>a</i>	204.2 ± 20.8 <i>ab</i>	170.8 ± 4.2 <i>a</i>	0.0270 ± 0.0020 <i>ab</i>	0.0342 ± 0.0002 <i>a</i>	1.20 ± 0.15 <i>a</i>
North Central Hardwood Forests	391.7 <i>a</i>	208.3 <i>ab</i>	183.3 <i>a</i>	0.0286 <i>ab</i>	0.0328 <i>a</i>	1.14 <i>a</i>
Northwest Glaciated Plains	377.1 ± 43.7 <i>a</i>	208.3 ± 20.8 <i>ab</i>	168.7 ± 22.9 <i>a</i>	0.0294 ± 0.0010 <i>b</i>	0.0354 ± 0.0004 <i>a</i>	1.24 ± 0.05 <i>a</i>
Western Corn Belt Plains	362.5 ± 8.3 <i>a</i>	154.2 ± 25.0 <i>b</i>	208.3 ± 16.7 <i>a</i>	0.0249 ± 0.0013 <i>ab</i>	0.0326 ± 0.0018 <i>a</i>	1.34 ± 0.40 <i>a</i>

**Table 3.5: Mean values of leaf traits of *D. oligosanthos* separated by ecoregion. Means within columns with different letters are statistically significant ( $P < 0.05$ ).**

Trait	SLA (cm <sup>2</sup> g <sup>-1</sup> )	LDMC	Fresh Leaf Thickness (mm)	C:N	$\delta^{13}\text{C}$ (‰)
Central Irregular Plains	184.0 ± 7.9 $a$	0.344 ± 0.006 $a$	0.184 ± 0.002 $ab$	31.81 ± 2.42 $a$	-27.39 ± 0.44 $abc$
Flint Hills	203.4 ± 11.0 $a$	0.295 ± 0.010 $b$	0.190 ± 0.007 $ab$	29.33 ± 1.37 $ab$	-28.09 ± 0.20 $a$
Nebraska Sandhills	170.4 ± 9.6 $a$	0.324 ± 0.009 $ab$	0.212 ± 0.010 $a$	22.88 ± 1.37 $bc$	-26.54 ± 0.11 $b$
North Central Hardwood Forests	197.1 ± 8.6 $a$	0.281 ± 0.014 $b$	0.167 ± 0.011 $b$	24.09 ± 1.12 $bc$	-26.86 ± 0.22 $bc$
Western Corn Belt Plains	218.7 ± 10.7 $a$	0.286 ± 0.009 $b$	0.180 ± 0.004 $ab$	20.92 ± 1.54 $c$	-27.87 ± 0.32 $ac$

**Table 3.6: Mean values of leaf traits of *P. virgatum* separated by ecoregion. Means within columns with different letters are statistically significant ( $P < 0.05$ ).**

Trait	SLA (cm <sup>2</sup> g <sup>-1</sup> )	LDMC	Fresh Leaf Thickness (mm)	C:N	$\delta^{13}\text{C}$ (‰)
Central Irregular Plains	164.1 ± 13.4 $ac$	0.357 ± 0.028 $ab$	0.212 ± 0.009 $a$	37.15 ± 8.24 $a$	-13.63 ± 0.08 $a$
Flint Hills	131.4 ± 4.4 $b$	0.393 ± 0.009 $b$	0.199 ± 0.009 $a$	37.15 ± 2.22 $a$	-13.27 ± 0.06 $a$
Nebraska Sandhills	130.8 ± 8.4 $ab$	0.387 ± 0.013 $b$	0.222 ± 0.004 $a$	26.60 ± 2.67 $a$	-13.26 ± 0.06 $a$
North Central Hardwood Forests	155.8 ± 4.2 $abc$	0.336 ± 0.013 $ab$	0.179 ± 0.001 $a$	23.16 ± 1.49 $a$	-13.13 ± 0.21 $a$
Northwest Glaciated Plains	190.3 ± 7.9 $c$	0.308 ± 0.017 $a$	0.210 ± 0.006 $a$	24.86 ± 1.93 $a$	-13.42 ± 0.15 $a$
Western Corn Belt Plains	161.5 ± 10.3 $abc$	0.328 ± 0.016 $ab$	0.207 ± 0.003 $a$	31.91 ± 7.53 $a$	-13.46 ± 0.10 $a$

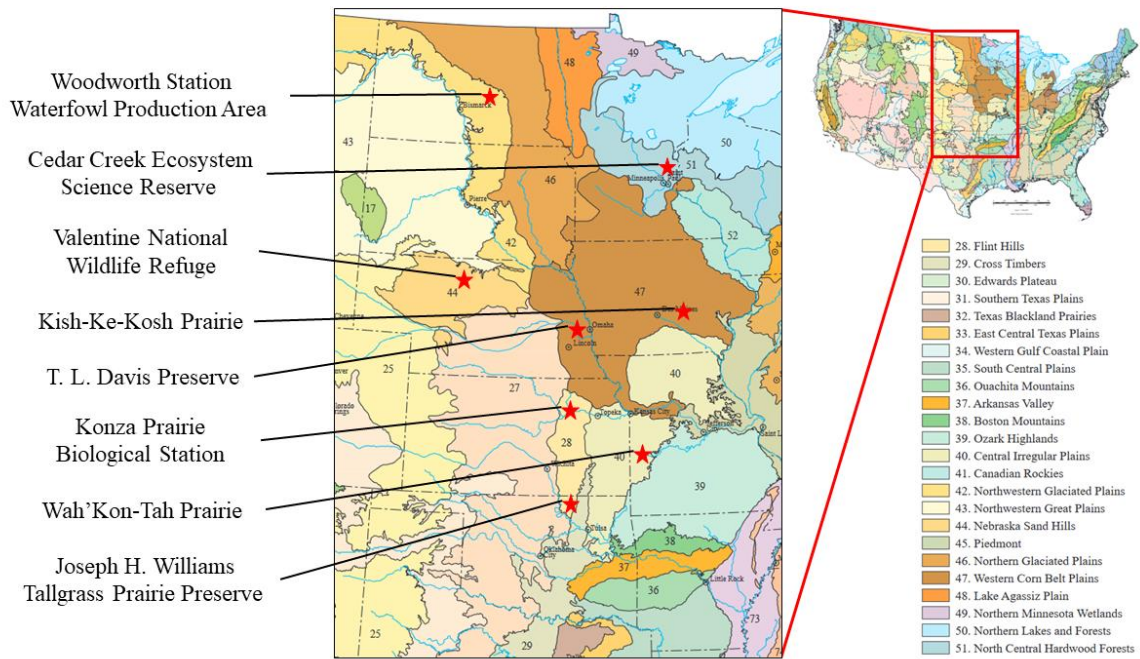


**Figure 3.1: A map of the grassland sites and their ecoregions (US Environmental Protection Agency, 2013).**

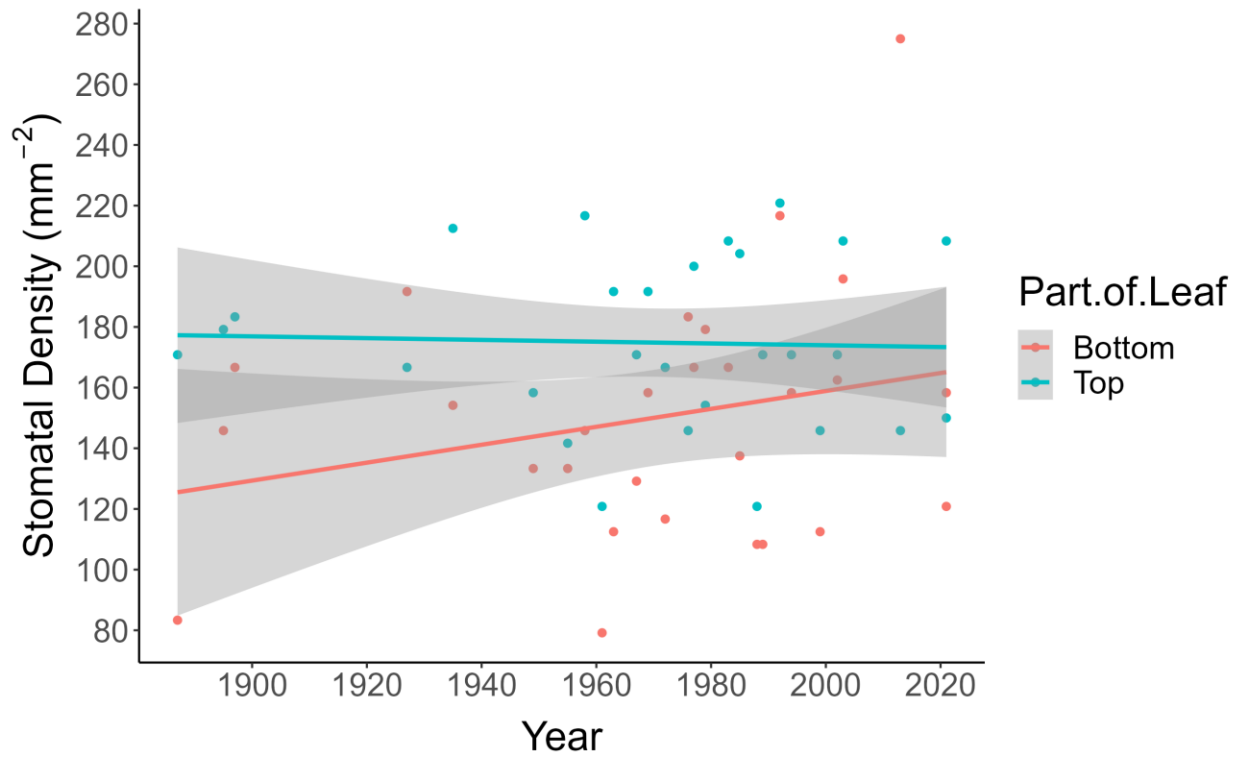


**Figure 3.2: The change in stomatal densities of the abaxial ( $R^2 = 0.06492$ ;  $P = 0.1907$ ) and adaxial ( $R^2 = 0.001344$ ;  $P = 0.8531$ ) surfaces of *P. virgatum* leaves from the years 1887 – 2021.**

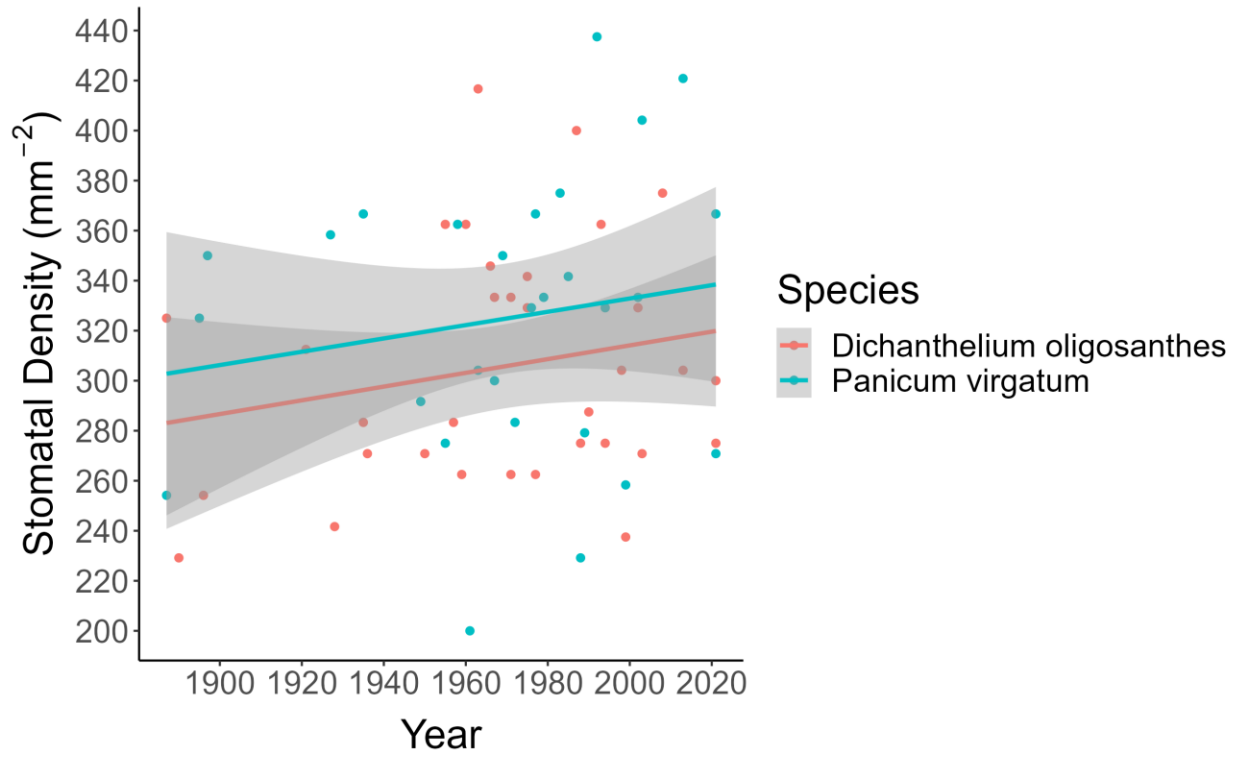


**Figure 3.3: The change in total stomatal densities of *D. oligosanthes* ( $R^2 = 0.04249$ ;  $P = 0.2498$ ) and *P. virgatum* ( $R^2 = 0.02825$ ;  $P = 0.3926$ ) leaves from the years 1887 – 2021.**

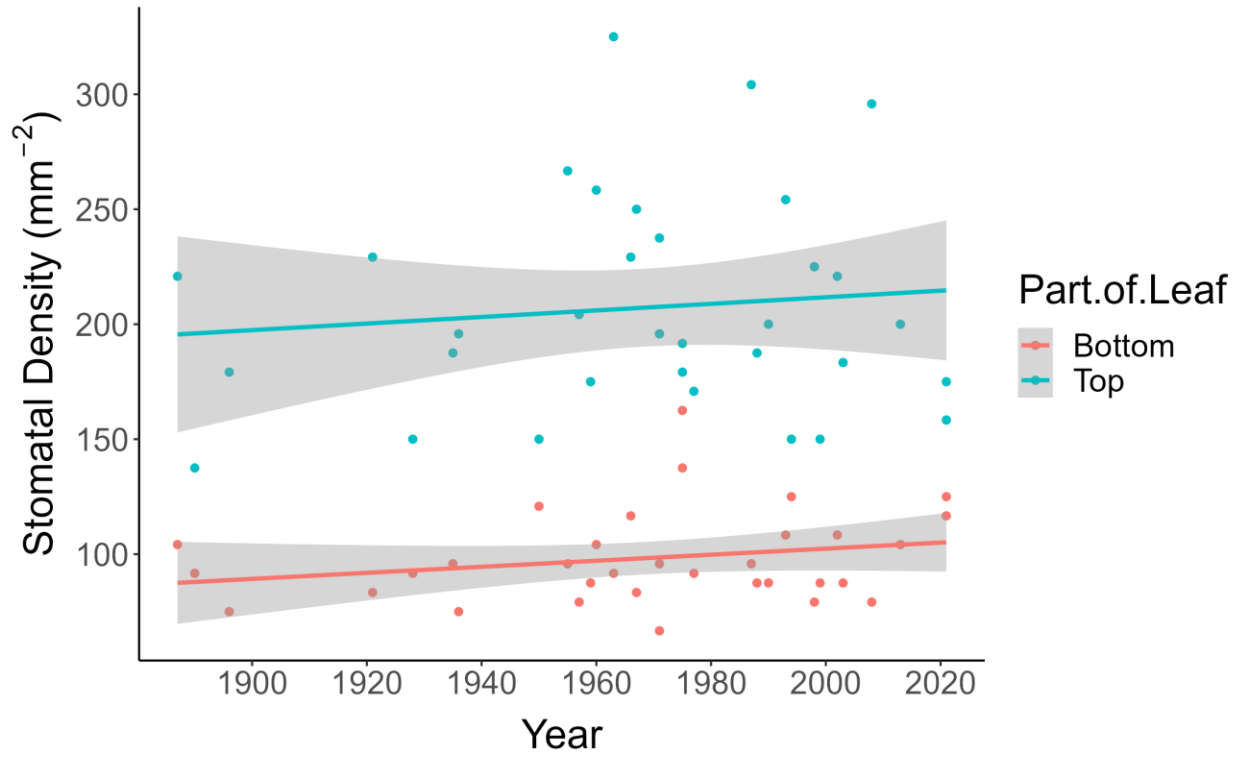


**Figure 3.4:** The change in stomatal densities of the abaxial ( $R^2 = 0.05433$ ;  $P = 0.1918$ ) and adaxial ( $R^2 = 0.01172$ ;  $P = 0.5487$ ) surfaces of *D. oligosanthos* leaves from the years 1887 – 2021.

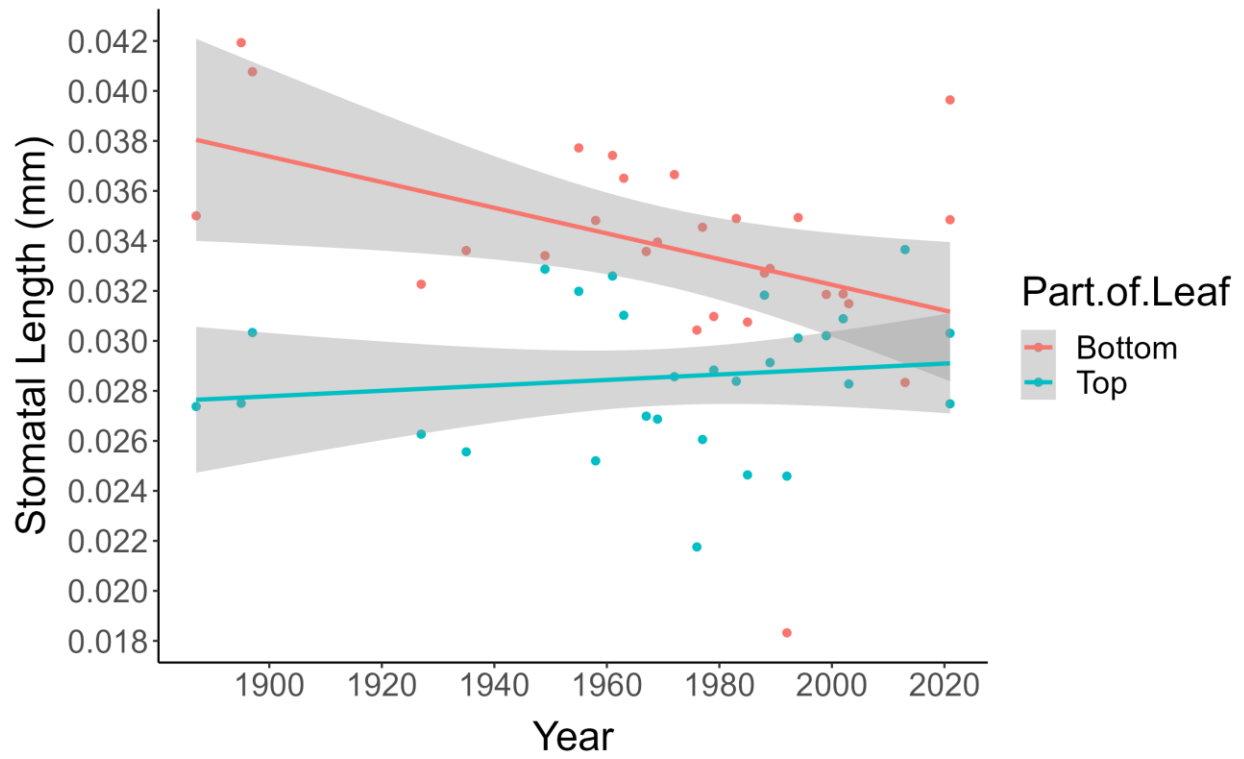


**Figure 3.5: The change in stomatal lengths of the abaxial ( $R^2 = 0.1748$ ;  $P = 0.02685$ ) and adaxial ( $R^2 = 0.01798$ ;  $P = 0.4964$ ) surfaces of *P. virgatum* leaves from the years 1887 – 2021.**

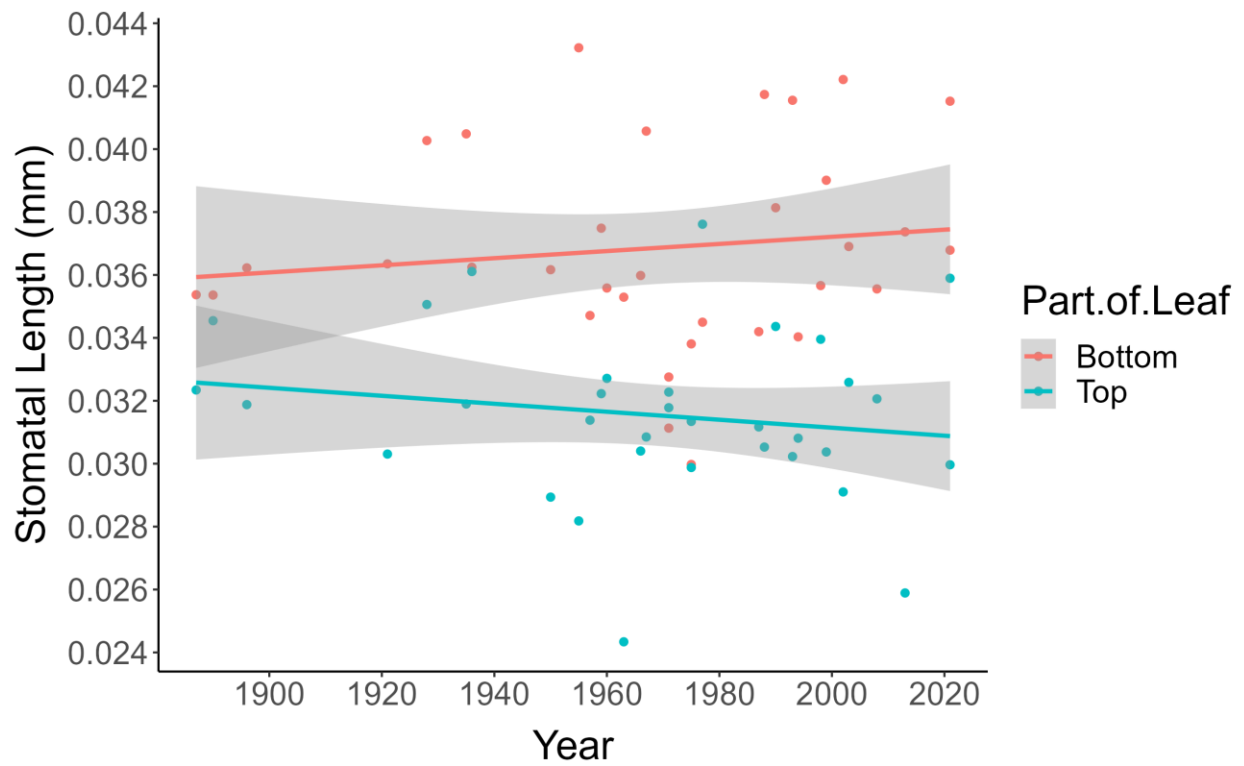


**Figure 3.6: The change in stomatal lengths of the abaxial ( $R^2 = 0.01594$ ;  $P = 0.4838$ ) and adaxial ( $R^2 = 0.02762$ ;  $P = 0.3553$ ) surfaces of *D. oligosanthos* leaves from the years 1887 – 2021.**

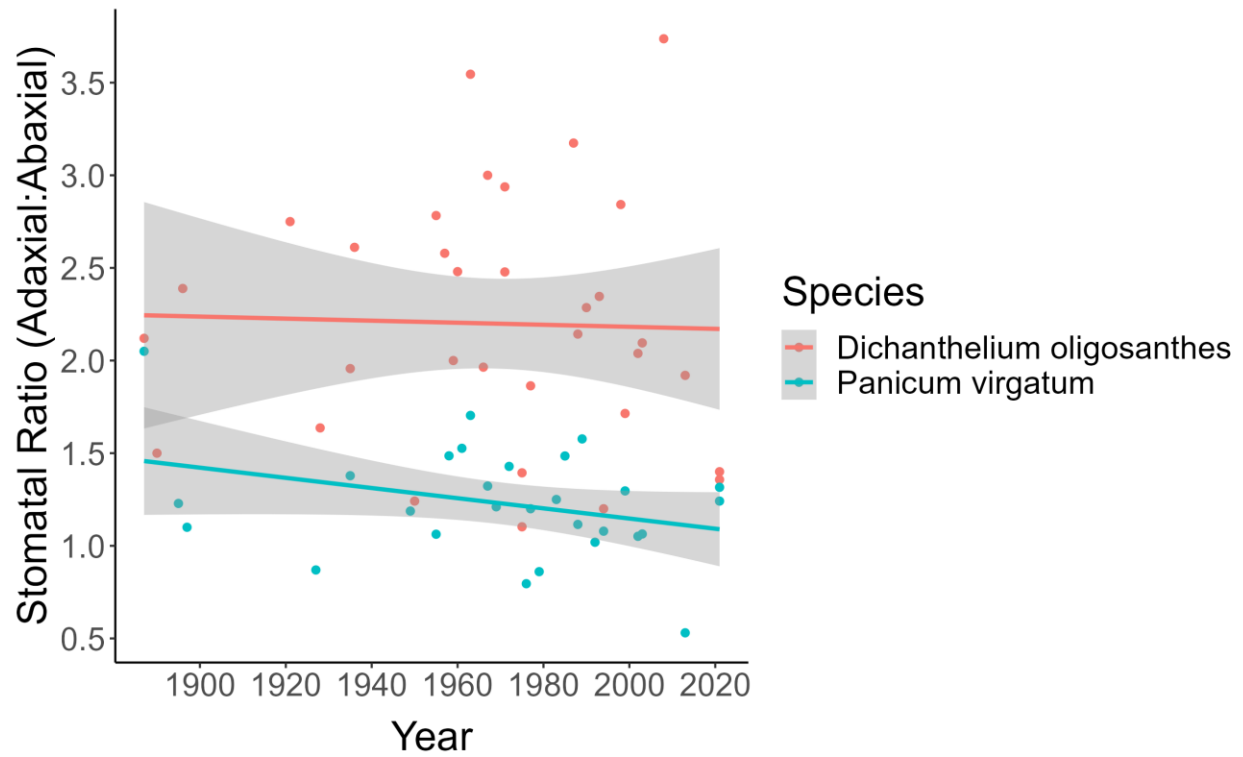


**Figure 3.7: The change in stomatal ratios (adaxial:abaxial) of *D. oligosanthes* ( $R^2 = 0.0008576$ ;  $P = 0.8715$ ) and *P. virgatum* ( $R^2 = 0.1052$ ;  $P = 0.09219$ ) leaves from the years 1887 – 2021.**

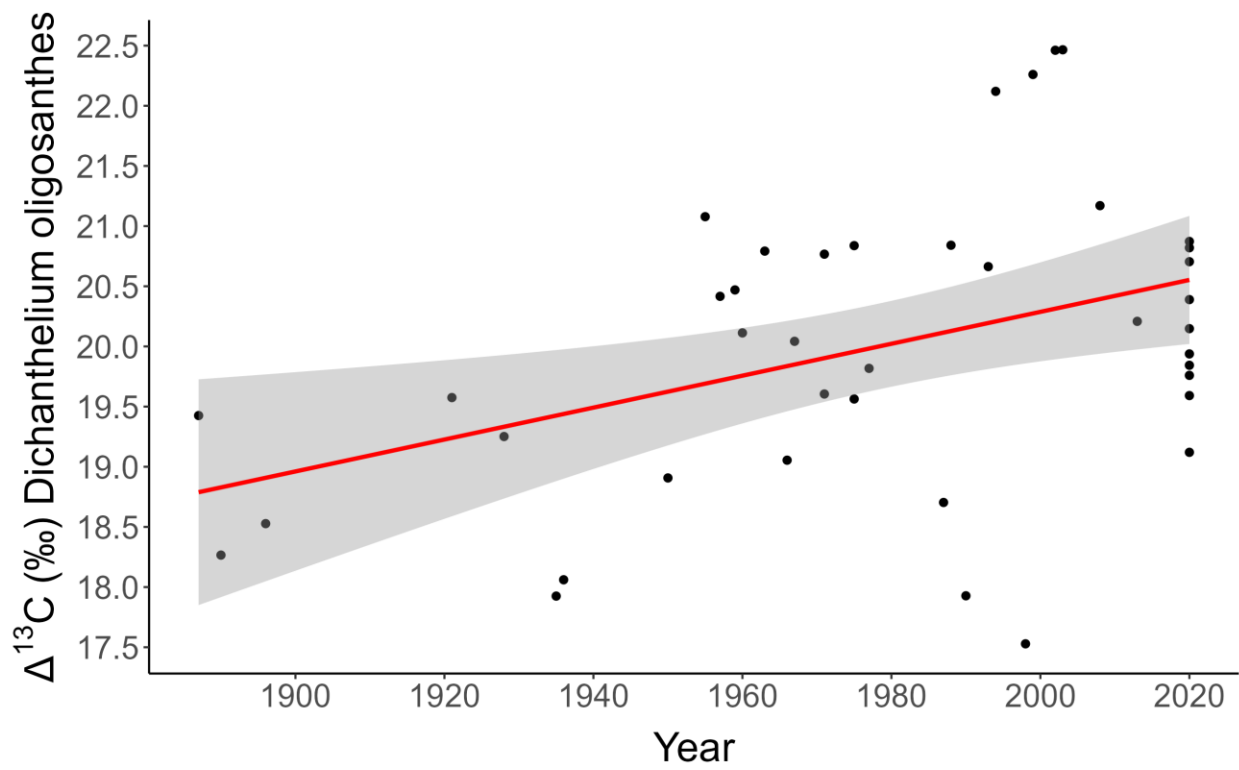


**Figure 3.8: The change in  $\Delta^{13}\text{C}$  of *D. oligosanthes* leaves from the years 1887 – 2020 ( $R^2 = 0.17$ ;  $P = 0.007394$ ).**

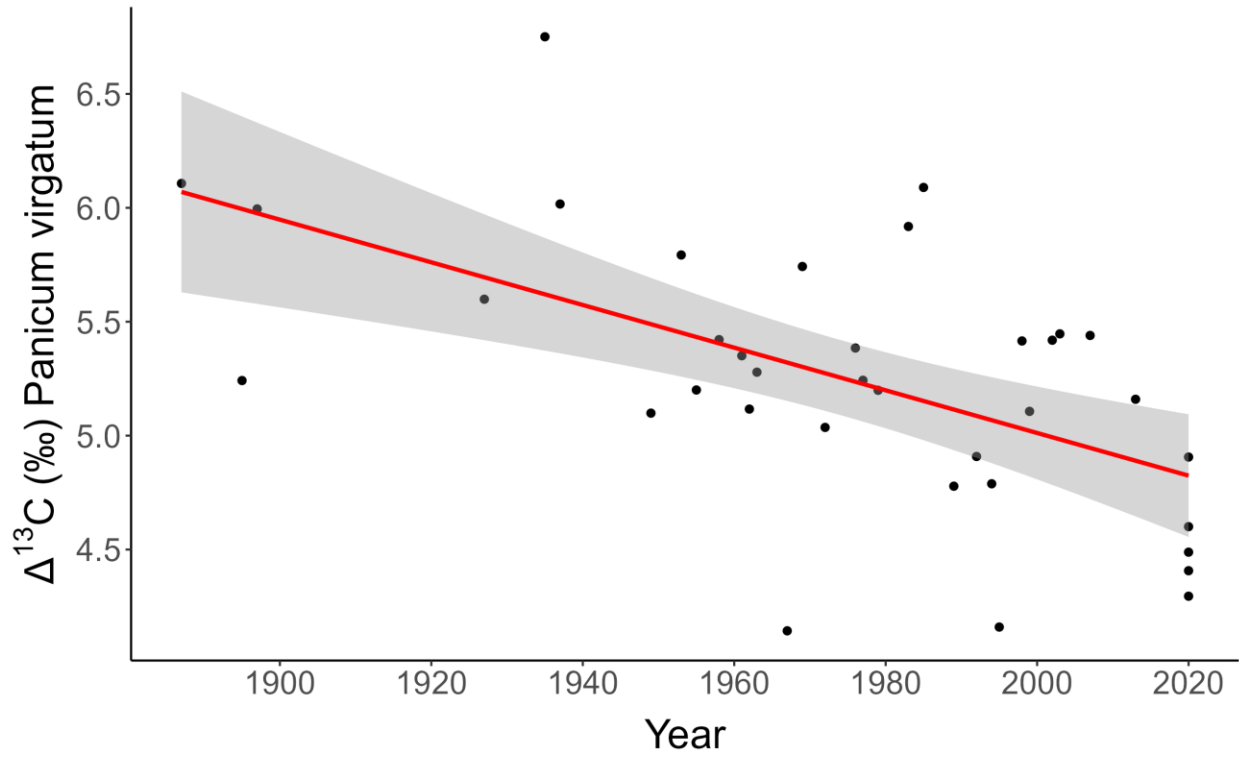


**Figure 3.9: The change in  $\Delta^{13}\text{C}$  of *P. virgatum* leaves from the years 1887 – 2020 ( $R^2 = 0.3276$ ;  $P = 0.0002649$ ).**

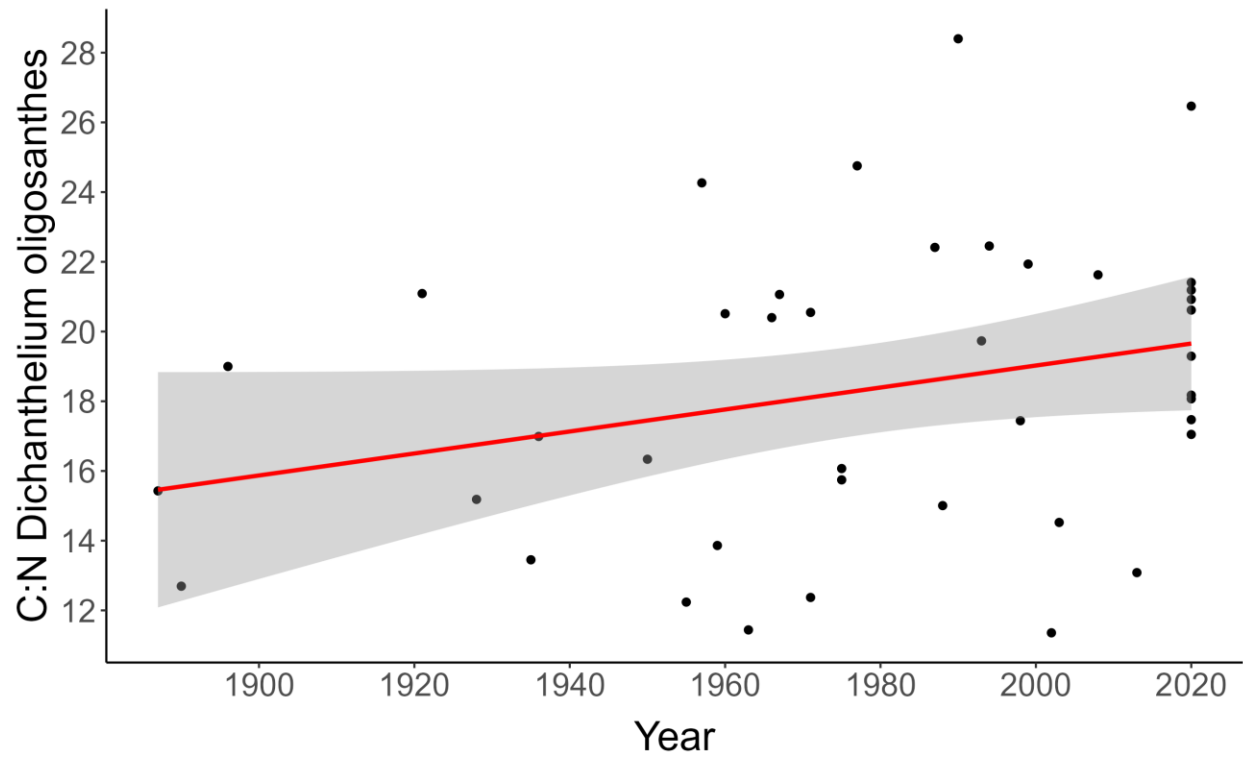


**Figure 3.10: The change in C:N of *D. oligosanthes* leaves from the years 1887 – 2020 ( $R^2 = 0.08207$ ;  $P = 0.06939$ ).**

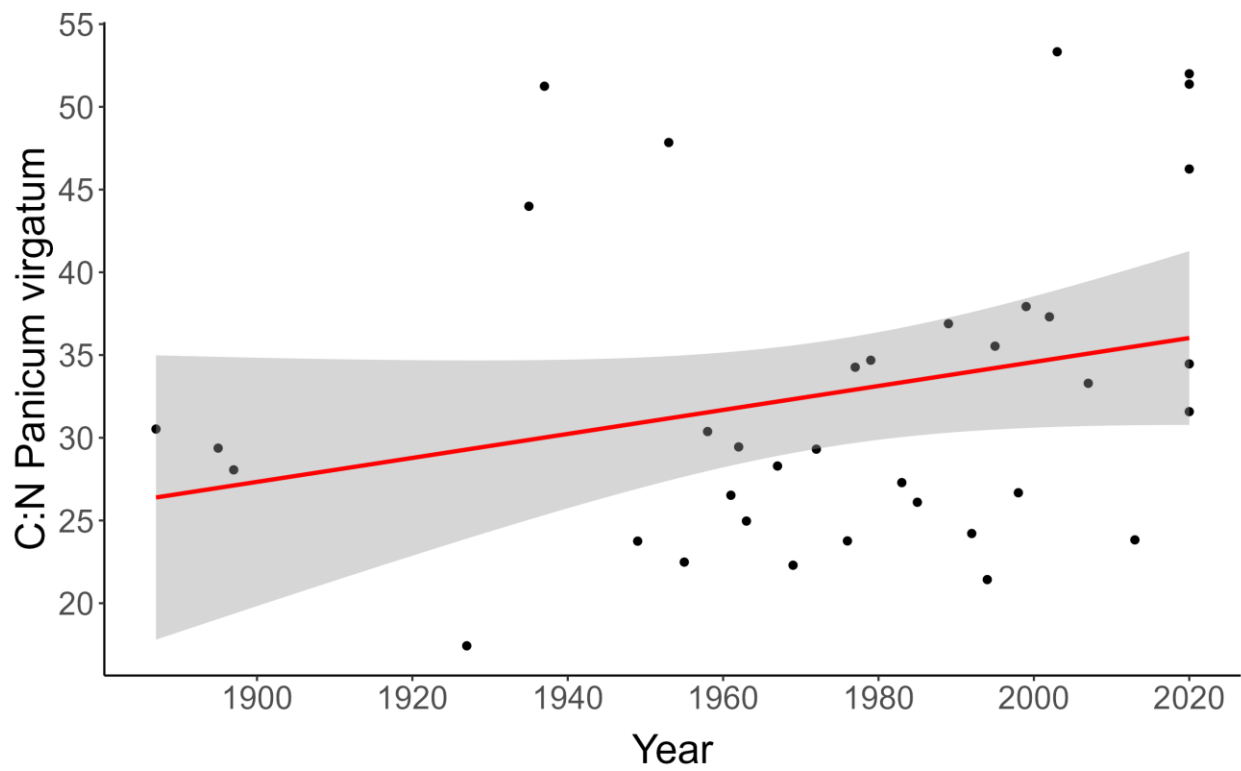


**Figure 3.11: The change in C:N of *P. virgatum* leaves from the years 1887 – 2020 ( $R^2 = 0.07127$ ;  $P = 0.1155$ ).**

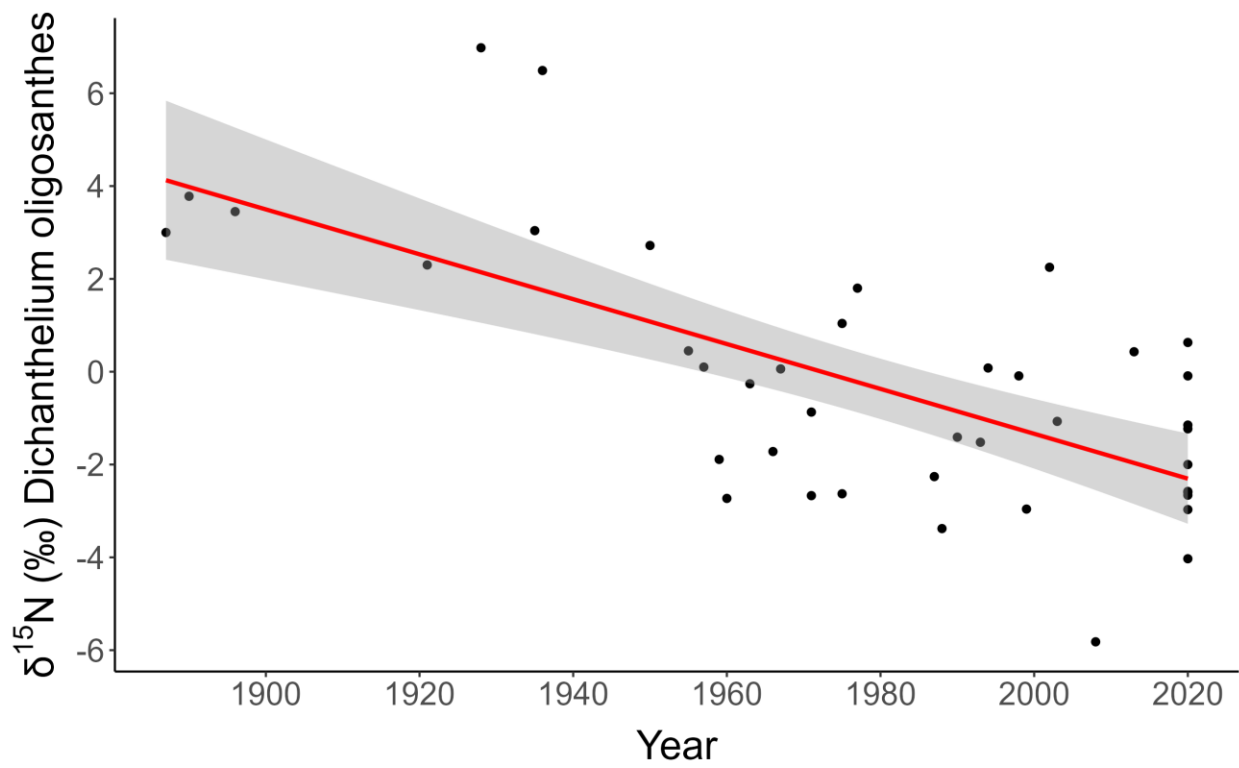


**Figure 3.12: The change in  $\delta^{15}\text{N}$  of *D. oligosanthes* leaves from the years 1887 – 2020 ( $R^2 = 0.4493$ ;  $P = 1.636e^{-06}$ ).**

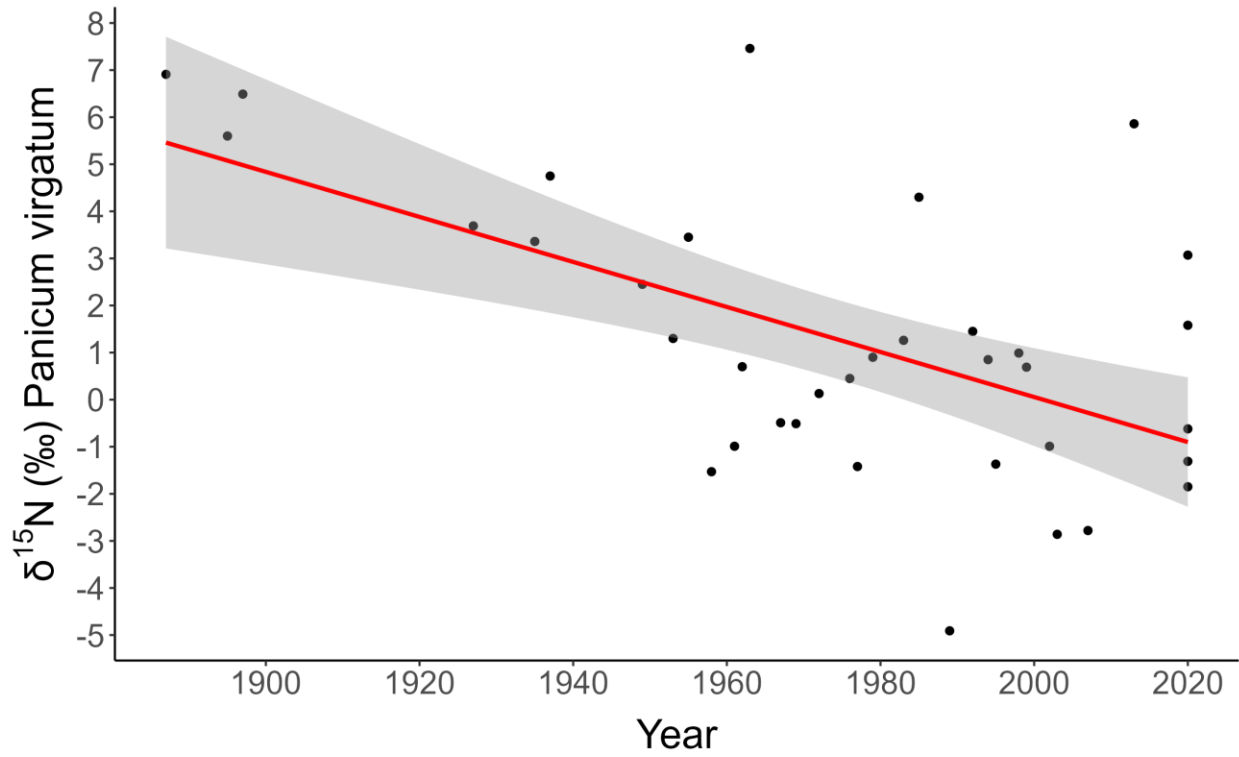


**Figure 3.13: The change in  $\delta^{15}\text{N}$  of *P. virgatum* leaves from the years 1887 – 2020 ( $R^2 = 0.3282$ ;  $P = 0.0002608$ ).**

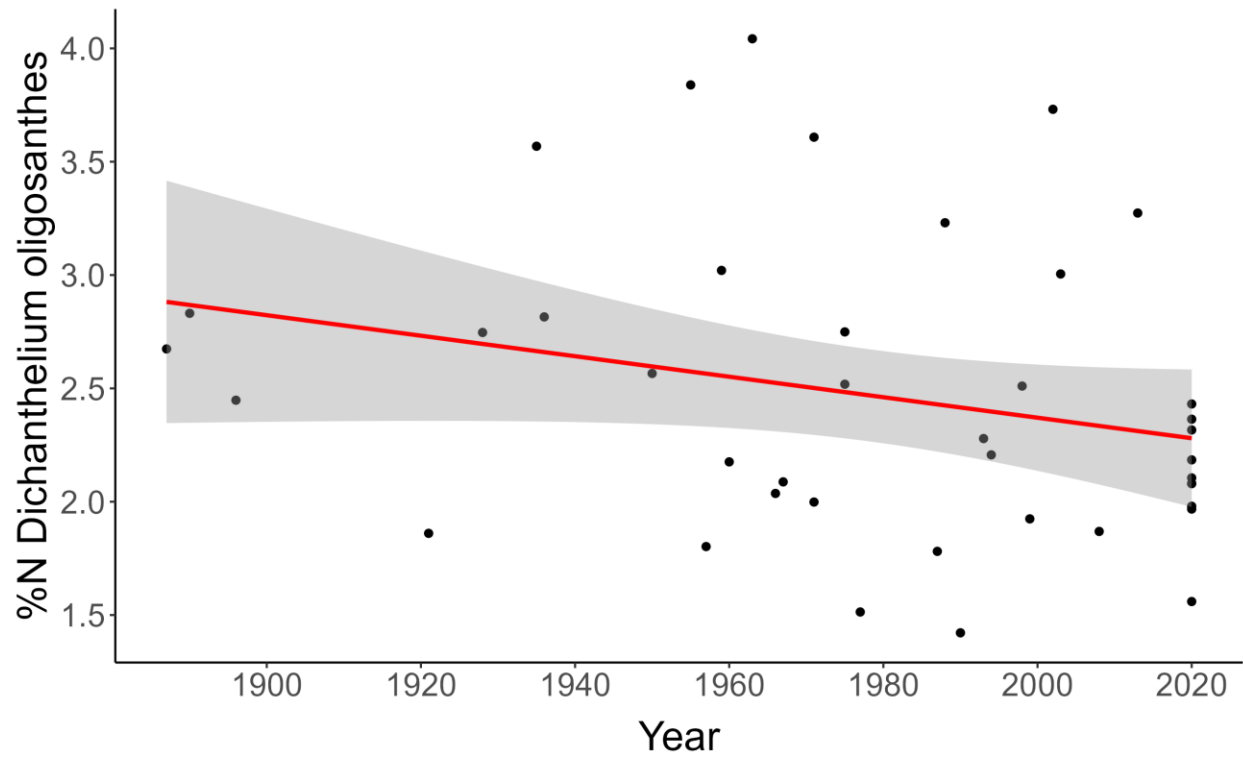


**Figure 3.14: The change in %N of *D. oligosanthes* leaves from the years 1887 – 2020 ( $R^2 = 0.06826$ ;  $P = 0.09895$ ).**

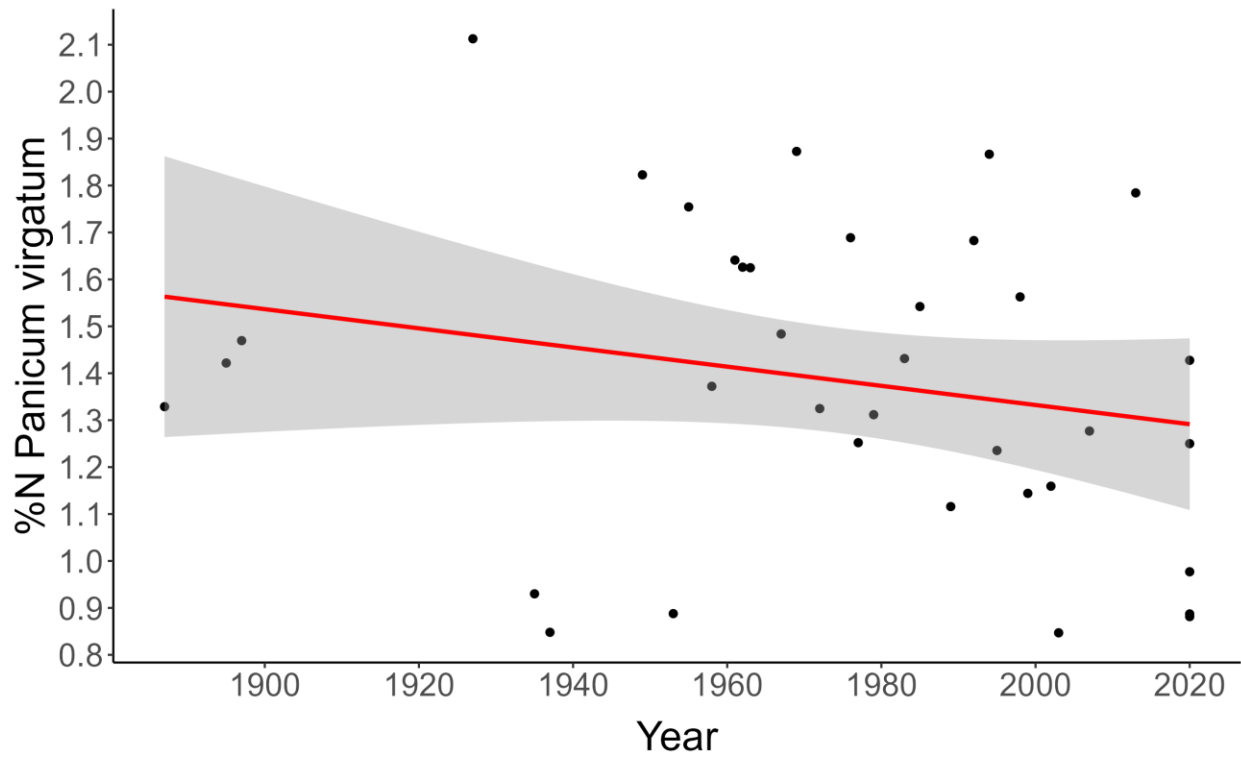


**Figure 3.15: The change in %N of *P. virgatum* leaves from the years 1887 – 2020 ( $R^2 = 0.0002608$ ;  $P = 0.1997$ ).**

## Chapter 4 - Conclusion

The grass family Poaceae is one of the most successful plant families on Earth. Grassy ecosystems cover over 25% of the Earth's terrestrial surface (Asner *et al.*, 2004) and grass species are found on every continent, including Antarctica. Poaceae comprises over 11,500 species of grasses (Soreng *et al.*, 2017), and the tremendous diversity among grass species has facilitated their success across a wide range of climatic and environmental conditions. Grasses and grass-dominated ecosystems function as essential drivers of global biogeochemical cycling (Scurlock & Hall, 1998) and are critical to the success of humanity, as grasses are utilized worldwide for food, fiber, and fuel (Tilman *et al.*, 2002; Glémin & Bataillon, 2009).

Despite the critical importance of Poaceae, grasses have historically been overlooked by ecologists in favor of non-grass species. Grasses are routinely underrepresented in trait databases such as the TRY database (Kattge *et al.*, 2011), especially C<sub>4</sub> grasses. While C<sub>4</sub> grasses account for less than half of all grass species (Osborne *et al.*, 2014), they often dominate the landscapes in which they occur (Strömberg, 2011), accounting for nearly a quarter of gross terrestrial productivity worldwide (Still *et al.*, 2003). Therefore, it is vital to increase our understanding of grass trait variability if we are to understand and predict how global change is affecting, and will continue to affect, grassy ecosystems. The goal of this thesis was to further understand the natural variability among Poaceae across spatial, temporal, and taxonomic scales in the Great Plains region of the United States.

In Chapter 2, I explored three methods of organizing grass species for use in grassland ecosystem models to better understand how trait diversity varies among grass species. The purpose of this chapter was to assess alternatives to plant functional types (PFTs) for use in Land Surface Models, which group grasses by their photosynthetic pathway. This method ultimately

underestimates trait diversity within Poaceae, especially among C<sub>4</sub> grass lineages (Griffith *et al.*, 2020). To this end, I measured 11 structural and physiological traits commonly used in grassland ecosystem models on 75 naturally-occurring species of grass. I then compared whether functional types grouped by photosynthetic pathway (C<sub>3</sub> or C<sub>4</sub>), life history (annual or perennial), or evolutionary history (tribe or C<sub>4</sub> lineage) best explained variation in traits. My results showed that grass traits are best understood within the context of their evolutionary history.

Photosynthetic pathway only revealed significant differences among physiological traits and life history primarily explained variation in structural traits. Evolutionary history, however, was found to significantly explain differences found in both structural and physiological traits when species were grouped by either tribe or C<sub>4</sub> lineage. These findings suggest that replacing PFTs with a grouping strategy that accounts for evolutionary history, such as lineage-based functional types (LFTs), would improve the predictions of grassland ecosystem models.

In Chapter 3, I examined spatial and temporal variability of leaf traits for two species of Panicoid grasses, *Dichanthelium oligosanthes* subsp. *scribnerianum* (C<sub>3</sub>) and *Panicum virgatum* (C<sub>4</sub>). Temporal trait variability was assessed by measuring traits on herbarium specimens from 1887-2020 from the Kansas State University Herbarium (KSC) and the McGregor Herbarium at the University of Kansas (KANU). Stomatal traits (total density, length, and adaxial:abaxial density) predominately did not vary over time for either species – a finding that contrasts with the results of many measurements on non-Poaceae species (Woodward & Kelly, 1995) – despite an increase of roughly 120 ppm in atmospheric CO<sub>2</sub> over this time period.  $\Delta^{13}\text{C}$  increased through time in *D. oligosanthes* but decreased in *P. virgatum*, which was the first time a temporal decrease in  $\Delta^{13}\text{C}$  for a C<sub>4</sub> species has been reported in the literature. Spatial trait variability was assessed by measuring leaf traits across eight different sites representing six

unique ecoregions of the Great Plains of North America. While few changes in stomatal traits were found (likely due to small sample sizes), differences in other leaf traits (SLA, LDMC, fresh leaf thickness, C:N, and  $\delta^{13}\text{C}$ ) were found across ecoregions, likely driven by spatial variation in precipitation and temperature. These results highlight how trait variation across spatial scales has influenced the ability of these species to persist across vast regions of the Great Plains of North America. These findings demonstrate the need to include representatives of Poaceae in more trait studies, as grass species are vastly under-represented in trait-based ecological research and likely respond differently than non-grass species to climatic and environmental change.

To accurately predict how grassland ecosystems may respond to future environmental change, it is first necessary to understand how dominant grasses of those ecosystems function. The traits of grass species can be used as predictors of plant performance (Violle *et al.*, 2007) and subsequently incorporated into grassland ecosystem models. This thesis has contributed to the understanding of how grass traits vary spatially, temporally, and by evolutionary lineage in the Great Plains region of the United States. The results of these studies provide additional evidence that including evolutionary history – rather than relying solely on life history or photosynthetic pathway – would improve the accuracy of ecosystem models aimed at predicting grassland responses to future climatic and environmental change.

## References

- Asner GP, Elmore AJ, Olander LP, Martin RE, Harris AT. 2004.** Grazing systems, ecosystem responses, and global change. *Annual Review of Environment and Resources* **29**: 261–299.
- Glémin S, Bataillon T. 2009.** A comparative view of the evolution of grasses under domestication. *New Phytologist* **183**: 273–290.

- Kattge J, Díaz S, Lavorel S, Prentice IC, Leadley P, Bönisch G, Garnier E, Westoby M, Reich PB, Wright IJ, et al. 2011.** TRY - a global database of plant traits. *Global Change Biology* **17**: 2905–2935.
- Osborne CP, Salomaa A, Kluyver TA, Visser V, Kellogg EA, Morrone O, Vorontsova MS, Clayton WD, Simpson DA. 2014.** A global database of C<sub>4</sub> photosynthesis in grasses. *New Phytologist* **204**: 441–446.
- Scurlock JMO, Hall DO. 1998.** The global carbon sink: a grassland perspective. *Global Change Biology* **4**: 229–233.
- Soreng RJ, Peterson PM, Romaschenko K, Davidse G, Teisher JK, Clark LG, Barberá P, Gillespie LJ, Zuloaga FO. 2017.** A worldwide phylogenetic classification of the Poaceae (Gramineae) II: an update and a comparison of two 2015 classifications. *Journal of Systematics and Evolution* **55**: 259–290.
- Still CJ, Berry JA, Collatz GJ, DeFries RS. 2003.** Global distribution of C<sub>3</sub> and C<sub>4</sub> vegetation: carbon cycle implications. *Global Biogeochemical Cycles* **17**: 6-1-6–14.
- Strömberg CAE. 2011.** Evolution of grasses and grassland ecosystems. *Annual Review of Earth and Planetary Sciences* **39**: 517–544.
- Tilman D, Cassman KG, Matson PA, Naylor R, Polasky S. 2002.** Agricultural sustainability and intensive production practices. *Nature* **418**: 671–677.
- Violle C, Navas M-L, Vile D, Kazakou E, Fortunel C, Hummel I, Garnier E. 2007.** Let the concept of trait be functional! *Oikos* **116**: 882–892.
- Woodward FI, Kelly CK. 1995.** The influence of CO<sub>2</sub> concentration on stomatal density. *New Phytologist* **131**: 311–327.